APPENDIX A

Manuscript entitled "*Effects of Modulating of Osteoactivin Expression on Osteoblast Differentiation*" by Abdulhafez A. Selim, Thomas A. Owen, Mario C. Rico, Steve L. Smock, Julian L. Castaneda, Reem A. Kanaan, Mary F. Barbe, Steven N. Popoff and Fayez F. Safadi.

Effects of Modulating of Osteoactivin Expression on Osteoblast Differentiation

Abdulhafez A. Selim[1], Thomas A. Owen[2], Mario C. Rico[1], Steve L. Smock[2], Julian L. Castaneda[1], Reem A. Kanaan[1], Mary F. Barbe[1], Steven N. Popoff [1]and Fayez F. Safadi[1]

[1] Department of Anatomy and Cell Biology, Temple University, School of Medicine, Philadelphia, PA
[2]Department of Cardiovascular and Metabolic Diseases, Pfizer Global Research and Development, Groton, CT

Running Title: Osteoactivin in osteoblasts

Abdulhafez A. Selim: abdu94@yahoo.com
Thomas A. Owen: Thomas_a_owen@groton.pfizer.com
Mario Rico: marior@temple.edu
Steve L. Smock:
Julian Casteaneda: Jucastaneda@msn.com
Reem A. Kanaan: kanaanreem@hotmail.com
Mary Barbe: mbarbe@temple.edu
Steven N. Popoff:

Corresponding Author:
Fayez F. Safadi, Ph.D
Assistant Professor, Department of Anatomy and Cell Biology
Temple University School of Medicine
3400 North Broad Street
Philadelphia, PA 19140
Voice: (215) 707-5655
Fax: (215) 707-2966
e-mail: fsafadi@temple.edu

SUMMARY

Previously, our laboratory examined differential gene expression in bone from normal and osteopetrotic (op) rats and isolated a novel complementary DNA (cDNA), termed osteoactivin (OA), that was overexpressed in op when compared to normal bone. Subsequent in situ hybridization and immunohistochemical localization demonstrated that OA messenger RNA (mRNA) and protein are expressed by osteoblasts. In primary osteoblast cultures, OA mRNA levels exhibited a temporal pattern of expression at highest levels during the later stages of matrix maturation and matrix mineralization. In this study, we attempted to block OA expression using OA antisense oligonucleotides. Blockage of OA expression in primary osteoblast cultures markedly decreased osteoblast differentiation markers, including alkaline phosphatase (ALP) activity, osteocalcin production, nodule formation, and calcium deposition. Conversely, the cytomegalovirus (CMV)-OA construct was generated and used to examine the effect of OA overexpression on MC3T3-E1 osteoblast differentiation. OA transient overexpression markedly increased osteoblast differentiation markers, including ALP activity, osteocalcin production, nodule formation and calcium deposition, compared to cultures transfected with an empty vector. OA overexpression also markedly induced expression of core binding factor 1 (Cbfa1), a master osteoblast transcription factor. Collectively, OA gain of expression or loss of expression in osteoblast cultures significantly induced and inhibited osteoblast differentiation respectively. These data suggested that OA plays a major role in the regulation of osteoblast differentiation.

INTRODUCTION

The initial identification of OA emerged from studies using an animal model of osteopetrosis, the op mutation in rats. This model was used to examine differential gene expression in bone from normal and op mutant rats that have a severe skeletal phenotype resulting from abnormalities associated with skeletal development.[1] A novel cDNA that is highly up-regulated in op compared to normal bone was identified using the technique of mRNA differential display.[2] Subsequent cloning and sequencing of the full-length cDNA revealed a sequence with homology to the previously reported human nmb,[3] murine nmb,[4] melanocyte specific protein (Pmel 17),[5] and DC-HIL (dendritic cell heparan sulfate proteoglycan integrin-dependent ligand).[6] No previous studies were done to examine the functional role of one of these genes in osteoblast development.

OA patterns of expression in vitro and in vivo suggested that OA might play an important role in

osteoblast development.[2] Tissue distribution of OA expression measured by RT-PCR analysis showed that OA is expressed at the highest level in bone and primary osteoblast cultures, with much lower levels of expression in other tissues such as brain, heart, and skeletal muscle.[2] In situ hybridization findings demonstrated intense staining of OA mRNA in osteoblasts lining bone surfaces in vivo.[2] Microarray analysis showed that OA expression increased in the fracture repair model, with time following fracture reaching a maximum at 2 weeks postfracture.[7] These findings showed that OA is expressed by osteoblasts, and its level of expression is highest at the sites of active osteogensis. OA temporal expression in osteoblast culture was examined, and the level of OA expression in primary osteoblast culture increased progressively as the cells differentiate with maximum expression during the final stage of matrix mineralization.[2] OA expression was also correlated with the expression of osteoblast-related genes, such as alkaline phosphates and osteocalcin in primary cell cultures.[2] Given these observations, we sought to assess whether OA plays a functional role in osteoblast development and function. Osteoblasts are the cells that are lining bone surfaces and responsible for bone matrix production. Osteoblasts originate from mesenchymal cells that have the ability to proliferate and differentiate into preosteoblasts and then into mature osteoblasts. Appropriate signals (eg, hormones, cytokines, and growth factors) are needed for the process of osteoblast differentiation.[8] The stages of osteoblast development and differentiation in the culture system have been well characterized. Primary osteoblast cultures undergo 3 distinct stages beginning with cell proliferation (day 0-7), followed by a period of matrix maturation (day 7-14), and ending with a stage of matrix mineralization (day 14-21).[9] The proliferation stage is associated with high levels of expression of histone 4, transforming growth factor-beta (TGF-β), collagen type I and fibronectin, followed by the stage of matrix maturation which is associated with high levels of expression of ALP. The last stage is the stage of matrix mineralization that is associated with maximum expression of osteocalcin (OC), osteopontin, and bone sialoprotein .[10] Temporal expression of osteoblast-related genes during different stages provide markers reflective of various stages of osteoblast differentiation and maturation in vitro.[10]

Our findings indicate a critical role for OA in osteoblast development with up and down regulation of osteoblast differentiation markers associated with up and down regulation of OA expression in vitro. These data suggest that OA plays a physiologically relevant role in bone development.

MATERIALS AND METHODS

Osteoblast Cultures

For primary osteoblast culture, calveria were harvested from neonatal rats (1-3 day old) and cleaned free of periosteum and endocranial dura in Ca^{++}/Mg^{++} free phosphate buffered saline (PBS) containing 200 units/ml penicillin and 200 μg streptomycin on ice. Each calverium was cut along the suture lines (sagital and coronal) and the pieces were transferred to siliconized Ehrlenmeyer flasks (Sigma, MO) and digested with trypsin/collagenase solution (0.25% trypsin and 0.1% collagenase P) in PBS. This enzymatic digest were repeated three times. Cells from the first digest were discarded and cells from the second and third digests were pooled, washed twice in MEM (Hank's) containing 10% fetal bovine serum (FBS), and resuspended in MEM (Earle's) containing 10% FBS. The cells were filtered through a 200 μm mesh metal screen filter (Fisher Scientific-Millipore filter and screen), counted, and plated at an appropriate concentration (i.e. 5 x 10^5 cells/100 mm plate) in MEM (Earl's) containing 10% FBS. On the third day of culture, the initial plating medium were replaced with MEM containing 10% FBS and ascorbic acid (25 μg/ml). On the seventh day of culture and every 2-3 days thereafter, the medium were replaced with MEM (Earle's) containing 10% FBS, ascorbic acid and β-glycerophosphate (10 μM). The mouse osteoblast cell line MC3T3-E1 (MC) was obtained from ATCC (ATCC Inc., VA) and routinely maintained in growth medium consisting of αMEM (Invitrogen, CA) containing 10% fetal bovine serum (Invitrogen), 100 units/ml penicillin, 100 μg/ml streptomycin , 25 μg/ml ascorbic acid and 10 μM β-glycerophosphate (Sigma) and medium were changed every 3-4 days.

Oligonucleotides Transfection

Primary osteoblasts were cultured as described above, when cells reached sub-confluent (50-60%), they were transfected with 0.5 μM of OA anti-sense or sense using oligofectamine (Invitrogen) according to the manufacturer's protocol. Oligonucleotides were synthesized of 20 base phosphorothioate-modified oligonucleotides (Sigma). The sequence of OA antisense oligos was (5'-CCCTAGTCCCATCCACCAGG-3') and the sequence of sense oligos was (5'- GGGCGTCTCTGAAAGGTAACG-3'). The sequence of OA antisense oligos was rigorously analyzed by Blast search and no homologies were found. Preliminary experiments were conducted to determine effective oligonucleotides concentration that was not toxic to the cells. Transfection efficiency was determined using green fluorescent (FITC) labeled oligos (Sigma). Primary osteoblast cultures were transfected with FITC oligos as described above then transfection efficiency was evaluated by counting

FITC-labeled cells versus total number of cells. Percentage of FITC labeled to total number of cells was calculated and 25% transfection efficiency was reproducibly achieved.

CMV-OA Transfection

Rat cDNA OA protein coding region was generated by RT-PCR using the following primers 5'PO4-ATGGAAAGTCTCTGCGGGGTCC-3' (designed at the initiating methionine ATG start codon) and 5'-CATACATGCACAGAAGAGTGGGTTCC-3' (designed at the 3' untranslated region of the rat OA with 20 bp past the termination codon TAA). The generated PCR product (1767) was cloned into the pCR3.1 TOPO vector which has cytomegalovirus (CMV) promoter (Invetrogen, CA) and LA Taq kit (Pan Vera, WI) was used to minimize potential PCR generated errors. MC3T3-E1 cells were cultured and when reached sub-confluent (50-60%), they were transfected with either CMV-OA (OA cDNA under CMV promoter), CMV- Empty Victor (E.V) or CMV- green fluorescent protein (GFP) constructs at a dose of 10 µg DNA/100-mm dish overnight using lipofectamine (Invetrogen) according to the manufacturer's protocol. Transfection efficiency was determined using the CMV- green fluorescent protein (GFP) construct. Briefly, MC3T3-E1 osteoblast like cells was transfected with CMV-GFP construct (10 µg DNA/100mm dish) then transfection efficiency was determined by calculating the percent of cells expressing GFP versus total number of cells using fluorescent microscopy. We routinely achieved about 30% transfection efficiency.

RNA Isolation

Cell layers were harvested and frozen in liquid nitrogen and stored at –80C. Cells were homogenized in Trizol, separated into aqueous and organic layer by chloroform, RNA remained in the aqueous layer was recovered by isopropyl alcohol precipitation. Pellets were washed again with 70% ethanol to clear RNA from DNA contamination.

RT-PCR Analysis

Two µg total RNA isolated from cell cultures were reverse transcribed to cDNA at 42°C for 50 minutes in a volume of 20 µl containing the following components: 1X first strand buffer (5X= 250 mM Tris, pH 8.3, 375 mM

KCl and 15 mM $MgCl_2$), 0.5 mM dNTP mix, 10 mM dithiothreitol (DTT), 0.5 µg oligo (dT) (12 –18 nucleotide) and 20 U Superscript II (RNase H-free reverse transcriptase) (Invitrogen). The reaction was then terminated at 70°C for 15 minutes, and 1 U RNase H (Invitrogen) was added to the reaction mixture, followed by incubation at 37°C for 10 minutes to remove the RNA. One µl aliquots of the generated cDNA was amplified in 50 µl of PCR reaction mixture containing 1 nM primer sets, 10 µl 10X Advantage buffer (Invitrogen), 10 nM dNTP mix, 1 µl DMSO and 1 µl Advantage polymerase mix (Clonetech, CA). The primers for osteoactivin are (sense: 5'-CCAGAAGAATGACCGGAACTCG-3' and anti-sense: 5'-CAGGCTTCCGTGGTAGTGG-3'). These primers were designed from the 5' end of the protein-coding region starting at a position 729 bp from the ATG start codon to position 1280. The primers for 18S are (sense: 5'-ACTTTCGATGGTAGTCGCCGTGC-3' and anti-sense: 5'-ATCTGATCGTCTTCGAACCTCCGA-3'). The primers for osteocalcin are (sense: 5'-TCTGACAAACCTTCAGTCC-3' and antisense: 5 ` AAATAGTGATACCGTAGATGCG-3'). The primers for G3PDH are (sense: 5'- ACCACAGTCCATGCCATCAC-3' and anti-sense: 5'- TCCACCACCCTGTTG CTGTA-3'). The primers for Cbfa1 are (sense: 5'- TCTGACAAACCTCATGTCC-3' and antisense: 5'AAATAGTGATACCGTAGATGCG-3'). PCR were performed using Perkin-Elmer GeneAmp PCR System 9600 (Perkin-Elmer, CT). PCR parameters for osteoactivin are: denaturation step at 94°C for 3 minutes, followed by 25 cycles of 94°C for 20 seconds, 62°C for 20 seconds and 68°C for 20 seconds; with final extension step at 68°C for 7 minutes. The expected osteoactivin PCR product is 552 bp. PCR parameters for 18S were: denaturation step at 94°C for 3 minutes, followed by 30 cycles of 94°C for 30 seconds, 65°C for 30 seconds and 68°C for 30 seconds; with final extension step at 72°C for 7 minutes. The expected 18S PCR product is 700bp. PCR parameters for osteocalcin are: denaturation step at 95°C for 3 minutes, followed by 30 cycles of 95°C for 60 seconds, 55 °C for 2 minutes and 72 °C for 1 minute; with final extension step at 72 °C for 7 minutes. The expected osteocalcin PCR product is 198 bp. PCR parameters for G3PDH are: denaturation step at 94°C for 3 minutes, followed by 35 cycles of 94°C for 45 seconds, 60 °C for 2 minutes and 72 °C for 2 minute; with final extension step at 72 °C for 7 minutes. The expected G3PDH PCR product is 452 bp. PCR parameters for Cbfa1 are: denaturation step at 94°C for 3 minutes, followed by 35 cycles of 94°C for 2 minutes, 60 °C for 30 second and 72 °C for 1 minute with final extension step at 72 °C for 10 minutes. The expected Cbfa1 PCR product is 632 bp. PCR products were analyzed by 1% agarose gel electrophoresis stained with ethidium bromide. A 100-bp ladder was used as a molecular weight marker (Invitrogen).

Antibody Preparation

Anti-OA antibody was raised against peptide that represents the sequence between amino acids 551-568. This peptide was selected because of its potential antigenicity and screened against the protein database to assure lack of homology with any known sequences. Chickens were immunized and the precipitated crude IgY was purified by affinity chromatography on Sepharose 4B derivatiesed with the antigen (immunizing peptide) (Zeneca, UK).

Western Blot Analysis and Protein Isolation

Protein samples isolated from cell cultures were mixed with equal volumes of 2X SDS sample buffer, boiled for 5 minutes, centrifuged for 5 minutes and subjected to 10% SDS-PAGE gel. Membrane was blocked with 5% milk, 1% BSA in Tris-buffered saline (TBS) and 0.1% Tween-20 (TTBS) for 2 hours and incubated with anti-chicken OA primary antibody (1μg/ml) overnight at 4°C. The blot was washed three times in TTBS each time for 15 minutes then incubated with HRP-conjugated donkey anti-chicken IgY secondary antibody (0.2 μg/ml) for two hours at room temperature. Signal was detected by ECL (Pierce, IL). For Protein isolation, cultured osteoblasts plates were rinsed three times with ice cold PBS. Cell layers were then harvested into protein extraction buffer (RIPA buffer), consisting of 50 mM Tris-HCl; pH 7.5; 135 mM NaCl; 1% Triton X-100, 0.1% sodium deoxycholate; 2 mM EDTA; 50 mM NaF; 2 mM sodium orthovanadate; 10 μg/ml aprotinin; 10 μg/ml leupeptin; 1 mM PMSF. Osteoblast cell pellets were homogenized in RIPA buffer then homogenates were incubated for 60 minutes at 4 °C, centrifuged and supernatant were collected and stored at -80C. Total protein concentration was measured using a bicinchoninic acid (BCA) protein assay (Pierce, IL).

MTT and Cell Counting assays

At day 5 of the culture (primary or MC3T3-E1osteoblasts), cells were incubated with 100 μl/well MTT substrate (3-[4,5-Dimethylthiazol-2-yl]-2,5-diphenyltertrazolium bromide) (Sigma Chemicals) for 4 hours at 37 °C. Cells were then washed with PBS then 500 μl/well of solublizer (20% (W/V) SDS in 50% DMF) was added and samples were read at 570 nm using ELISA plate reader. For cell counting assay, cells were trypsinized then they were counted by haemocytometer.

Alkaline Phosphatase Activity Measurement

At day 14 of the culture (primary or MC3T3-E1 osteoblasts), cell layer was washed with PBS and extracted in 150 mMTris pH 9.0/0.1mM $ZnCl_2$/0.1 mM $MgCl_2$ (TZM buffer) with 1% Triton X-100 for 30 minutes at 37 °C. Cell layer were scraped, vortexed and an aliquot mixed with p-nitrophenol (Sigma P104) substrate in 10x TZM buffer (Sigma). Alkaline phosphatase activity results (substrate release nmol/minute) were normalized to the total protein content. Total protein content was determined from matched cultures using BCA Peirce protein assay kit.

Alkaline Phosphatase Histochemistry

At day 14 of primary osteoblast culture, cells were rinsed once with PBS and fixed in 4% Para formaldehyde for 10 minutes, rinsed with dH_2O. Fresh substrate of 1ml Naphthol AS MX-BI, 1ml FRV and 1 ml sodium nitrite (Sigma) were mixed together and dissolved in 45 ml distilled water according to manufacturer's protocol. Substrate was then added onto the dishes and incubated for 45 minute at room temperature (RT). The dishes were rinsed in tab water, drained and air dried. Pictures were taken from randomly selected fields using *Nikon* inverted microscope.

Osteocalcin Measurement

At day 21 of the culture, osteocalcin concentration in serum free conditioned media was measured using commercially purchased sandwich ELISA kit (Biomedical Technologies Inc., MA). Briefly, a series of standards prepared from rat whole serum were used to generate standard curve (0.78 ng/ml - 50 ng/ml). Conditioned media and standards were incubated in ELISA plates, washed in PBS and incubated with anti-rat osteocalcin at 37 °C for 1 hour. Wells were washed and incubated with peroxidase-conjugated secondary antibody for 1 hour at RT. Tetramethyl benzidine (TMB) substrate was added to the wells and samples were incubated for 30 minutes in the dark in RT. Absorbance was read at 450nm using ELISA plate reader (Perkin Elmer Wallac, CT) within 15 minutes. Osteocalcin concentration values (ng/ml) were normalized to the total protein content. Total protein content was determined from matched cultures using BCA Peirce protein assay kit.

Calcium Measurement

At day 21 of the culture, cell layers were rinsed with cold PBS then hydrolyzed in 400 µl 0.5 N HCl. Aliquots were mixed with calcium binding reagent (o-cresolphthalein complexone and 8-hydroxyquinoline) in 250 nM 2-Amino-2-Methyl-1, 3 Propanediol buffer (Sigma Chemicals) and read at 575 nm using Beckman spectrophotometer. Concentration of calcium ions were calculated from comparison to a standard of known optical density (OD) using this equation: (A_{575} sample/ A_{575} standard) x (concentration of standard) and data were expressed as µg calcium/well.

Histochemical Staining of Mineralized Nodules.

At day 21 of the culture, cell layers were washed in Hank's balanced salt solution, fixed with 4% Para formaldehyde for 10 minutes at RT, stained with 3% silver nitrate solution for 1 hour under high intensity light at RT. Cell layers were then washed with dH_2O, fixed with 5% sodium thiosulfate for 2 minutes at RT, washed with dH_2O and allowed to air dry. For Alizarin red, cell layers were rinsed with PBS and fixed for 15 minutes at 4°C with 2% paraformaldehyde in PBS. Fixed cultures were rinsed with dH_2O, and stained by incubation with 1mg/ml AR-S (SIGMA) for 20 minutes. Cell layers were then washed five times with dH_2O followed by a 15 minutes rinse with PBS with gentle rotation to reduce nonspecific AR-S stain. Pictures were taken from different fields using *Nikon* inverted microscope.

Image Analysis

Pictures were taken using *Nikon* inverted microscope from different fields. Images for mineralized nodules stained with alizarin red were analyzed using *ImageJ* software (NIH, DC). The average size for mineralized nodules in control cultures was 800 pixels which is equivalent to $1.6x10^{-3}mm^2$. Images for mineralized nodules stained with von Kossa were analyzed using *BIOQUANT* software (Bioquant Image Analysis Inc, TN). The average size for mineralized nodules in control cultures was 1000 pixels which is equivalent to $2x10^{-3}mm^2$.

Data Presentation and Analysis

Data were presented as a percent of control where control is cells not transfected. The average absorbance of MTT assay in control samples was 0.75 OD at 575 nm in primary osteoblast cultures and 1.05 in MC3T3-E1 osteoblast cultures. The average cell number/well in 12 well plates was $0.9x10^5$ in primary osteoblast culture and

$1.35x10^5$ in MC3T3-E1 osteoblast culture. The average value for alkaline phosphatase activity in control samples was 110nM substance release/min in primary osteoblast culture and 145nM substance release/min in MC3T3-E1 osteoblast culture. The average value for calcium content/ well in 12 well plates in the control samples was 60 µg/well in primary osteoblast culture and 95 µg/well in MC3T3-E1 osteoblast cultures. The average value for osteocalcin concentration in control samples was 5ng/mg protein /ml in primary osteoblast culture and 8.5 ng/mg protein/ml in MC3T3-E1 osteoblast cultures. For all quantitative data, differences between individual groups were analyzed for statistical significance using the appropriate test. For two group comparison, statistical analysis of the data was achieved by unpaired two-tailed student *t* test. For multiple group comparison, analysis of variance (ANOVA) was used to evaluate the effect of one variable on multiple independent groups. In the event of a significant group effect, individual pairs of means were compared using Bonferroni post-hoc test. Any *P* value > 0.05 was considered statistically significant.

RESULTS

OA antisense Oligonucleotides Block OA Expression in Primary Osteoblast Culture.

Given that OA is expressed throughout the primary osteoblast culture period, gradually increasing to reach a maximum expression level at the end of the culture period,[2] we next asked whether OA is a critical factor in osteoblast proliferation and/or differentiation, using an antisense oligonucleotides approach. Antisense technology was developed to inhibit gene expression by utilizing oligonucleotides complementary to the mRNA, which encodes the target gene. This approach constitutes a very efficient and specific means to artificially regulate gene expression.[11] Seven different OA antisense oligonucleotides (OA-AS oligos) were designed, and the sequence of each was vigorously analyzed by Blast search to assure lack of homology with any other known genes. We first screened these 7 OA-AS oligos for their ability to block OA expression in cultures of RAT-2 fibroblast cells, since these cells constitutively express high levels of OA. These cells are derived from a 5-bromo-2'-deoxyuridine resistant strain of Fisher rat fibroblast 3T3-cell line.[12] OA expression was determined by RT-PCR analysis (Figure 1 - A). Densitometric analysis showed that 5 of the OA-AS oligos (1, 3, 4, 5 and 7) down-regulated OA expression, ranging from 68% to 99% when compared to mock (scrambled) oligonucleotides or transfection reagent treated control cultures (Figure 1 -B). Next, effect of OA-AS oligos treatment on OA expression in primary osteoblast cultures was examined. Transfection efficiency was evaluated using FITC-

conjugated oligonucleotides and 25% transfection efficiency was reproducibly obtained (data not shown). Preliminary studies were carried out to determine the effective oligonucleotide concentration that was not toxic to primary osteoblast cells (data not shown). Primary osteoblast cultures were transfected with 0.5 μM of OA-AS oligo-1 or sense oligonucleotides then OA mRNA and protein expression were examined by RT-PCR and Western Blot analyses respectively. OA-AS oligos markedly reduced OA expression and protein production (Figure 1 - C, D, E and F).

Inhibition of OA Expression Has No Effect on Osteoblast Proliferation or Viability.

Since OA is expressed throughout the culture period,[2] we examined the effect of OA-AS oligos on osteoblast development at the first (proliferation period), second (matrix maturation), and third week (matrix mineralization) in culture. Primary osteoblast cultures were either not transfected or transfected with 0.5 μM of sense or OA-AS oligos. At day 5 of culture, MTT assay (Figure 2 - A) and cell number counting (Figure 2 - B) were performed. MTT assay is routinely used to examine the effect of different factors on mammalian cells viability, cell number and proliferation.[13] OA antisense had no significant effect on osteoblast viability or proliferation (Figure 2). These results suggest that OA had a minimal role during the proliferation phase of primary osteoblast cultures.

Inhibition of OA Expression Blocks Primary Osteoblast Differentiation.

We further examined the effect of OA-AS oligos on primary osteoblast cultures during differentiation phases: matrix formation phase (day 7-14) and matrix mineralization phase (day 14-21). It has been established that osteoblast differentiation could be evaluated by different conventional markers, such as ALP,[14] osteocalcin expression,[15] calcium deposition, and nodule formation .[16] We examined the effect of OA-AS oligos on ALP activity (a marker for the matrix maturation stage; Figure 3 - A) and production (Figure 3 - B and C) at day 14. We also examined the effect of OA-AS oligos on osteoblast differentiation markers during the mineralization stage, including nodule formation (Figure 4 - A and B), nodule size (Figure 4 - C) calcium deposition (Figure 4 - D), and osteocalcin production at day 21 (Figure 4 - E). OA-AS oligos significantly inhibited ALP activity and production at day 14 (Figure 3), nodule formation (Figure 4 - A, B and C), calcium deposition (Figure 4 - D), and osteocalcin production at day 21 (Figure 4 - E). These data suggest that loss of OA expression significantly

inhibited osteoblast differentiation independent of cell proliferation.

OA Over-expression Induces MC3T3-E1 Osteoblast Differentiation in Culture

To further address the putative functional role of OA in osteoblast differentiation suggested by antisense oligonucleotides transfection, we next questioned whether osteoblast differentiation is altered when OA is over-expressed in MC3T3-E1 osteoblast cells. OA over-expression was achieved by transient transfection of MC3T3-E1 osteoblast cultures with a CMV-OA construct. MC3T3-E1 osteoblast like cells were used because of these advantages: First, it allows increased transfection efficiency compared to primary osteoblasts. Second, MC3T3-E1 follows the same pattern of primary osteoblast development and differentiation in culture.[17] Third, MC3T3-E1 expresses OA at much lower level than primary osteoblast (data not shown) and this reduces the background that might interfere with OA over-expression. Using a CMV- green fluorescent protein (GFP) control vector, we reproducibly obtained a maximal efficiency transfection of 30%, which resulted in a fourfold increase in OA levels observed by RT-PCR (Figure 5) and Western blot analyses (data not shown). In order to examine the role of OA in osteoblast proliferation, osteoblast cultures were transfected with CMV-OA or CMV- empty vector (E.V). Then, at day 5 of culture, MTT assay (Figure 6 - A) and cell number counting (Figure 6 - B) were performed. OA over-expression had no significant effect on osteoblast viability or proliferation (Figure 6).

The effect of OA over-expression on osteoblast differentiation markers during matrix maturation and matrix mineralization stages was examined and it was found that OA over-expression significantly induced ALP activity at day 14 (Figure 7 - A), calcium deposition (Figure 7 - B), nodule formation (Figure 7 - C, D, and E), osteocalcin (OC) production (Figure 7 - F), and OC gene expression (Figure 7 - G) at day 21.

OA over-expression also markedly induced Cbfa1 expression (Figure 8). Cbfa1 is a transcription factor that was found to be a "master" gene for the process of osteoblast differentiation and development.[18] Cbfa1 induces the expression of different genes that regulate osteoblast function, such as osteocalcin, osteonectin, and bone sialoprotein.[19] Cbfa1 expression starts early and increases with time in culture, reaching the maximum at the end of culture period.[20] Collectively, gain of OA expression markedly induced osteoblast differentiation markers and Cbfa1 expression in vitro.

DISCUSSION

In the present study, we examined loss and gain of OA expression and its functional role in osteoblast development in vitro. For this purpose, OA gene expression was manipulated using antisense oligonucleotides to down-regulate OA expression and CMV-OA construct to induce OA expression. OA expression was effectively modulated in osteoblast cultures (Figures 1 and 5). This approach was successfully used to examine the role of orphan nuclear estrogen receptor-related receptor alpha (αERR) in osteoblast differentiation and function.[21]

Examination of how OA affects osteoblast development would help in understanding its functional role. Osteoblast-related proteins can influence osteoblast development in different ways. TGF-β and 1alpha, 25-dihydroxyvitamin D3 affect osteoblast development mainly during the proliferation period.[22] Bone morphogenetic proteins mainly affect osteoblast differentiation.[23] Connective tissue growth factor affects both osteoblast proliferation and differentiation.[24] The effect of modulation of OA expression on osteoblast development was examined and was found that inhibition or induction of OA expression had no significant effect on osteoblast proliferation or viability (Figures 2 and 6, respectively). These data were supported by studies on human glioma cell lines showing that OA over-expression did not affect their proliferation or cell cycle phases.[25]

We further examined the role of OA during osteoblast differentiation stages, and found that loss of OA expression significantly inhibited osteoblast differentiation markers (Figures 3 and 4). On the other hand, gain of OA expression significantly induced osteoblast differentiation markers (Figures 7 and 8). These data suggest a critical role for OA in the process of osteoblast differentiation. These data were supported by previous in vivo findings showing that OA expression increased in the fracture repair model, with time following fracture reaching a maximum at 2 weeks postfracture.[7]

OA has high homology to proteins that regulates melanocyte differentiation and function such as Pmel-17 and murine nmb. Pmel 17 (a melanocyte specific gene) may function as a catalyst in melanin biosynthesis and take part in melanocyte differentiation.[5] Murine nmb also plays an important role in melanin biosynthesis and development of the retinal pigment epithelium .[4] Osteoblast and melanocytes have shared embryological origin. During early vertebrate development, neural crest cells emerge from the dorsal neural tube, migrate into the periphery, and form a wide range of derivatives. Crest cells from all axial levels form neurons, glia, and melanocytes; the cranial crest additionally generates skeletal derivatives such as bone and cartilage (ear and facial).[26] The shared developmental origin (neural crest) of melanocytes and osteoblast has implications at molecular and clinical levels. At molecular level, there is growing number of genes that found to regulate both

melanocyte and osteoblast functions. BMP2 [27] and TGF-β1 [28] (major regulators of osteoblast development in vivo and in vitro) were found to play a major role in melanocyte development. On the other hand, alpha melanocyte stimulating hormone (αMSH) (a major regulator of melanocyte development) was recently found to play an important role in regulation of osteoblast development. [29] At the clinical level, osteoporosis-pseudoglioma syndrome (OPPG) (a rare autosomal recessive disorder) is characterized by severe juvenile-onset osteoporosis and congenital or early-onset blindness due to retinal dysplasia. The gene responsible was recently identified to be the low density lipoprotein receptor-related family member LRP5. [30] LRP5 is expressed by osteoblasts in situ and play an important role in osteoblast development .[31] Pigmentary glaucoma syndrome also (a significant cause of human blindness) was linked to stop codon mutation in murine glycoprotein nmb (Gpnmb) [32] that has high homology (71%) with OA and has temporal pattern of expression in primary osteoblast cultures.[4] Collectively, these studies suggest that OA protein and its protein family might be involved in regulation of both osteoblast and melanocyte differentiation and functions.

OA also has high homology to proteins that regulate cell migration such as DC-HIL and human nmb. DC-HIL preferentially expressed by the dendritic cell line (XS52), might be involved in transendothelial migration of dendritic cells.[6] Human nmb is also implicated in regulation of migration of melanoma malignant cells.[3] Cell migration and matrix remodeling are key events in tissue repair and restructuring. In fracture repair process, osteoblasts are responsible for the production of new bone matrix during bone remodeling.[32] Interestingly, there are a number of osteoblast-related genes that are involved in osteoblast migration as well as differentiation, such as osteopontin,[33] periostin,[34] osteoblast-specific factor-1 ,[35] osteonectin,[36] bone morphogenetic protein 2 (BMP2),[37] and Cbfa1.[38] Recently, it was found that OA expression significantly induced human glioma cell migration in vitro and in vivo.[22] Previously mentioned studies suggest that OA might regulate osteoblast migration in addition to its role in osteoblast differentiation. These 2 roles are very essential during fracture repair, especially for fractures that are healing poorly.[39]

OA is expressed in osteoblast cells in vitro and in vivo[2] and appears to have a critical role in osteoblast differentiation in vitro. These findings indicate that OA may have an important function in the formation and turnover of the skeleton, but the mechanism by which it does so (ie, through affecting osteoblast migration and chemotaxis) remains to be established.

The identification of novel anabolic agents in bone, and perhaps even more important, gaining insights into their mechanisms of action, are subjects of intense clinical interest. Various diseases or conditions cause either localized or systemic bone loss, including various forms of osteoporosis, certain malignancies, and inflammation.[40] Osteoporosis is a systemic disorder characterized by a gradual reduction in bone mass (osteopenia) to a point where the skeleton is compromised, which leads to bone fragility and increased susceptibility to fractures of the hip, spine, and wrist.[41] In the United States it is estimated that $10 billion to $15 billion are spent annually for the treatment of osteoporotic fractures. Identification of factors that have potential therapeutic application would have a beneficial effect, either locally (as in fracture repair or localized osteopenia) or systemically (as in generalized osteoporosis). In conclusion, OA plays a critical role in osteoblast differentiation in vitro, and characterization of that role in osteoblast development represents a step in that direction.

REFERENCES

1. Marks SC Jr and Popoff SN. (1989) *Am J Anat.* **86**:325-334.

2. Safadi FF, Xu J, Smock SL, Rico MC, Owen TA, Popoff SN. (2001) *J Cell Biochem.* **84**:12-26.

3. Weterman MA, Ajubi N, van Dinter IM, Degen WG, van Muijen GN, Ruitter DJ, and Bloemers HP (1995) *Int J Cancer.* **60**:73-81.

4. Bachner D, Schroder D, Gross G. (2002) *Brain Res Gene Expr Patterns.* **October;1(3-4):**159-165.

5. Kwon BS, Kim KK, Halaban R, Pickard RT. (1994) *Pigment Cell Res.* **7**:394-397.

6. Shikano S, Bonkobara M, Zukas PK, Ariizumi K. (2001) *J Biol Chem.* **276**:8125-8134.

7. Hadjiargyrou M, Lombardo F, Zhao S, Ahrens W, Joo J, Ahn H, Jurman M, White DW and Rubin CT. (2002) *J Biol Chem.* **277**:30177-30182.

8. Ducy P, Karsentry G. (1995) *Mol Cell Biol.* **15**:1858-1869.

9. Lian JB, Stein GS. (1995) *Iowa Orthop J.* **15**:118-140.

10. Owen TA, Aronow M, Shalhoub V, Barone LM, Wilming L, Tassinari MS, Kennedy MB, Pockwinse S, Lian JB and Stein GS (1990) *J Cell Physiol.* **143**:420-430.

11. Toulme JJ, Verspieren P, Boiziau C, Loreau N, Cazenave C, Thuong NT. (1990) *Ann Parasitol Hum Comp.* **1(suppl)**:11-14.

12. Topp WC. (1981) *Virology.* **113**:408-411.

13. Alley MC, Scudiero DA, Monks A, Hursey ML, Czerwinski MJ, Fine DL, Abbott BJ, Mayo JG, Shoemaker RH and Boyd MR. (1988) *Cancer Res.* **48(3)**:589-601.

14. Aubin JE, Liu F, Malaval L, Gupta AK. (1995) *Bone.* **August;17(suppl 2)**:77S-83S.

15. Lian JB, Stein GS, Bortell R, Owen TA . (1991) *J Cell Biochem.* **45(1)**:9-14.

16. Stein GS, Lian JB, Owen TA. (1990) *FASEB J.* **4(13)**:3111-3123.

17. Choi JY, Lee BH, Song KB, Park RW, Kim IS, Sohn KY, Jo JS and Ryoo HM. (1996) *J Cell Biochem.* **61**:609-618.

18. Karsenty G. (2000) *Semin Cell Dev Biol.* **11**:343-346.

19. Ducy P. (2000) *Dev Dyn.* **219(4)**:461-471.

20. Banerjee C, Hiebert SW, Stein JL, Lian JB, Stein GS. (1996) *Proc Natl Sci USA.* **93**:4968-4973

21. Bonnelye E, Merdad L, Kung V, Aubin JE. (2001) *J Cell Biol.* **53**:971-984.

22. Gurlek A, Kumar R. (2001) *Crit Rev Eukaryot Gene Expr.* **11(4)**:299-317.

23. Hay E, Hott M, Graulet AM, Lomri A, Marie PJ. (1999) *J Cell Biochem.* **72(1)**:81-93.

24. Nishida T, Nakanishi T, Asano M, Shimo T, Takigawa M. (2000) *J Cell Physiol.* **184(2)**:197-206.

25 Rich JN, Shi Q, Hjelmeland MD, Cummings TJ, Kuan CT, Bigner DD, Counter CM, Wang XF. (2003) *J Biol Chem.* **278(18)**:15951-15957. Epub 2003 Feb 17.

26. McGonnell IM, Graham A. (2002) *Curr Biol.* **12(9)**:767-71

27. Martinez-Esparza M, Solano F, Garcia-Borron JC. (1999) *Cell Mol Biol (Noisy-le-grand).* **45(7)**:991-1000.

28. Kanzler B, Foreman RK, Labosky PA, Mallo M. (2000) *Development.* **127(5)**:1095-104.

29. Lim SK, Li SZ, Rhee Y, Chung SS, Jin YJ, Yook JI. (2002) *Yonsei Med J.* **43(4)**:500-10.

30. Lev D, Binson I, Foldes AJ, Watemberg N, Lerman-Sagie T. (2003) *Isr Med Assoc J.* **5(6)**:419-21.

31. Gong Y, Slee RB, Fukai N, Rawadi G, Roman-Roman S, Reginato AM, Wang H, Cundy T, Glorieux FH, Lev D, Zacharin M, Oexle K, Marcelino J, Suwairi W, Heeger S, Sabatakos G, Apte S, Adkins WN,

Allgrove J, Arslan-Kirchner M, Batch JA, Beighton P, Black GC, Boles RG, Boon LM, Borrone C, Brunner HG, Carle GF, Dallapiccola B, De Paepe A, Floege B, Halfhide ML, Hall B, Hennekam RC, Hirose T, Jans A, Juppner H, Kim CA, Keppler-Noreuil K, Kohlschuetter A, LaCombe D, Lambert M, Lemyre E, Letteboer T, Peltonen L, Ramesar RS, Romanengo M, Somer H, Steichen-Gersdorf E, Steinmann B, Sullivan B, Superti-Furga A, Swoboda W, van den Boogaard MJ, Van Hul W, Vikkula M, Votruba M, Zabel B, Garcia T, Baron R, Olsen BR, Warman ML; Osteoporosis-Pseudoglioma Syndrome Collaborative Group. (2001) *Cell.* **107(4)**:513-23.

32. Liu X, Kohyama T, Kobayashi T, Abe S, Kim HJ, Reed EC, Rennard SI. (2003) *Osteoporos Int.* **14(3)**:235-242. Epub 2003 Apr 10.

33. Zohar R, Cheifetz S, McCulloch CA, Sodek J. (1998) *Eur J Oral Sci.* **106 (suppl 1)**:401-407.

34. Gillan L, Matei D, Fishman DA, Gerbin CS, Karlan BY, Chang DD. (2002) *Cancer Res.* **62(18)**:5358-5364.

35. Yang X, Tare RS, Partridge KA, Roach HI, Clarke NM, Howdle SM, Shakesheff KM, Oreffo RO. (2003) *J Bone Miner Res.* **18(1)**:47-57.

36. Sodek J, Zhu B, Huynh MH, Brown TJ, Ringuette M. (2002) *Connect Tissue Res.* **43(2-3)**:308-319.

37. Kawaguchi J, Kii I, Sugiyama Y, Takeshita S, Kudo A. (2001) *J Bone Miner Res.* **16(2)**:260-269.

38. Sun L, Vitolo M, Passaniti A. (2001) *Cancer Res.* **61(13)**:4994-5001.

39. Steinbrech DS, Mehrara BJ, Rowe NM, Dudziak ME, Luchs JS, Saadeh PB, Gittes GK, Longaker MT. (2000) *Plast Reconstr Surg.* **105(6)**:2028-2038.

40. Cushenberry LM and de Bittner MR. (2002) *Ann Pharmacother.* **36**:671-678.

41. NIH consensus development panel on osteoporosis prevention, 2001.

Figure Legends

Figure 1. Inhibition of OA expression in primary osteoblast culture by OA antisense oligonucleotides. (A) Seven different OA antisense oligonucleotides were tested for their ability to block constitutive OA mRNA expression in the RAT-2 cell line. Different OA antisense oligonucleotides were transfected into RAT-2 cells (lanes 1-7), followed by RT-PCR, using OA specific primers. Controls included cells treated with the transfection reagent only or cells transfected with scrambled oligonucleotides (mock). OA cDNA was used as a template for PCR positive control. 18S was used as an internal PCR control. No template indicates no cDNA was added and used as a negative control. (B) Densitometric analysis for RT-PCR in (A), ratio was expressed as percent of maximum expression. (C) Primary osteoblast cultures were transfected with 0.5 μM of sense or OA antisense-1 (OA-AS1) oligonucleotides and RT-PCR for OA was performed at day 21 of the culture. 18S was used as an internal PCR control. M= ladder. (D) Densitometric analysis of RT-PCR gel represents the ratio of OA over 18S expression. (E) Western blot analysis of OA in primary osteoblast cultures transfected with 0.05 μM of sense or OA-AS oligos. Anti-OA antibody detected 2 protein bands corresponding to non-glycosylated OA protein (~65 kDa) and glycosylated OA (~95 kDa). Equal loading of proteins across lanes was verified by reprobing the blot for β-tubulin. (F) Densitometric analysis for Western blot in (E).

Suggested location: close to results in page 10

Figure 2. OA-AS oligos had no effect on osteoblast proliferation or viability. Primary osteoblasts were either not transfected or transfected with 0.5 μM of sense or OA-AS oligos. At day 5 of the culture, MTT (A) and cell counting (B) assays were performed. Results are expressed as a percent of control, where cells not treated (No Tx) are 100 %.

Suggested location: close to results in page 11

Figure 3. OA-AS oligos decreased ALP activity and production. Primary osteoblast cultures were either not transfected or transfected with 0.5 μm of sense or OA-AS oligos, then ALP activity was measured at day 14, as shown in (A). Parallel cultures transfected with sense (B) or OA-AS oligos (C) were histochemically stained for ALP. Data in (A) were presented as a percent of control where not treated culture (No Tx) is 100%. ** represents $P < 0.01$ when OA-AS oligos treated culture compared to either No Tx or sense treated cultures. In (B) and (C) pictures were taken using a *Nikon* inverted microscope at 40x magnification. Insets showing scanned images for stained wells

Suggested location: close to results in page 11

Figure 4. OA-AS oligos reduced nodule formation, calcium deposition, and osteocalcin production at day 21. Primary osteoblasts were either not transfected or transfected with 0.5 μM of sense or OA-AS oligos. At day 21 of the culture, nodule formation was evaluated by alizarin red staining: (A) Primary cultures transfected with sense, (B) cultures transfected with OA-AS oligos and (C) size of stained mineralized nodules. In a parallel culture, calcium deposition (D) and osteocalcin production (E) were measured. In (A) and (B), pictures were taken using a *Nikon* inverted microscope at 100x magnification. In (C), (D) and (E) data were presented as a percent of control where cells not treated (No Tx) is 100%. *represents $P < 0.05$ when OA-AS oligos treated cultures compared to either No Tx or sense treated cultures.

Suggested location: close to results in page 11

Figure 5. OA over-expression in MC3T3-E1 osteoblast culture. MC3T3-E1 osteoblast cultures were transfected with CMV-green fluorescent protein (GFP) or CMV-OA then RT-PCR for OA was performed, as shown in (A). (B) Densitometric analysis of RT-PCR represents the ratio of OA over 18S expression. 18S was used as PCR internal control. M = 100bp ladder.

Suggested location: close to results in page 12

Figure 6. OA over-expression had no effect on osteoblast proliferation or viability. MC3T3-E1 osteoblasts like cells were either not transfected or transfected with CMV-empty vector (E.V) or CMV-OA. At day 5 of the culture, MTT (A) and cell number counting (B) assays were performed. Results are expressed as a percent of control where cells not treated (No Tx) are 100 %.

Suggested location: close to results in page 12

Figure 7. OA over-expression induced osteoblast differentiation markers. MC3T3-E1 osteoblast cultures were either not transfected or transfected with CMV-empty vector (EV) or CMV-OA, then cultures were terminated at 14 or 21 days for assessment of differentiation markers. (A) ALP activity measured at day 14. At day 21 of culture, calcium deposition (B), nodule formation evaluated by von Kossa staining for cultures transfected with CMV-EV (C) or CMV-OA (D), size of mineralized nodules (E), osteocalcin production (F) and RT-PCR for osteocalcin gene expression (G) were examined. In (A), (B), (E) and (F), data were presented as a percent of control where cells not treated (No Tx) or cells treated with CMV-EV are 100%. * represents $P < 0.05$ and ** represents $P < 0.01$ when CMV-OA transfected culture compared to not transfected or CMV-EV transfected cultures. In (C) and (D), pictures were taken using a *Nikon* inverted microscope at 40x magnification. In (G), RT-PCR for 18S was used as PCR internal control.

Suggested location: close to results in page 12

Figure 8. Cbfa1 expression induced by OA over-expression in MC3T3-E1 osteoblast culture. MC3T3-E1 osteoblasts were transfected with CMV-EV or CMV-OA. (A) RT-PCR for Cbfa1 gene expression at day 14. (B) Densitometric analysis of RT-PCR in (A). G3PDH was used as PCR internal control.

Suggested location: close to results in page 12.

FIGURE#1

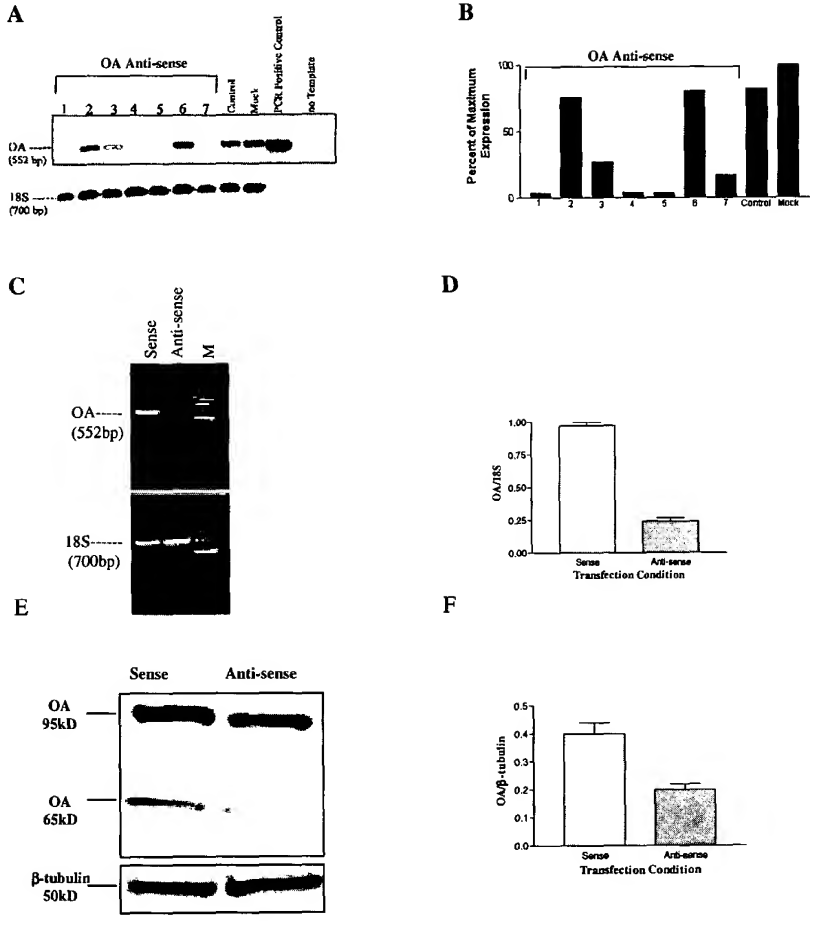

FIGURE#2

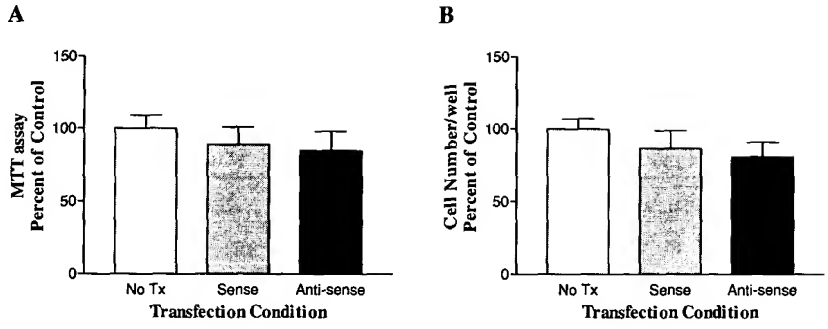

FIGURE#3

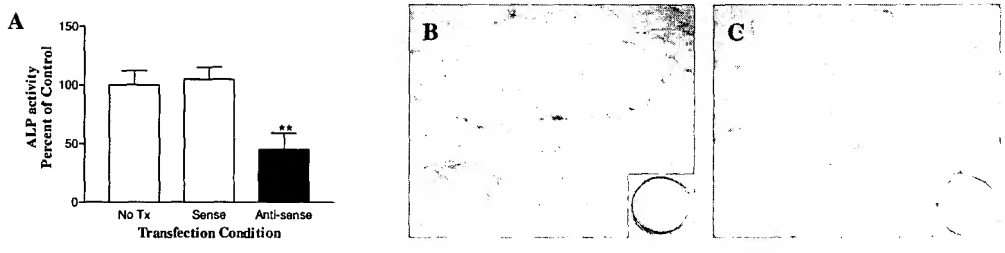

FIGURE#4

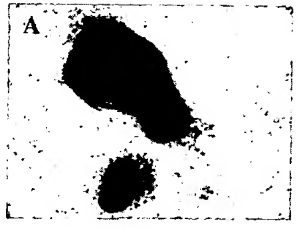

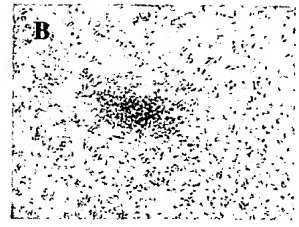

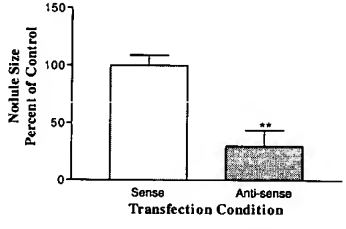

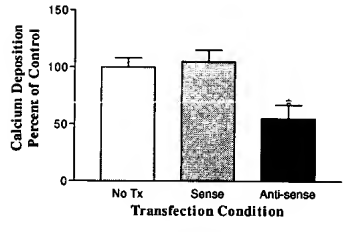

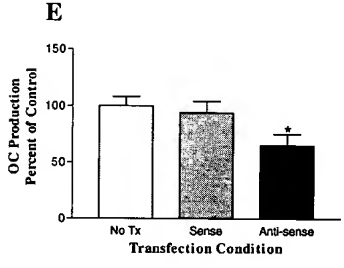

FIGURE#5

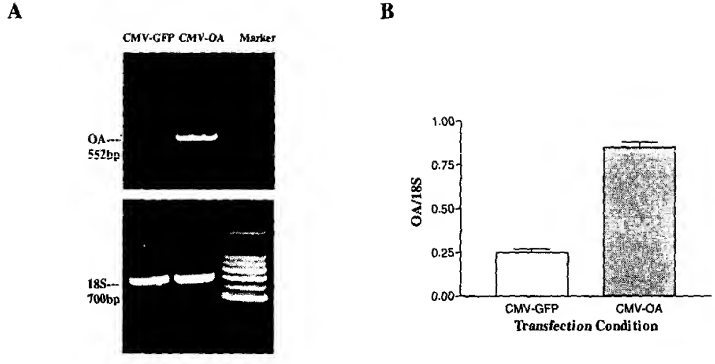

FIGURE#6

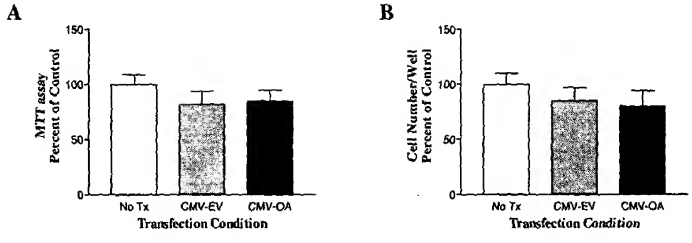

FIGURE#7

Osteoactivin in osteoblasts

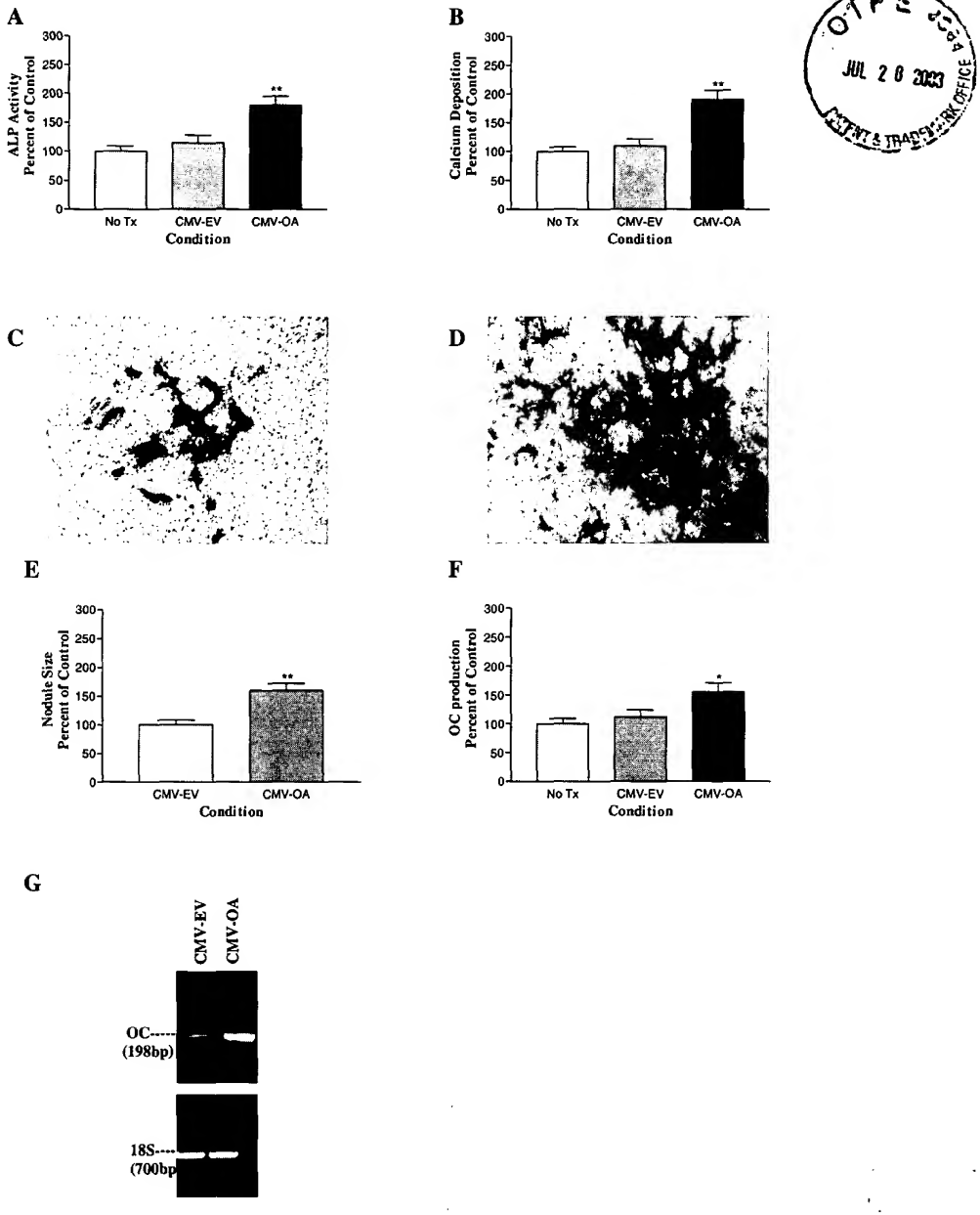

FIGURE#8

A

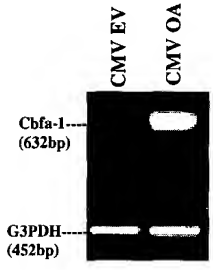

B

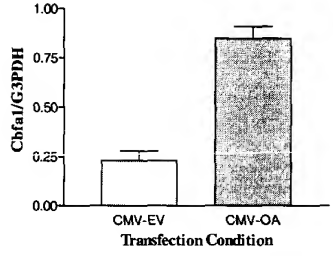

APPENDIX B

Declaration under 37 C.F.R. § 1.132 by Dr. Steven N. Popoff

PATENTS
U.S.S.N. 09/943,075
Attorney Docket No. PFI-015/71369.262

IN THE UNITED STATES PATENT AND TRADEMARK OFFICE

Applicant:	Steven N. Popoff *et al.*	Art Unit:	1632
Serial No.:	09/943,075	Examiner:	Scott D. Priebe
Filing Date:	August 30, 2001	Conf. No.	7695
Title:	**Osteoactivin Protein and Nucleic Acids Encoding the Same, Compositions and Methods of Stimulating Bone Differentiation**		

CERTIFICATION UNDER 37 C.F.R. § 1.8(a)

I hereby certify that this correspondence is being deposited with the United States Postal Service as first class mail in an envelope addressed to Mail Stop Non-Fee Amendment, Commissioner for Patents, P.O. Box 1450, Alexandria VA 22313-1450 on the date shown below.

Date of mail deposit

Sharon R. Matthews

Mail Stop Non-Fee Amendment,
Commissioner for Patents
P.O. Box 1450
Alexandria, VA 22313-1450

DECLARATION UNDER 37 C.F.R. § 1.132
(In Re Katz Declaration)

Dear Sir:

I, Steven N. Popoff, Ph.D., declare the following:

1. I am an applicant of the above-identified patent application (hereinafter "Application") and a co-inventor of the subject matter described and claimed therein. Specifically, I am the co-inventor, with Fayez F. Safadi, Thomas A. Owen and Steven L. Smock of the subject matter described and claimed in this Application for the claims drawn to rat nucleic acid molecules encoding osteoactivin, means of their expression and methods of their use.

2. I have reviewed the claims pending in the Application as of April 25, 2003, as well as those being proposed for Amendment in response to the Office Action mailed April 25, 2003.

3. I am also one of eight co-authors of the GenBank® submission containing the nucleic acid and amino acid sequences listed in GenBank® Accession No. AF184983, dated October 21, 1999. The other authors of this submission include Xu, J., Safadi, F. F., Smock, S.L., Rosenzweig, A.B., Odgren, P.R., Marks, S.C., Jr., and Owen, T.A.

4. The nucleic acid and protein sequences described in GenBank® Accession No. AF184983, dated October 21, 1999, cited by the Examiner against this Application, describes our own work.

5. Fayez F. Safadi, Thomas A. Owen, Steven L. Smock and I conceived of the work resulting in the sequences listed at GenBank® Accession No. AF184983.

6. Xu, J., Rosenzweig, A.B., Marks, S.C. Jr. and Odgren, P.R. were not named as co-inventors on the Application because they did not conceive of the claimed invention but were involved in this project after its conception in non-inventive capacities. Xu, J., Rosenzweig, A.B., Marks, S.C. Jr. and Odgren, P.R. were named as co-authors on the GenBank® submission for their contribution to this project after it had been conceived by us. Specifically, Xu, J. was a graduate student and Rosenzweig, A. B. was a technician in my laboratory; both worked on this project under my supervision and direction. Marks, S.C., Jr. and Odgren, P.R. were consultants who helped in some of the follow-up studies to characterize the over-expression of osteoactivin in osteopetrotic bone. None of them took part in the inventive process.

I further declare that all statements made herein of my own knowledge are true and that all statements made on information and belief are believed to be true; and further that the statements were made with the knowledge that willful false statements and the like so made are punishable by fine or imprisonment, or both, under Section 1001 of Title 18 of the United States Code and that such willful false statements may jeopardize the validity of the application or any patent issuing thereon.

7/24/03

Date

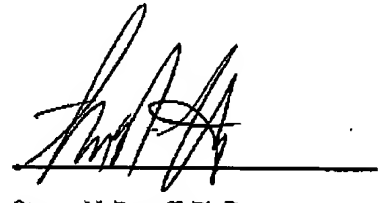

Steven N. Popoff, Ph.D.

APPENDIX C

The references cited on page 9, last paragraph namely:

1. Blaese, R.M. et al. *Science* **270**:475-480, 1995;
2. Bordignon, C. et al. *Science* **270**:470-475, 1995
3. Onodera et al. *Blood* **91**:30-36, 1996; and
4. Grossman, M. et al. *Nat.Genet.* **6**:335-341, 1994
5. Lee, J. Y. et al. *Hum. Gene Ther.* **13**:1201-1211, 2002

are attached for the Examiner's perusal.

becco's minimum essential medium (DMEM) in the presence of polybrene (8 μg/ml) as described (18). Cells were washed twice in phosphate-buffered saline (PBS), resuspended in fresh medium, and cultured for 3 to 4 days. Transduced cells were tested for the presence of helper virus and cryopreserved until use.
36. BM mononuclear cells were obtained as a Ficoll fraction and grown for 2 to 3 days in complete DMEM at a density of 6×10^5 to 8×10^5 cells/cm^2 (35). T cell depletion and progenitor cell enrichment were obtained as described (3, 35). Gene transfer was carried out by multiple infection cycles with cell-free, helper virus–tested viral supernatants in the presence of polybrene (8 μg/ml) (35). BM cells were maintained in a long-term culture system over adherent layers without addition of exogenous growth factors, and infected during the first 3 days of culture. Transduced cells were tested for the presence of helper virus and cryopreserved until use. At that time, the transduced cells were washed, resuspended in normal saline containing 4% human albumin, and reinfused into the patient.
37. C. Bordignon *et al.*, *Proc. Natl. Acad. Sci. U.S.A.* 86, 6748 (1989).
38. PHA blasts or antigen-specific T cells were cloned by limiting dilution. The relative frequencies of transduced cells was obtained by comparing the precursor frequency in the absence and presence of G418 (800 μg/ml). G418-resistant T cell clones were isolated and maintained as described (44, 45).
39. The relative frequencies of transduced BM progenitor cells were obtained by comparing the frequency of CFU-G, CFU-GM, BFU-E, and CFU-GEMM cells in the absence and presence of increasing doses of G418 (0.7, 1.0, 1.5 mg/ml) as described (37). In selected experiments, individual G418-resistant colonies were collected for analysis of vector transduction and expression.
40. M. J. Barnett *et al.*, *Blood* 84, 724 (1994).
41. C. Bordignon *et al.*, data not shown.
42. J. Sambrook, E. F. Fritsch, T. Maniatis, *Molecular Cloning: A Laboratory Manual* (Cold Spring Harbor Laboratory, Cold Spring Harbor, NY, ed. 2, 1989).
43. P. J. Southern and P. Berg, *J. Mol. Appl. Genet.* 1, 327 (1982).
44. A. Lanzavecchia, *Nature* 314, 537 (1985).
45. P. Panina-Bordignon *et al.*, *Eur. J. Immunol.* 19, 2237 (1989).
46. Y. Choi *et al.*, *Proc. Natl. Acad. Sci. U.S.A.* 86, 8941 (1989).
47. E. Y. Loh, J. F. Elliot, S. Cwirla, L. L. Lanier, M. M. Davis, *Science* 243, 217 (1989).
48. T cell receptor V_β-chain usage was analyzed on transduced T cell lines by reverse transcriptase–PCR. Briefly, total RNA was reverse transcribed with oligo(dT) and oligo(dG) primers and subjected to PCR with V_α- or C_β-specific oligonucleotides (46) or to anchored PCR with a C_β-specific oligonucleotide as described (47). Amplified products were analyzed by agarose gel electrophoresis.
49. We are indebted to L. Ruggieri and A. Wack for performing some of the ex vivo and in vitro analyses of gene transfer frequency; to the nurses and clinical staff of the Clinica Pediatrica, School of Medicine, University of Brescia, for skilled and dedicated care; to A. Arrighini and A. Crescenzo for clinical assistance in the extended care of the two patients; to A. Plebani for dosing specific antibody production; to M. Hershfield, P. Dallabona, and A. Ballabio for helpful discussions; and to Enzon, Inc., and Ophan Europe for providing PEG-ADA before commercial distribution. Supported by grants from Telethon, the Italian National Research Council, and the Italian Ministry of Health (IV-VII AIDS Projects).

26 May 1995; accepted 27 September 1995

T Lymphocyte–Directed Gene Therapy for ADA$^-$ SCID: Initial Trial Results After 4 Years

R. Michael Blaese,* Kenneth W. Culver, A. Dusty Miller, Charles S. Carter, Thomas Fleisher, Mario Clerici,† Gene Shearer, Lauren Chang, Yawen Chiang, Paul Tolstoshev, Jay J. Greenblatt, Steven A. Rosenberg, Harvey Klein, Melvin Berger, Craig A. Mullen,‡ W. Jay Ramsey, Linda Muul, Richard A. Morgan, W. French Anderson§

In 1990, a clinical trial was started using retroviral-mediated transfer of the adenosine deaminase (ADA) gene into the T cells of two children with severe combined immunodeficiency (ADA$^-$ SCID). The number of blood T cells normalized as did many cellular and humoral immune responses. Gene treatment ended after 2 years, but integrated vector and ADA gene expression in T cells persisted. Although many components remain to be perfected, it is concluded here that gene therapy can be a safe and effective addition to treatment for some patients with this severe immunodeficiency disease.

The possibility of using gene transfer as a therapy for human disease has great appeal. The decision to enter clinical trials awaited the development of safe and efficient techniques of gene transfer and improved understanding of the basic pathology and biology underlying likely candidate diseases and target cells. The advent of useful retroviral vectors that permitted relatively high efficiency gene transfer and stable integration was a critical advance (*1*, *2*), as was the demonstration that this procedure of gene transfer could be effectively and safely used in humans (*3*).

Severe combined immunodeficiency secondary to a genetic defect in the purine catabolic enzyme adenosine deaminase [ADA$^-$ SCID] is characterized by defective T and B cell function and recurrent infections, often involving opportunistic pathogens. Large amounts of deoxyadenosine, an ADA substrate, are present in these patients; deoxyadenosine is preferentially converted to the toxic compound deoxyadenosine triphosphate in T cells, disabling the immune system (*4*).

Because this disease is curable by allogeneic bone marrow transplantation given without pretransplantation cytoreductive conditioning, it was initially assumed that gene therapy should be directed at the bone marrow stem cell. However, initial attempts to use stem cell gene transfer in primates resulted in only low-level, transient gene expression, insufficient for clinical use. The observation that the only donor cells detected in some patients "cured" by allogeneic bone marrow transplantation was their T cells—the others remaining ADA-deficient (*5*)—raised the possibility that T cell–directed gene therapy also might be a useful treatment.

The introduction of enzyme replacement with ADA-containing erythrocytes (*6*) or with bovine ADA conjugated with polyethylene glycol (PEG-ADA) (*7*) has made this approach feasible. PEG-ADA has provided noncurative, life-saving treatment for ADA$^-$ SCID patients; with this treatment, most patients have experienced weight gain and decreased opportunistic infections. Full immune reconstitution has been less regularly achieved with enzyme therapy. T cell function as measured by in vitro mitogen responses improved in most patients, but fewer patients recovered consistent immune responses to specific antigens [for instance, as measured by normal delayed-type hypersensitivity (DTH) skin test reactivity] (*8*–*10*). Nearly all PEG-ADA–treated patients showed increased peripheral T cell counts, which provided a source of T cells for gene correction not available without enzyme therapy. Furthermore, enzyme treatment could be continued during the gene therapy trial so that the ethical dilemma of withholding or stopping a life-saving therapy to test an unknown treatment could be avoided.

The adenosine deaminase complementary DNA (cDNA) (*11*) is 1.5 kb and fits within a retroviral vector. With the use of an ADA-containing retroviral vector, ADA-deficient T cell lines were transduced to express normal amounts of ADA; this rendered them normally resistant to intoxication and growth inhibition when challenged with deoxyadenosine (*12*, *13*). Next, studies in mice, rabbits, and nonhuman primates using T cells modified with retroviral vectors showed normal cell survival and function after their reintroduction into recipient animals (*14*). Finally, Bordignon and colleagues (*15*) showed that ADA gene–corrected T cells acquired a survival advantage compared with uncorrected ADA-deficient cells when transplanted into immunodeficient, but ADA-

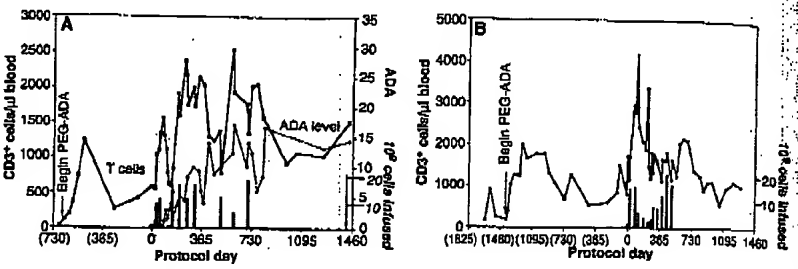

Fig. 1. Peripheral blood T cell counts since the time the diagnosis of ADA deficiency was made, dates of treatments, and the total number of cells infused for each patient. ADA level is measured in nanomoles of adenosine deaminated per minute per 10^9 cells. Vertical bars indicate the dates of cell infusion, and their height represents the total number of nonselected cells infused at each treatment. The T cell numbers represent total CD3-bearing T cells determined by standard flow cytometric analysis. (**A**) Patient 1 began gene therapy on 14 September 1990 (protocol day 0) and received a total of 11 infusions. Cellular ADA enzyme level is indicated by the dashed line. ADA activity was determined as described (*13*, *25*). Values shown are the mean of duplicate samples and represent EHNA-sensitive ADA enzyme activity. (**B**) Patient 2 began gene therapy on 31 January 1991 (protocol day 0) and received of a total of 12 infusions.

normal BNX recipient mice.

The clinical protocol used here has been described elsewhere (*16*). Patients with documented ADA$^-$ SCID were eligible if they did not have a human lymphocyte antigen–matched sibling as a potential donor for marrow transplantation and if they had been treated with PEG-ADA for at least 9 months without full immune reconstitution. T cells were obtained from their blood by apheresis, induced to proliferate in culture, transduced with the ADA retroviral vector LASN, culture-expanded, and then reinfused into the patient after 9 to 12 days (*17*). No selection procedure was used to enrich for gene-transduced cells.

The clinical histories and ADA gene mutations of each patient have been reported (*18*, *19*). Patient 1 presented with infection at 2 days of age and had recurrent infections and very poor growth until 26 months of age, when the diagnosis of ADA deficiency was established and she was started on PEG-ADA [30 U per kilogram of body weight per week (30 U/kg/week)]. Treatment with PEG-ADA enzyme for approximately 2 years had resulted in significant, but incomplete, benefit. With PEG-ADA she gained weight, had fewer infections, and transiently developed a normal peripheral blood T cell count (Fig. 1A), and her T cells had acquired the ability to respond to mitogens in vitro. However, significant immune deficiency persisted, including recurrence of her T lymphopenia (Fig. 1A), DTH skin test anergy (Table 1), depressed in vitro immune reactivity to specific antigens such as tetanus toxoid, failure to generate normal cytotoxic T cells to viral antigens or allogeneic cells, defective immunoglobulin production and absent or weak antibody responses to several vaccine antigens, and borderline isohemagglutinin titers (Table 1). At 4 years of age, she was enrolled in this trial.

The course of disease in patient 2 (who was 9 years old when enrolled in the trial) was milder than that seen in classic SCID (*19*). She had her first serious infection at age 3, and septic arthritis at age 5; the diagnosis was finally established at age 6 when significant lymphopenia with ADA deficiency was confirmed. This patient had an excellent initial improvement in peripheral T cell numbers after the start of PEG-ADA therapy (30 U/kg/week) at age 5, but lymphopenia recurred in the third and fourth years of enzyme treatment (Fig. 1B). During the year before gene therapy, repeated evaluation of her immune system showed persisting immunodeficiency, but less severe than that in patient 1. Despite 4 years of enzyme treatment, DTH skin test reactivity was absent (Table 1), cytotoxic T cells to viral antigens and allogeneic cells were deficient, and isohemagglutinins were barely detectable. However, illustrating the variability seen in the responses of patient 2 over time, blood lymphocytes that were cryopreserved from the day the clinical trial began and tested later showed normal cytotoxic activity to allogeneic cells.

Within 5 to 6 months of beginning gene therapy, the peripheral blood T cell counts for patient 1 (Fig. 1A) rapidly increased in number and stabilized in the normal range and have remained normal since that time (*20*). ADA enzyme activity, nearly undetectable in her blood lymphocytes initially, progressively increased in concentration during the first 2 years of treatment to reach a level roughly half the concentration found in heterozygous carriers (expressing only one intact ADA allele) and has re-

Table 1. DTH skin test reactivity and isohemagglutinin titers in sera of each patient at various times during the treatment protocol. Skin tests were applied as Multitest (Pasteur Merieux, Lyon, France) and scored according to the manufacturer's instructions 48 to 72 hours after being placed. Seven antigens were placed on the dates indicated, although only five were technically satisfactory on day 1252 for patient 1 and on day 1118 for patient 2. Isohemagglutinin titers were determined by standard blood bank techniques (*34*). Ninety five percent of normal children over the age of 2 years will have a titer of ≥1:16 and 82% will have a titer ≥1:32 (*35*). ND, not done. For the DTH skin tests, positive tests were elicited; T, tetanus toxoid; D, diphtheria toxoid; C, *Candida albicans*; P, Proteus antigen; S, streptococcal antigen; OT, old tuberculin.

Protocol day	Isohemagglutinins	DTH skin tests
	Patient 1	
−9	16	None (0/7)
115	256	ND
251	128	ND
314	32	T, D, C
455	32	T, D, C, S, P
510	64	ND
707	32	ND
1252	ND	*D*, C, P
	Patient 2	
−122	4	None (0/7)
−9	4	ND
90	256	ND
186	128	ND
291	128	ND
501	128	T, D, C, S, OT
676	64	ND
957	16	ND
1118	ND	T, D, S, P

R. M. Blaese, C. A. Mullen, W. J. Ramsey, National Center for Human Genome Research, National Institutes of Health (NIH), Building 49, Room 2A03, Bethesda, MD 20892, USA, and National Cancer Institute (NCI), NIH, Bethesda, MD 20892, USA.
K. W. Culver, M. Clarici, G. Shearer, J. J. Greenblatt, S. A. Rosenberg, NCI, NIH, Bethesda, MD 20892, USA.
A. D. Miller, Fred Hutchinson Cancer Research Center, Seattle, WA 98104, USA.
C. S. Carter, T. Fleisher, H. Klein, Clinical Center, NIH, Bethesda, MD 20892, USA.
L. Chiang and W. F. Anderson, National Heart, Lung, and Blood Institute (NHLBI), NIH, Bethesda, MD 20892, USA.
Y. Chiang and P. Tolstoshev, Genetic Therapy, Gaithersburg, MD 20878, USA.
M. Berger, Department of Pediatrics, Case Western Reserve University School of Medicine, Cleveland, OH 44106, USA.
L. Muul, National Center for Human Genome Research, NIH, Bethesda, MD 20892, USA.
R. A. Morgan, National Center for Human Genome Research, NIH, Bethesda, MD 20892, USA, and NHLBI, NIH, Bethesda, MD 20892, USA.

*To whom correspondence should be addressed at the National Center for Human Genome Research. E-mail: mblaese@nchgr.nih.gov
†Present address: Cattedra Di Immunogia, Universita Milano, Milan 20133, Italy.
‡Present address: Division of Pediatrics, M. D. Anderson Cancer Center, Houston, TX 77030, USA.
§Present address: Norris Cancer Center, University of Southern California School of Medicine, Los Angeles, CA 90033, USA.

mained at that level since (Fig. 1A). Thus, both the reconstituted number of peripheral blood T cells and the elevated T cell ADA enzyme concentration have persisted since the patient's last treatment, indicating that peripheral T cells can have an unexpectedly long life-span and that gene expression from the retroviral vector has not been silenced over this period.

Patient 2, who had variable immune reactivity before enrollment, responded to the institution of lymphocyte infusions, with her peripheral T cell count rapidly increasing to levels in the high normal range (Fig 1B). Beginning with infusion 5, which included protocol modifications to partially deplete CD8 cells from the initially cultured cell population (*21*), her T cell count fell into the mid-normal range, where it persisted throughout the treatment period and for a year after the last cell infusion. In contrast to those in patient 1, ADA enzyme levels in the circulating T cells of patient 2 did not rise significantly above the small amounts seen before gene therapy treatment (~1.5 nmol/10^8 cells per minute).

The differences in final lymphocyte ADA concentration are consistent with the levels of gene transfer reached in these patients. For several months in the second protocol year during which cell infusions were not given, LASN vector sequences detected by polymerase chain reaction (PCR) maintained a stable frequency in the peripheral blood of patient 1 at a level greater than the PCR-positive control standard containing the equivalent of 0.3 vector copies/cell (Fig. 2). By contrast, although vector-containing cells were also stably detected throughout a similar period in patient 2, their level reached only a value equivalent to 0.1 to 1.0% of her circulating cells carrying the inserted ADA vector.

The principal contributor to the difference in the final frequency of LASN vector–modified T cells in patients 1 and 2 was the low gene transfer efficiency in the cells of patient 2; this was consistently only a tenth or less of what was routinely achieved in the cells from patient 1. Despite the gross differences in the final proportion of vector-containing cells reached in these two patients, both CD4 and CD8 T cell populations from each have remained consistently positive for integrated vector sequences since the first infusion through protocol day 1480 for patient 1 and through protocol day 1198 for patient 2 (Fig. 2).

To more accurately measure the proportion of vector-containing cells in patient 1, we performed quantitative Southern (DNA) hybridization analysis for vector sequence on DNA isolated from her peripheral blood T cells at different days during the course of this protocol. On protocol days 816 and 1252, which represent samples taken 109 and 545 days after the last treatment, the vector concentration was at the level of approximately one vector copy per cell (Fig. 3). Longitudinal studies of samples obtained throughout the study show that this large amount of integrated vector was reached by infusion 8 (D707) and that it has remained in this range since that time (*22*).

The use of a restriction endonuclease that cuts only once within the vector sequence does not give detectable bands (Fig. 3), indicating that the population of blood T cells at these dates is not oligoclonal with respect to integrated vector. Vector-derived mRNA was readily detected by reverse transcription (RT)–PCR at these same times (Fig. 3), confirming that vector expression persisted and was correlated with the presence of ADA enzyme activity in her circulating T cells.

To evaluate the effect of gene therapy on the immune function of these two patients in addition to its beneficial effect on T cell numbers, we performed a panel of immunologic studies both before, and at various times after, treatment. DTH skin test reactivity to common environmental and vaccine antigens tests the overall competence of the cellular immune system because a response depends on the full complement of cellular functions, not just cell proliferation or secretion of a single cytokine (Table 1). Patient 1 was anergic before our protocol treatment despite nearly 2 years of PEG-ADA treatment. Eight months after the initiation of gene therapy (protocol day 251), she had a brisk DTH response to a single intradermal skin test with tetanus toxoid. By protocol day 455, DTH responses to five of seven antigens were present, and this increased responsiveness has persisted, through day 1252.

Before the protocol, patient 2 had no positive DTH skin test (Table 1). At protocol day 501, five positive DTH skin tests were elicited, and this increased DTH reactivity had persisted when she was last tested on day 1118. She also acquired palpable lymph nodes and visible tonsils during the period of protocol treatment.

To corroborate the improved immune function indicated by these DTH tests, we evaluated the capacity of peripheral T cells from our patients to produce interleukin-2 (IL-2) or to kill antigenic target cells in vitro. In several patients treated with PEG-ADA, in vitro T cell proliferative responses to mitogens may normalize, whereas responses to specific antigens are less improved (*7–10*). During PEG-ADA treatment before gene therapy, T cells from patient 1 produced IL-2 in response to stimulation with

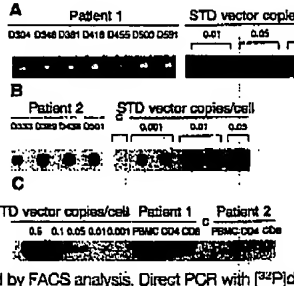

Fig. 2. PCR evaluation of the frequency of LASN vector-positive cells in the blood of patients 1 and 2 at various protocol days. (**A**) Cells from patient 1 for protocol days (D) 304 to 591 (see Fig. 1A). PCR analysis was performed as described (*26*) in an ethidium-stained gel. (**B**) Cells from patient 2 for protocol days (D) 333 to 501 (see Fig. 1B). PCR products were probed with ^{32}P-labeled *neo* gene as described (*26*). (**C**) Purified CD4$^+$ and CD8$^+$ cell subpopulations from patient 1 (D1480) and patient 2 (D1198) prepared by separation of peripheral blood mononuclear cells (PBMCs) by fluorescence-activated cell sorting (FACS). The purity of the separated T cell subpopulations from which DNA was extracted exceeded 98%, as confirmed by FACS analysis. Direct PCR with [^{32}P]deoxycytosine triphosphate was performed as described (*27*). Standards (STD) were prepared from DNA obtained from cell mixtures of a known proportion of LASN-transduced cells containing a single vector insert mixed with vector-negative cells. C, vector-negative control cells.

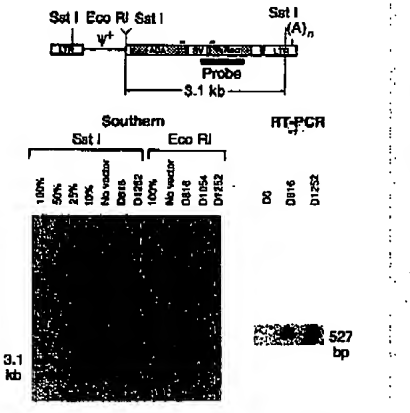

Fig. 3. Quantitative Southern hybridization analysis of DNA prepared from the blood mononuclear cells of patient 1 on protocol days (D) 816 and 1252 (*28*). DNA digested with Sst I should yield a single restriction fragment of 3.1 kb containing both the vector *neo* and ADA genes. Eco RI cuts only once within the vector sequence, and therefore a detectable band would indicate that a predominant clone with a single unique vector integration site was present in that blood sample. None was detected. Polyadenylated mRNA was extracted from the patient cells on days 0, 816, and 1252 and analyzed for vector message by RT-PCR (*29*). The primer locations used are indicated as short solid lines above the vector diagram. SV, SV40 early promoter; $(A)_n$, polyadenylation site; Ψ, extended retrovirus packaging signal. Hatched regions indicate protein coding regions.

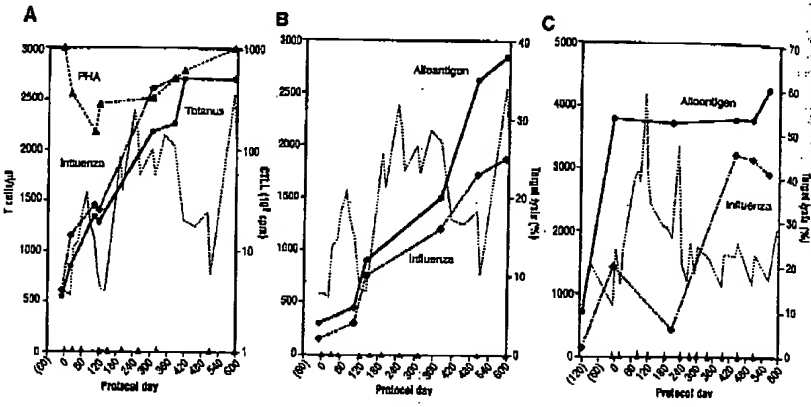

Fig. 4. Evaluation of the in vitro cellular immune responses of blood T cells from patients 1 and 2 at various times before and during the gene therapy trial. At least two normal subjects were included concurrently in each assay, and only those in which the controls responded appropriately are included here. (**A**) Production of IL-2 by cultured cells from patient 1 after stimulation with the mitogen PHA and with the specific antigens tetanus toxoid and influenza A virus as described (*30*). IL-2 was quantitated by bioassay measuring the proliferation of the IL-2–dependent T cell line CTLL at a 1:2 dilution of the lymphocyte culture supernatant. The fine dashed line indicates the patient's T cell count for reference. Solid triangles along the base line indicate the dates of cell infusion. (**B**) In vitro killing of a ^{51}Cr-labeled, influenza A–infected autologous B cell line and a ^{51}Cr-labeled allogeneic target B cell line by blood T cells from patient 1 as described (*37*). Lysis (as percent specific isotope release during a 6-hour incubation of effector and target cells at a ratio of 60:1) was measured after in vitro pre-stimulation for 7 days. Solid triangles along the base line indicate the dates of cell infusion. (**C**) In vitro killing of a ^{51}Cr-labeled, influenza A–infected autologous B cell and a ^{51}Cr-labeled allogeneic target B cell line by blood T cells from patient 2 as described above.

the mitogen phytohemagglutinin (PHA) (Fig. 4A) but were unable to produce IL-2 in response to stimulation with influenza A virus or tetanus toxoid, despite repeated immunization with these antigens. Over the first months of gene therapy, IL-2 production improved and became normal after 1 year (Fig. 4A). Again before gene therapy, patient 1's T cells failed to show significant cytolytic reactivity against either allogeneic cells or influenza A–infected target cells. Almost mirroring the steady increase in IL-2 production, she acquired normal in vitro cytolytic T cell responses to these antigens, reaching normal values in her second year of treatment (Fig. 4B).

The results of these cytolytic assays for patient 2 are shown in Fig. 4C. Tests done 120 days before the beginning of gene therapy also showed impaired responses. However, cells that were obtained at the time of the first gene therapy infusion, cryopreserved, and subsequently tested some months later showed a normal cytolytic response to allogeneic cells. After a year on gene therapy, cytolytic T cell activity against influenza also became normal.

To evaluate the effects of our treatment on humoral immune function in these patients, we measured antibody responses to several antigens. Despite their PEG-ADA treatment, both patients 1 and 2 had only low or borderline titers of isohemagglutinins on repeated testing before gene therapy. Each patient showed significant elevations in the levels of these antibodies within 90 to 115 days of beginning treatment with gene-modified cells (Table 1). Isohemagglutinins are antibodies that react with group A and B red blood cell antigens and occur spontaneously as a result of environmental exposure to cross-reacting antigens. Isohemagglutinin responses are, therefore, less dependent on the timing of previous immunizations than are responses to common vaccine antigens. After gene therapy, each patient also had improvement in antibody responses to vaccines to *Hemophilus influenzae* B (HIB) and tetanus toxoid (Fig. 5). With enzyme therapy alone, peripheral lymphocytes from each patient were unable to produce immunoglobulin M (IgM) in vitro after stimulation with pokeweed mitogen (PWM), but made robust responses after a year on the gene therapy protocol (Fig. 5A). Immunoglobulin production to PWM depends on T cells; these results further confirm the reconstitution of T cell function associated with gene therapy.

The effects of this treatment on the clinical well-being of these patients is more difficult to quantitate. Patient 1, who had been kept in relative isolation in her home for her first 4 years, was enrolled in public kindergarten after 1 year on the protocol and has missed no more school because of infectious disease than her classmates or siblings. She has grown normally in height and weight and is considered to be normal by her parents. Patient 2 was regularly attending public school while receiving PEG-ADA treatment alone and has continued to do well clinically. Chronic sinusitis and headaches, which had been a recurring problem for several years, cleared completely a few months after initiation of the protocol.

This trial of retroviral-mediated gene transfer shows that the survival of reinfused transduced peripheral blood T cells is prolonged in vivo; the erroneous assumption that T cells would not have such long-term survival was often cited as a potential problem with this treatment strategy. Patient 1 has had a normal total peripheral T cell count since the last cell infusion, and the proportion of her circulating T cells carrying vector DNA has remained stable over that period. Further, expression of the ADA transgene under the influence of the retroviral long terminal repeat (LTR) promoter has persisted for a long period in vivo without obvious extinction. There have been swings in the level of ADA enzyme in her peripheral lymphocytes throughout the period of observation, but the level of blood ADA enzyme activity at 4 years (protocol day 1480) is equivalent to that found immediately after the last cell infusion 2 years earlier (Fig. 1A). Although the data have not yet been completely analyzed, blood obtained after 5 years showed continuation of this trend with, again, a normal T lymphocyte count and an equivalent ADA level.

The mechanism by which our treatment aided immune reconstitution in patient 2 is less clear. The responses of patient 2 to some in vitro immunologic tests were variable before beginning our treatment protocol, ranging from little or no detectable response to nearly normal responses on the blood sample from the day gene therapy began. This patient produced a normal antibody response to immunization with bacteriophage φX174 about a year before beginning gene therapy (*8*). Although we have shown several examples of depressed cellular and humoral immune responses that strongly improved after gene therapy, this highly variable immune reactivity while patient 2 was on PEG-ADA therapy alone complicates interpretation of the contribution of our therapy. There was a temporal relation between initiation of gene therapy and a normalized peripheral T cell count,

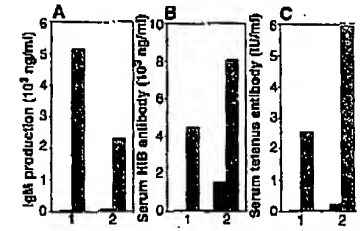

Fig. 5. Humoral immune function of patients 1 and 2 before (solid bars) and after (hatched bars) gene therapy. (**A**) IgM production by the patient's peripheral blood mononuclear cells in cultures stimulated with the T cell–dependent polyclonal activator PWM performed as described (*32*). "Before" samples were from D(−9). Follow-up cultures were at D500 (patient 1) and D560 (patient 2). In each case, the patient's cells stimulated with the T cell–independent B cell stimulant EBV (*33*) produced normal amounts of IgM (not shown), indicating intact B cell function before and after gene therapy, as expected. At least two normal subjects were included concurrently in each assay, and only those in which the controls responded appropriately are included here. (**B**) Serum antibody response to *Hemophilus influenzae* B. Patient 1 had failed to respond to two immunizations while on PEG-ADA alone [D(−9) shown]. Her response at protocol D591 is shown, after immunization. Patient 2 had some HIB-specific antibodies present before therapy [D(−122)], whose amounts increased without additional immunization during the protocol (D560). (**C**) Serum tetanus antibody. Patient 1 had negligible response to five separate tetanus immunizations before gene therapy [D(−48) shown] but responded briskly at D731, 24 days after reimmunization. Serum titers for patient 2 are shown for D(−9), 140 days after immunization while on PEG-ADA alone, and after receiving gene therapy (D592), 32 days after a booster tetanus immunization.

improved DTH, appearance of tonsils and palpable lymph nodes, normalized isohemagglutinin response, and improved PWM response, as well as other factors. In view of the relatively low level of ADA gene transfer achieved in this patient, the potential contribution of the infusions of the culture-activated T cells to the patient's response must also be considered. Perhaps ex vivo T cell activation somehow bypassed a differentiation block that PEG-ADA alone was unable to relieve. Despite the low final percentage gene transfer achieved, a 1% level of ADA gene–corrected cells could represent 10^9 to 10^{10} ADA-expressing T cells distributed throughout the body that could readily contribute to immune improvement.

Since the beginning of the trial, the dose of PEG-ADA enzyme given to each of our patients has been decreased by more than half (patient 1, 14 U/kg/week; patient 2, 10 U/kg/week), during which time their immune function has improved. By contrast, worsened immune function has been seen in other ADA$^-$ SCID patients when their dose of enzyme has been similarly reduced (*10*, *23*). We do not want to expose these patients to the potential risk of recurrent immunodeficiency by completely stopping PEG-ADA enzyme treatment until we have better information about the quality and duration of the immune improvement achieved by this first-generation gene therapy trial. The role of continued exogenous enzyme treatment will be clarified here or in companion studies attempting stem cell gene correction (*24*).

The safety of retroviral-mediated gene transfer has been a central concern. At least in the short and intermediate term, no problems have appeared in any clinical trial using these vectors. In the longer term, the theoretical potential for retroviral vectors to cause insertional mutagenesis remains the primary concern. To date, there has been no indication that malignancy associated with this process will be a complication of retroviral-mediated gene transfer.

Our trial here has demonstrated the potential efficacy of using gene-corrected autologous cells for treatment of children with ADA$^-$ SCID. Eleven children with this disease have been enrolled in various gene therapy protocols, each using different strategies and retroviral vector designs and focusing on different target cell populations. The experience gained from these approaches should provide guidance for gene therapy as a treatment for this disorder as well as for a larger array of inherited and acquired diseases.

REFERENCES AND NOTES

1. K. Shimotohno and H. M. Temin, *Cell* 26, 67 (1981); R. Mann, R. C. Mulligan, D. Baltimore, *ibid.* 33, 153 (1983); S. Watanabe and H. M. Temin, *Proc. Natl. Acad. Sci. U.S.A.* 79, 5986 (1982); A. D. Miller, D. J. Jolly, T. Friedmann, I. M. Verma, *ibid.* 80, 4709 (1983); E. Gilboa *et al.*, *Biotechniques* 4, 504 (1986); D. Armentano *et al.*, *J. Virol.* 61, 1647 (1987); A. D. Miller and G. J. Rosman, *Biotechniques* 7, 980 (1989).
2. A. D. Miller and C. Buttimore, *Mol. Cell. Biol.* 6, 2895 (1986).
3. S. A. Rosenberg *et al.*, *N. Engl. J. Med.* 323, 570 (1990).
4. R. Hirschhorn, *Birth Defects* 19, 73 (1983); E. R. Giblett, J. E. Anderson, F. Cohen, B. Pollara, H. J. Meuwissen, *Lancet* ii, 1067 (1972); M. S. Coleman *et al.*, *J. Biol. Chem.* 253, 1619 (1978); A. R. Cohan *et al.*, *Proc. Natl. Acad. Sci. U.S.A.* 75, 472 (1978); J. Donofrio *et al.*, *J. Clin. Invest.* 62, 884 (1978); D. A. Carson, J. Kaye, S. Matsumoto, J. E. Seegmiller, L. Thompson, *Proc. Natl. Acad. Sci. U.S.A.* 76, 2430 (1979); R. L. Wortmann, B. S. Mitchell, N. L. Edwards, I. H. Fox, *ibid.*, p. 2434; D. A. Carson, J. Kaye, D. B. Wasson, *J. Immunol.* 126, 348 (1981); P. E. Daddona *et al.*, *J. Clin. Invest.* 72, 483 (1983); R. Hirschhorn *et al.*, *ibid.* 64, 1130 (1979); R. Hirschhorn *et al.*, *ibid.* 71, 1887 (1983); P. E. Daddona, B. L. Davidson, J. L. Pedrignon, W. N. Kelley, *J. Biol. Chem.* 260, 3875 (1985); A. L. Akeson, D. A. Wigginton, J. J. Hutton, *J. Cell. Biochem.* 39, 217 (1989).
5. R. H. Buckley *et al.*, *J. Immunol.* 136, 398 (1986); M. L. Markert, M. S. Hershfield, R. I. Schiff, R. H. Buckley, *J. Clin. Immunol.* 7, 389 (1987); L. Wijnaendts, F. Le Deist, C. Griscelli, A. Fischer, *Blood* 74, 2212 (1989); A. M. Yeager, *Pediatr. Ann.* 17, 694 (1988); R. J. O'Reilly, C. A. Keever, T. N. Small, J. Brochstein, *Immunodefic. Rev.* 1, 273 (1989); C. A. Keever *et al.*, *Clin. Immunol. Immunopathol.* 48, 261 (1988); W. Friedrich *et al.*, *Lancet* i, 761 (1984); W. Friedrich *et al.*, *Eur. J. Pediatr.* 144, 125 (1985); G. M. Silber *et al.*, *Clin. Immunol. Immunopathol.* 44, 317 (1987).
6. S. H. Polmar *et al.*, *N. Engl. J. Med.* 295, 1337 (1976); F. C. Schmalstieg *et al.*, *J. Pediatr.* 93, 597 (1978); J. B. Ziegler, C. H. Lee, M. B. Van der Weyden, A. S. Bagnara, J. Beveridge, *Arch. Dis. Child.* 55, 452 (1980); A. Rubinstein, R. Hirschhorn, M. Sicklick, R. A. Murphy, *N. Engl. J. Med.* 300, 387 (1979); R. Hirschhorn, P. S. Papageorgiou, H. H. Kasarwala, L. T. Taft, *ibid.* 303, 377 (1980); S. H. Polmar, *Semin. Hematol.* 17, 30 (1980); J. J. Hutton *et al.*, *J. Clin. Invest.* 68, 413 (1981); E. G. Davies, R. J. Levinsky, D. R. Webster, H. A. Simmonds, D. Perrett, *Clin. Exp. Immunol.* 50, 303 (1982).
7. M. S. Hershfield *et al.*, *N. Engl. J. Med.* 316, 589 (1987).
8. H. D. Ochs *et al.*, *Blood* 80, 1163 (1992).
9. M. S. Hershfield and S. Chaffee, in *Treatment of Genetic Disease*, R. J. Desnick, Ed. (Churchill-Livingstone, New York, 1991), p. 169; J. D. Chun *et al.*, *Ann. Allergy* 70, 462 (1993).
10. K. Weinberg *et al.*, *J. Clin. Invest.* 92, 596 (1993).
11. S. H. Orkin *et al.*, *J. Biol. Chem.* 258, 12753 (1983); D. Valerio *et al.*, *Gene* 25, 231 (1983); D. A. Wiginton, G. S. Adrian, R. L. Friedman, D. P. Suttle, J. J. Hutton, *Proc. Natl. Acad. Sci. U.S.A.* 80, 7481 (1983).
12. P. W. Kantoff *et al.*, *Proc. Natl. Acad. Sci. U.S.A.* 83, 6563 (1986); D. B. Kohn, J. E. Selegue, M. Ballow, R. M. Blaese, *Pediatr. Res.* 21, 313A (1987); D. B. Kohn *et al.*, *Blood Cells* 13, 285 (1987); D. B. Kohn, W. F. Anderson, R. M. Blaese, *Cancer Invest.* 7, 179 (1989).
13. D. B. Kohn *et al.*, *J. Immunol.* 142, 3971 (1989).
14. K. W. Culver, W. F. Anderson, R. M. Blaese, *Hum. Gene Ther.* 2, 107 (1991); K. W. Culver *et al.*, *Proc. Natl. Acad. Sci. U.S.A.* 88, 3155 (1991); K. W. Culver *et al.*, *Hum. Gene Ther.* 1, 399 (1990).
15. G. Ferrari *et al.*, *Science* 251, 1363 (1991).
16. R. M. Blaese *et al.*, *Hum. Gene Ther.* 1, 327 (1990).
17. Peripheral T cells from the patients were collected by apheresis, isolated by density gradient centrifugation, washed extensively, and then cultured in 24-well culture plates in medium supplemented with 100 to 1000 IU/ml of recombinant IL-2 and 10 ng/ml of OKT3 to stimulate T cell proliferation. After 24 hours, half the medium was removed and replaced with supernatant containing the LASN retroviral vector supplemented with IL-2 and protamine (10 μg/ml) to give an initial multiplicity of infection of 1. The LASN vector contains the human ADA cDNA under the transcriptional control of the promoter-enhancer in the retroviral LTR and a neomycin phosphotransferase gene (*neo*) controlled by an internal SV40 promoter [R. A. Hock, A. D. Miller, W. R. A. Osborne, *Blood* 74, 876 (1989)] LASN was packaged with PA317 amphotropic retrovirus packaging cells (*2*). The LASN vector preparation, manufactured under good manufacturing practices by Genetic Therapy, Gaithersburg, MD, had a titer of 1×10^6 to 3×10^6. The cells were returned to the incubator and the transduction process repeated, with the addition of fresh retroviral supernatant and IL-2 twice daily for a total of three to five additions of vector. The cultured cells were transferred to gas-permeable culture bags at the conclusion of the transduction process. The proliferating T cell cultures were observed daily, split, and fed as necessary with periodic samples tested for viability and microbial contamination. Gene transfer efficiency was variable from treatment to treatment and patient to patient, ranging from 1 to 10% for patient 1 and 0.1 to 1% for patient 2. On days 9 to 12, the cultured cells were washed extensively with saline containing 0.5% human albumin and were then infused into the patient over a period of about 1 hour. During the 9 to 12 days of culture, the cell populations had expanded 17- to 135-fold. Preliminary studies testing the T cell receptor β gene repertoire showed that T cell cultures remained polyclonal for at least 3 weeks under these culture conditions. The culture period used in the clinical trial was held to half this time period to ensure a polyclonal T cell repertoire in the infused cell population.
18. M. S. Hershfield, S. Chaffee, R. U. Sorensen, *Pediatr. Res.* 33, S42 (1993); R. M. Blaese, *ibid.*, p. S49;

R. U. Sorenson, M. Berger, M. S. Hershfield, *ibid.* **27**, 162A (1990); I. Santisteban *et al.*, *J. Clin. Invest.* **82**, 2291 (1993).
19. Y. Levy *et al.*, *J. Pediatr.* **113**, 312 (1988).
20. The protocol was reviewed and approved by the Clinical Research Subpanels of the NCI and NHLBI, the NCI Cancer Treatment and Evaluation Program (CTEP), the NIH Biosafety Committee, the Human Gene Therapy Subcommittee, the Recombinant DNA Advisory Committee, the Director of NIH, and the U.S. Food and Drug Administration. Informed consent was obtained from the parents of each patient.
21. Beginning with culture 9 for patient 1 and culture 5 for patient 2, the patients' lymphocyte populations obtained by apheresis were fractionated by adherence to flasks coated with CD8 monoclonal antibodies (Applied Immune Sciences) following the manufacturer's instructions. This protocol modification for CD8 depletion was introduced because both patients were developing a progressively inverted CD4⁺/CD8⁺ ratio. This effect was apparently the result of preferential growth of $CD8^+$ cells during the last 4 to 5 days of culture and the subsequent persistence of these infused $CD8^+$ cells in the circulation. Consequently, each subsequent apheresis sampled the recently increased number of $CD8^+$ cells, and thus the skewing of the ratio of CD4 to CD8 cells became compounded with each additional treatment. By partially depleting the apheresis sample of $CD8^+$ cells by an immunoaffinity selection process, the later treatments for each patient consisted of cells with a more balanced phonotype. The perturbation in normal CD4⁺/CD8⁺ cell proportions did not have detectable untoward effects for either patient.
22. C. A. Mullen, K. W. Culver, R. A. Morgan, W. F. Anderson, R. M. Blaese, unpublished results.
23. K. Weinberg, unpublished observations; R. M. Blaese, unpublished observations.
24. D. B. Kohn *et al.*, *Nature Med.* **1**, 1017 (1995).
25. The ADA enzyme activity assay was performed in duplicate as described (*13*). Positive control cells were obtained from healthy normal donors and had a mean of 82 U (normal range, 66 to 102 U). Duplicate samples were run in the presence of the ADA enzyme inhibitor EHNA (30 μM). Specific ADA activity was calculated as total adenosine deaminating activity minus EHNA-resistant activity. EHNA-resistant activity represents metabolic activity of a nonspecific aminohydrolase present in human cells.
26. R. A. Morgan, K. Cornetta, W. F. Anderson, *Hum. Gene Ther.* **1**, 135 (1990).
27. B. A. Bunnell, L. M. Muul, R. R. Donahue, R. M. Blaese, R. A. Morgan, *Proc. Natl. Acad. Sci. U.S.A.* **92**, 7739 (1995).
28. Southern hybridization analysis for LASN vector consisted of the following: 10 μg of DNA was digested with Sst I and hybridized with a 728-bp Nco I fragment from LASN corresponding to the SV40 promoter and *neo* gene. DNA from K562-LASN cells served as a positive control.
29. RT-PCR analysis for LASN vector transcripts was as follows: 3 μg of polyadenylated RNA was treated with deoxyribonuclease and reverse-transcribed. The cDNA (0.3 μg) was amplified with LASN vector–specific primers in a 30-cycle PCR reaction. The oligonucleotides 5′-CAGCCTCTGCAGGGCAGAAC-3′ (corresponding to the 3′ end of the ADA gene in LASN) and 5′-GCCCAGTCATAGCCGAATAG-3′ (complementary to 5′ end of the *neo* gene in LASN) were used as primers. After electrophoresis and blotting, the sequences were hybridized with a 527-bp probe corresponding to the entire length of the predicted PCR product.
30. M. Clerici *et al.*, *J. Clin. Invest.* **84**, 1892 (1989).
31. M. Clerici *et al.*, *J. Immunol.* **146**, 2214 (1991); W. E. Biddison, F. E. Ward, G. M. Shearer, S. Shaw, *ibid.* **124**, 548 (1980).
32. T. A. Waldmann *et al.*, *Lancet* **ii**, 609 (1974).
33. H. Kirchner *et al.*, *J. Immunol.* **122**, 1310 (1979).
34. *AABB Technical Manual*, R. H. Walker, Ed. (American Association of Blood Banks, Bethesda, MD, ed. 11, 1993), pp. 622–623.
35. S. W. Fong, B. Y. Osgundah, W. F. Taylor, *Transfusion* **14**, 551 (1974).

36. The authors acknowledge suport technical and nursing support by C. Abik, K. Snitzer, A. Roop, M. Brown, F. May, R. Gutierlez, M. Yu, H. Goetzman, C. Wanrabe, B. Sink, and L. Top. In addition, we thank R. Sorensen for providing the initial patient blood samples, Applied Immune Sciences for CELLector T-150 flasks, and Genetic Therapy for clinical-grade LASN vector. Finally, we also thank our earlier collaborators D. B. Kohn, E. Gilboa, P. W. Kantoff, M. Egilis, R. Moen, K. Cornetta, A. Gillio, R. J. O'Reilly, and C. Bordignon for their contributions that helped prepare the way for this clinical trial.

30 June 1995; accepted 27 September 1995

Physical Map and Organization of *Arabidopsis thaliana* Chromosome 4

Renate Schmidt,* Joanne West, Karina Love, Zoë Lenehan, Clare Lister, Helen Thompson, David Bouchez, Caroline Dean†

A physical map of *Arabidopsis thaliana* chromosome 4 was constructed in yeast artificial chromosome clones and used to analyze the organization of the chromosome. Mapping of the nucleolar organizing region and the centromere integrated the physical and cytogenetic maps. Detailed comparison of physical with genetic distances showed that the frequency of recombination varied substantially, with relative hot and cold spots occurring along the whole chromosome. Eight repeated DNA sequence families were found in a complex arrangement across the centromeric region and nowhere else on the chromosome.

Arabidopsis thaliana has been adopted as a model organism for the analysis of complex plant processes by means of molecular genetic techniques (*1*). The increase in map-based cloning experiments makes the generation of a complete physical map of the *Arabidopsis* genome a high priority. In addition, the availability of such a map would enable the organization of the chromosome to be studied in more detail. Little is known about the organization of plant chromosomes, but the general picture is that of chromosomes carrying large numbers of dispersed [often retrotransposons (*2*)] and tandemly repeated DNA sequences (*3*). The relatively small (100 Mb) *Arabidopsis* genome has a much smaller number of repeated DNA sequences than do most other plant species; its five chromosomes contain ~10% highly repetitive and ~10% moderately repetitive DNA (*4*). The dispersion of most of these sequences among the low-copy DNA is unknown.

We discuss here a physical map, which we have presented on the World Wide Web (WWW) at URL: http://nasc.nott.ac.uk/JIC-contigs/JIC-contigs.html, of *Arabidopsis* chromosome 4, one of the two chromosomes carrying nucleolus organizing regions. The construction of this map allowed us to analyze the frequency of recombination along the whole chromosome, the integration of the physical with the cytogenetic map, the interspersion pattern of repeated and low-copy DNA sequences over the whole chromosome, and the arrangement of repeated DNA sequences over the centromeric region.

We generated the physical map by hybridizing probes to four yeast artificial chromosome (YAC) libraries (*5*), using colony hybridization experiments (*6*). The probes consisted of 112 markers genetically mapped to chromosome 4, 20 previously unmapped genes, random genomic fragments and sequences flanking transposable elements, and the 180–base pair (bp) repetitive element carried in pAL1 (*7*). Southern (DNA) blot analysis of YAC clones confirmed the colony hybridization results and revealed common restriction fragments in the different YAC clones hybridizing to a given marker. This demonstrated overlap between the inserts of the YAC clones. On the basis of these results, the YAC clones could be placed into 14 YAC contigs with a high degree of redundant YAC cover, ensuring an accurate map despite the presence of chimeric clones in the YAC libraries.

We generated YAC end fragments, using either inverse polymerase chain reaction (IPCR) or plasmid rescue (*8*), from YAC clones lying near the ends of each of the 14 contigs. The fragments were hybridized to Southern blots of YAC clones from adjacent contigs. In addition, YACs, as well as some of the end fragments generated by IPCR, were used to identify clones from a cosmid library of the Columbia ecotype (*9*). The cosmids were then used as new markers on the YAC libraries. These experiments reduced the number of contigs to four. In all but two instances, the end fragments revealed that the contigs were already overlapping. Experiments aimed at closing the last three gaps have been attempt

R. Schmidt, J. West, K. Love, Z. Lenehan, C. Lister, H. Thompson, C. Dean, Department of Molecular Genetics, Biotechnology and Biological Sciences Research Council, John Innes Centre, Colney, Norwich NR4 7UH, UK. D. Bouchez, Laboratoire de Biologie Cellulaire, Institut National de la Recherche Agronomique, 78026 Versailles Cedex, France.

*Present address: Max-Delbrueck Laboratory, Carl-von-Linne-Weg 10, D50829, Cologne, Germany.
†To whom correspondence should be addressed.

REFERENCES AND NOTES

1. The current EST database (dbEST release 091495) from the National Center for Biotechnology Information (Bethesda, MD) contains a total of 322,225 entries, including 255,645 from the human genome and 21,044 from *Arabidopsis*. Access is available via the World Wide Web (http://www.ncbi.nlm.nih.gov).
2. E. M. Meyerowitz and R. E. Pruitt, *Science* 229, 1214 (1985); R. E. Pruitt and E. M. Meyerowitz, *J. Mol. Biol.* 187, 169 (1986); I. Hwang *et al.*, *Plant J.* 1, 367 (1991); P. Jarvis *et al.*, *Plant Mol. Biol.* 24, 685 (1994); L. Le Guen *et al.*, *Mol. Gen. Genet.* 245, 390 (1994).
3. D. Shalon, thesis, Stanford University (1995); ——— and P. O. Brown, in preparation. Microarrays were fabricated on poly-L-lysine–coated microscope slides (Sigma) with a custom-built arraying machine fitted with one printing tip. The tip loaded 1 μl of PCR product (0.5 mg/ml) from 96-well microtiter plates and deposited ~0.005 μl per side on 40 slides at a spacing of 500 μm. The printed slides were rehydrated for 2 hours in a humid chamber, snap-dried at 100°C for 1 min, rinsed in 0.1% SDS, and treated with 0.06% succinic anhydride prepared in buffer consisting of 50% 1-methyl-2-pyrrolidinone and 50% boric acid. The cDNA on the slides was denatured in distilled water for 2 min at 90°C immediately before use. Microarrays were scanned with a laser fluorescent scanner that contained a computer-controlled XY stage and a microscope objective. A mixed gas, multiline laser allowed sequential excitation of the two fluorophores. Emitted light was split according to wavelength and detected with two photomultiplier tubes. Signals were read into a PC with the use of a 12-bit analog-to-digital board. Additional details of microarray fabrication and use may be obtained by means of e-mail (pbrown@cmgm.stanford.edu).
4. F. M. Ausubel *et al.*, Eds., *Current Protocols in Molecular Biology* (Greene & Wiley Interscience, New York, 1994), pp. 4.3.1–4.3.4.
5. Polyadenylated [poly(A)$^+$] mRNA was prepared from total RNA with the use of Oligotex-dT resin (Qiagen). Reverse transcription (RT) reactions were carried out with a StrataScript RT-PCR kit (Stratagene) modified as follows: 50-μl reactions contained 0.1 μg/μl of *Arabidopsis* mRNA, 0.1 ng/μl of human AChR mRNA, 0.05 μg/μl of oligo(dT) (21-mer), 1× first strand buffer, 0.03 U/μl of ribonuclease block, 500 μM deoxyadenosine triphosphate (dATP), 500 μM deoxyguanosine triphosphate, 500 μM dTTP, 40 μM deoxycytosine triphosphate (dCTP), 40 μM fluorescein-12-dCTP (or tissamine-5-dCTP), and 0.03 U/μl of StrataScript reverse transcriptase. Reactions were incubated for 60 min at 37°C, precipitated with ethanol, and resuspended in 10 μl of TE (10 mM tris-HCl and 1 mM EDTA, pH 8.0). Samples were then heated for 3 min at 94°C and chilled on ice. The RNA was degraded by adding 0.25 μl of 10 N NaOH followed by a 10-min incubation at 37°C. The samples were neutralized by addition of 2.5 μl of 1 M tris-Cl (pH 8.0) and 0.25 μl of 10 N HCl and precipitated with ethanol. Pellets were washed with 70% ethanol, dried to completion in a speedvac, resuspended in 10 μl of H_2O, and reduced to 3.0 μl in a speedvac. Fluorescent nucleotide analogs were obtained from New England Nuclear (DuPont).
6. Hybridization reactions contained 1.0 μl of fluorescent cDNA synthesis product (5) and 1.0 μl of hybridization buffer [10× saline sodium citrate (SSC) and 0.2% SDS]. The 2.0-μl probe mixtures were aliquoted onto the microarray surface and covered with cover slips (12 mm round). Arrays were transferred to a hybridization chamber (3) and incubated for 18 hours at 65°C. Arrays were washed for 5 min at room temperature (25°C) in low-stringency wash buffer (1× SSC and 0.1% SDS), then for 10 min at room temperature in high-stringency wash buffer (0.1× SSC and 0.1% SDS). Arrays were scanned in 0.1× SSC with the use of a fluorescence laser-scanning device (9).
7. Samples of poly(A)$^+$ mRNA (4, 5) were spotted onto nylon membranes (Nytran) and crosslinked with ultraviolet light with the use of a Stratalinker 1800 (Stratagene). Probes were prepared by random priming with the use of a Prime-It II kit (Stratagene) in the presence of [^{32}P]dATP. Hybridizations were carried out according to the instructions of the manufacturer. Quantitation was performed on a PhosphorImager (Molecular Dynamics).
8. M. Schena and R. W. Davis, *Proc. Natl. Acad. Sci. U.S.A.* 89, 3894 (1992); M. Schena, A. M. Boyd, R. W. Davis, *Genes Dev.* 7, 367 (1993); M. Schena and R. W. Davis, *Proc. Natl. Acad. Sci. U.S.A.* 91, 8393 (1994).
9. H. Hotte *et al.*, *Plant J.* 4, 1051 (1993); T. Newman *et al.*, *Plant Physiol.* 106, 1241 (1994).
10. N. E. Morton, *Proc. Natl. Acad. Sci. U.S.A.* 88, 7474 (1991); E. D. Green and R. H. Waterston, *J. Am. Med. Assoc.* 266, 1966 (1991); C. Bellanne-Chantelot, *Cell* 70, 1059 (1992); D. R. Cox *et al.*, *Science* 265, 2031 (1994).
11. E. S. Kawasaki *et al.*, *Proc. Natl. Acad. Sci. U.S.A.* 85, 5698 (1988).

12. The laser fluorescent scanner was designed and fabricated in collaboration with S. Smith of Stanford University. Scanner and analysis software was developed by R. X. Xia. The succinic anhydride reaction was suggested by J. Mulligan and J. Van Ness of Darwin Molecular Corporation. Thanks to S. Theologis, C. Somerville, K. Yamamoto, and members of the laboratories of R.W.D. and P.O.B. for critical comments. Supported by the Howard Hughes Medical Institute and by grants from NIH [R21HG00450) (P.O.B.) and R37AG00198 (R.W.D.)] and from NSF (MCB9106011) (R.W.D.) and by an NSF graduate fellowship (D.S.). P.O.B. is an assistant investigator of the Howard Hughes Medical Institute.

11 August 1995; accepted 22 September 1995

Gene Therapy in Peripheral Blood Lymphocytes and Bone Marrow f r ADA$^-$ Immunodeficient Patients

Claudio Bordignon,* Luigi D. Notarangelo, Nadia Nobili, Giuliana Ferrari, Giulia Casorati, Paola Panina, Evelina Mazzolari, Daniela Maggioni, Claudia Rossi, Paolo Servida, Alberto G. Ugazio, Fulvio Mavilio

Adenosine deaminase (ADA) deficiency results in severe combined immunodeficiency, the first genetic disorder treated by gene therapy. Two different retroviral vectors were used to transfer ex vivo the human ADA minigene into bone marrow cells and peripheral blood lymphocytes from two patients undergoing exogenous enzyme replacement therapy. After 2 years of treatment, long-term survival of T and B lymphocytes, marrow cells, and granulocytes expressing the transferred ADA gene was demonstrated and resulted in normalization of the immune repertoire and restoration of cellular and humoral immunity. After discontinuation of treatment, T lymphocytes, derived from transduced peripheral blood lymphocytes, were progressively replaced by marrow-derived T cells in both patients. These results indicate successful gene transfer into long-lasting progenitor cells, producing a functional multilineage progeny.

Severe combined immunodeficiency associated with inherited deficiency of ADA (*1*) is usually fatal unless affected children are kept in protective isolation or the immune system is reconstituted by bone marrow transplantation from a human leukocyte antigen (HLA)–identical sibling donor (*2*). This is the therapy of choice, although it is available only for a minority of patients. In recent years, other forms of therapy have been developed, including transplants from haploidentical donors (*3*, *4*), exogenous enzyme replacement (*5*), and somatic-cell gene therapy (*6*–*9*).

We previously reported a preclinical model in which ADA gene transfer and expression successfully restored immune functions in human ADA-deficient (ADA$^-$) peripheral blood lymphocytes (PBLs) in immunodeficient mice in vivo (*10*, *11*). On the basis of these preclinical results, the clinical application of gene therapy for the treatment of ADA$^-$ SCID (severe combined immunodeficiency disease) patients who previously failed exogenous enzyme replacement therapy was approved by our Institutional Ethical Committees and by the Italian National Committee for Bioethics (*12*). In addition to evaluating the safety and efficacy of the gene therapy procedure, the aim of the study was to define the relative role of PBLs and hematopoietic stem cells in the long-term reconstitution of immune functions after retroviral vector–mediated ADA gene transfer. For this purpose, two structurally identical vectors expressing the human ADA complementary DNA (cDNA), distinguishable by the presence of alternative restriction sites in a nonfunctional region of the viral long-terminal repeat (LTR), were used to transduce PBLs and bone marrow (BM) cells independently. This procedure allowed identification of the origin of

C. Bordignon, N. Nobili, G. Ferrari, D. Maggioni, C. Rossi, P. Servida, F. Mavilio, Telethon Gene Therapy Program for Genetic Diseases, DIBIT, Istituto Scientifico H. S. Raffaele, Milan, Italy.

L. D. Notarangelo, E. Mazzolari, A. G. Ugazio, Department of Pediatrics, University of Brescia Medical School, Brescia, Italy.

G. Casorati, Unità di Immunochimica, DIBIT, Istituto Scientifico H. S. Raffaele, Milan, Italy.

P. Panina, Roche Milano Ricerche, Milan, Italy.

*To whom correspondence should be addressed.

cells, and their progeny, after gene transfer.

This combined therapy and marking strategy allowed us to investigate directly in humans some of the basic questions related to the potential of retroviral vectors for gene therapy in cells of the hemato-lymphopoietic lineages. Although gene transfer into human hematopoietic progenitors (*13*, *14*), peripheral blood stem cells (*15*), and PBLs (*16–18*) has been extensively demonstrated in vitro, the potential for long-term survival in vivo after the manipulations required for retroviral vector gene transfer remains to be proven. In addition, this study allowed us to study the feasibility of gene transfer into hematopoietic stem and progenitor cells, and the potential for long-term persistence of differentiated cells in a context different from high-dose chemotherapy and BM transplantation (*19–21*). In this system, however, the positive selection may represent an absolute requirement for favoring the appearance of vector-transduced cells.

In ADA$^-$ patients, failure of the immune system to develop is due to the sensitivity of lymphocytes or their precursors to the toxic effects of accumulated ADA substrates (*22*). Because it is possible to reduce the levels of toxic metabolites in ADA$^-$ cells by providing exogenous ADA (*23*), a nonselective form of ADA replacement (that is, transfusion of irradiated red cells from normal individuals) has been used to treat ADA$^-$ patients (*24*). An improved form of treatment was developed by covalent attachment of polyethylene glycol (PEG) to the purified bovine enzyme (*23*, *25*). PEGilation appears to block access of degradative enzymes, antibodies, and antigen-presenting cells to the protein surface, thereby inhibiting clearance from the circulation (*26–28*) and prolonging ADA plasma half-life from a few minutes to 24 hours (*23*). The main biochemical consequences of ADA deficiency are almost completely reversed by PEG-ADA treatment (*23*), resulting in an increase in circulating T lymphocytes and improvement of cellular immune functions (*23*, *29*).

In our study, treatment in two patients [G.B., patient 1; A.R., patient 2 (*30*); both about 2 years of age] was initiated with weekly intramuscular injections of increasing doses of PEG-ADA (20 and 30 U per kilogram of body weight) until plasma ADA activity could be maintained at least in the normal range of total blood activity. The range of ADA activity was stable between 20 and 40 μmol hour^{-1} ml^{-1}. Before initiation of treatment, both patients had nearly undetectable intracellular ADA activity, and lymphopenia was observed in both patients. Approximately 50% of blood mononuclear cells reacted with monoclonal antibodies to T cell surface antigens, and their proliferative response to mitogens ranged from virtually undetectable to 10% of normal controls. Both patients showed some response in mixed lymphocyte culture, although they produced no specific antibody and showed no antigen-restricted T cell response. Residual immune functions were probably due to previous irradiated red cell transfusions. During the first year of PEG-ADA treatment, lymphocyte counts and proliferative responses to phytohemagglutinin (PHA) normalized.

Immunological reconstitution resulted in increased isohemoagglutinin titer and in cellular and antibody responses to vaccination with teranus toxoid (TT) (*31*). Associated with reconstitution of immune functions was the complete reversion of all clinical signs of immunodeficiency. However, as reported elsewhere (*29*), the initial reconstitution in this case was limited by the failure to maintain PBL counts and, more markedly, antigen-specific and nonspecific proliferative responses. At that point, the two patients met the conditions that define PEG-ADA treatment failure, as reported in our approved clinical protocol (*12*). Failure of treatment was defined by an extensive number of laboratory parameters and immunological assays (*12*). In both patients, failure of treatment was observed in the absence of any acute illness or open infection episodes and was confirmed in three separate determinations. Waiting for potential recurrence of clinical symptoms such as infectious episodes, or failure of thriving, was considered to be inappropriate.

Early development of T cells obtained during PEG-ADA treatment was crucial to the implementation of the gene therapy protocol. Administration of PEG-ADA continued throughout the study period, although at decreasing amounts. Therefore, the relative role of gene-corrected cells and PEG-ADA treatment remains to be completely defined, an issue that will be addressed during the continuation of this study.

The aim of our study was to evaluate the safety and efficacy of the retroviral vector–mediated gene transfer procedure and to define the relative role of PBLs and BM stem and progenitor cells as effectors of long-term reconstitution of immune functions after gene transfer. For this purpose, we constructed two different retroviral vectors, DCAI and DCAm, expressing the human ADA cDNA under the control of its own promoter, which were used to infect PBLs and BM cells, respectively (Fig. 1). Both vectors are based on the double-copy (DC) design (*32*) and are structurally identical except for the presence of alternative restriction sites (Mlu I in DCAI and Bss HII in DCAm) in a nonfunctional region of the viral LTR (*33*). This feature allowed unequivocal tracing of the origin (BM or PBL) of the transduced cell progeny in the circulation by a simple polymerase chain reaction (PCR) analysis on genomic DNA (*34*). Both vectors were packaged in the amphotropic GP+*env* Am12 cell line (*33*). PBLs and T cell–depleted BM cells were transduced ex vivo either by multiple exposure to cell-free viral supernatant or by coculture with irradiated packaging cells (*35*, *36*). Gene transfer efficiency increased from 1 to 2.5% up to 40% in total PBLs, with the introduction in the procedure of a new packaging line and of cocultivation. Gene transfer efficiency into CFU-GM and BFU-E hematopoietic progenitors averaged 30 to 40%, as described (*37*). These frequencies were estimated by cloning in lim-

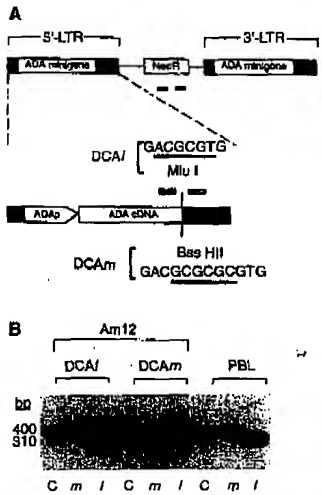

Fig. 1. (**A**) Structure of the DCAI (lymphocytes) and DCAm (marrow) proviruses. A human ADA minigene (promoter + full-length cDNA) was inserted into the LTR U3 region of a Moloney murine leukemia virus–derived retroviral vector (DCA) (*32*, *33*). For construction of two vectors that could be distinguished from each other after integration into the target cell genome, the unique Mlu I restriction site present in a functionally irrelevant region of the LTR in DCAI was converted into a Bss HII site in DCAm (enlarged map). The hatched boxes indicate the location of the PCR primers used to detect vector DNA in target cells and for vector identification. (**B**) PCR identification of the vector integrated into the lymphocytes of patient 1 3 months after initial administration of DCAI-transduced PBLs and DCAm-transduced BM cells, showing the PBL origin of the transduced circulating lymphocytes. C, control (uncut PCR product); *m*, marrow-specific Bss HII cut present in DCAm-transduced cells; *l*, lymphocyte-specific Mlu I cut present in DCAI-transduced cells. PCR amplification of DNA obtained from the DCAI and DCAm packaging cell lines (Am12) is shown as a control.

iting dilution (38) and semi-solid colony-forming assays (39), respectively, in the presence or absence of G418 and are the result of the steady improvement in both cell-free infection and cocultivation that we have produced in recent years (10, 11, 18, 37). In particular, our goal has been to increase gene transfer frequency while maintaining phenotype, immune repertoire, and in vivo potential for proliferation, differentiation, and survival. For this purpose, short cultivation time under conditions of low interleukin-2 (IL-2) concentration were developed for the activation and infection of PBLs (35), while BM cells were maintained in a long-term culture system over adherent layers without addition of exogenous growth factors, and were infected during the first 3 days of culture (36). This system produces minimal loss of differentiation capacity and potential for in vivo hematopoietic reconstitution (40). No G418 selection was applied to infected PBLs or BM cells before reinfusion. Transduction efficiency and production of the vector-derived ADA in infected cells was determined by PCR and thin-layer chromatography (TLC), respectively (41).

In vivo administration of genetically modified cells began in March 1992 for patient 1 and July 1993 for patient 2. Patient 1 received 7.24×10^8 DCAI-transduced lymphocytes and 0.35×10^8 DCAm-transduced progenitor cells in nine injections administered intravenously (i.v.) over a period of 24 months. Patient 2 received a slightly smaller number of cells in five injections over 10 months.

We began monitoring the persistence of vector-transduced cells at monthly (or bimonthly) intervals from the first infusion. Analyses were performed both on bulk populations of cells of different origin, for the indication of origin of transduced cells, and on clonal assays for quantitation of transduced BM and PBLs. Six months after the beginning of treatment, long-term survival of transduced cells was demonstrated in both patients by the presence of vector-derived sequences in the DNA extracted from peripheral blood mononuclear cells, total BM cells, mature granulocytes (Fig. 2A), individual T lymphocyte clones (Fig. 3), and BM progenitors (BFU-E, CFU-GM, and CFU-GEMM) in clonal culture (41). ADA production at levels substantially greater than observed in untransduced ADA$^-$ controls was observed in PBLs, BM, and granulocytes (Fig. 2C). The proportion of genetically modified cells in BM and circulating blood was monitored throughout the study by BM and T cell clonal assay in the presence of G418, and indirectly from the amount of ADA activity in total cell populations from BM and peripheral blood. In both patients, this proportion ranged between 5 and 30% of clonable BM progenitors and between 0.8 and 8.5% in PBLs. Total ADA activity ranged between 5 and 18% of normal values in both patients' nucleated cells in the blood. Sixteen months after discontinuation of treatment, ADA activity in total circulating nucleated cells was 126 nmol hour^{-1} per milligram of protein in patient 1 and 77 nmol hour^{-1} per milligram of protein in patient 2 (internal normal control, 1157 nmol hour^{-1} per milligram of protein; for method see legend to Fig. 2). At the same time, in patient 1, the frequency of transduced G418-resistant T cell was 4.76% and that of clonable BM progenitors was 25%; in patient 2 these frequencies were 2.0% and 17%, respectively. During this period in patient 1, and more recently in patient 2, ADA activity became reproducibly detectable also in circulating erythrocytes (Fig. 2C). Vector-derived ADA activity in individual T cell clones was comparable to, or higher than, that of normal controls (legend to Fig. 2C), as observed in T cells that survived in vivo selection in the human PBL-SCID mouse preclinical model (10, 11). ADA activity in Neo-resistant BM colonies also averaged normal levels (41).

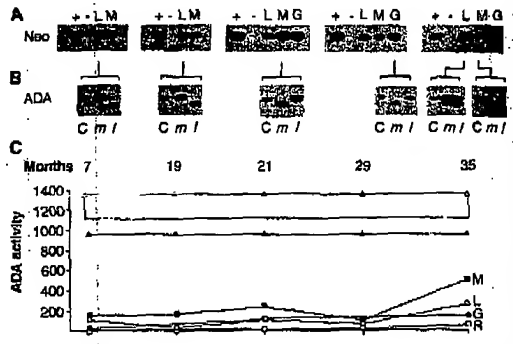

Fig. 2. Persistence of transduced hematopoietic cells in vivo and analysis of their origin. During 3 years after initiation of the gene therapy trial, persistence of transduced PBLs and BM cells, and expression of vector-derived ADA activity were documented at regular intervals. (**A**) Detection of transduced cells by PCR analysis for the NeoR gene was consistent throughout the follow-up of patient 1 in PBLs (L), BM cells (M), and circulating granulocytes (G). + and −, PCR-positive and negative controls, respectively. (**B**) Analysis of the identity of the integrated vector showed that vector-positive lymphocytes were initially all derived from long-lived transduced PBLs, as demonstrated by the presence of the DCAI-specific PCR pattern (7 and 19 months), whereas BM and granulocytes showed the DCAm-specific pattern (21, 29, and 35 months). Three years after initiation and 1 year after discontinuation of treatment, DCAm-specific signals started to appear in the DNA extracted from PBLs, indicating progressive conversion of the circulating, genetically modified lymphocyte pool from a predominantly PBL-derived to a BM progenitor–derived population (35 months). This observation was further confirmed by the analysis of Neo-resistant, peripheral blood T cell clones (Fig. 3). (**C**) In parallel, vector-derived ADA activity was monitored by TLC in total PBLs (L) and BM cells (M) of patient 1. G, granulocytes; R, red blood cells. Two positive controls are provided: ADA activity (mean ± SE) from a pool of normal individuals (△), and ADA activity from a polyclonal PBL line from the same patient transduced in vitro and selected in G418 (▲). Lysates were prepared from 1×10^6 cells in 10 μl of CGLB buffer by three cycles of freeze and thaw. ADA enzyme activity was analyzed by the ^{14}C-adenosine to ^{14}C-inosine conversion assay followed by TLC (37). Cell lysates from individual clones (~2×10^5 cells) were normalized for protein content by the BIO-RAD protein assay (Bio-Rad Laboratories GmbH, Munich, Germany). Positive and negative controls were, respectively, lysates from normal PBLs and uninfected, IL-2–stimulated ADA$^-$ PBLs, because IL-2 stimulation is reported to increase the efficiency of ADA expression in ADA$^-$ cells (37). TLC plates were exposed for 3 days in a PhosphorImager (Molecular Dynamics, Sunnyvale, California). Ratio of adenosine conversion is expressed as nmol hour^{-1} mg^{-1}.

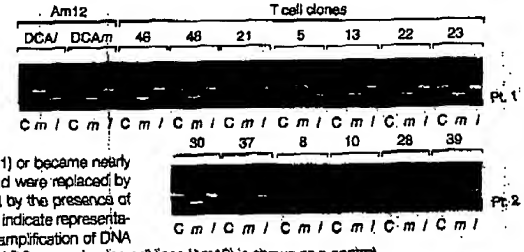

Fig. 3. Origin of T cell clones obtained from the peripheral blood of patient 1 (top) and patient 2 (bottom) 1 year after discontinuation of treatment. Clonable T cells containing the DCAI vector diminished markedly (patient 1) or became nearly undetectable (patient 2), and were replaced by BM-derived T cells, marked by the presence of the DCAm vector. Numbers indicate representative individual clones. PCR amplification of DNA obtained from the DCAI and DCAm packaging cell lines (Am12) is shown as a control.

Spontaneous revertants (ADA-positive, vector-negative) were not observed in either peripheral blood or BM.

Initially, the analysis of the retroviral vector amplified from the DNA of circulating lymphocytes indicated that genetically modified cells were derived from a pool of long-lived PBLs originally transduced with the DCAI vector (Fig. 1B). This finding was consistent throughout the period of administration of transduced PBLs and BM cells (Fig. 2B, at 7 and 19 months, for example), whereas total BM cells (Fig. 2B, at 21 and 35 months, for example) and circulating granulocytes (Fig. 2B, at 29 months, for example) always showed the DCAm-specific restriction pattern or marrow-derived cells. However, about 1 year after discontinuation of gene therapy, both PBL- and BM-derived lymphocytes were detectable in the circulation (Fig. 2B, at 35 months). At that time, Neo-resistant, clonable T cells containing the PBL-specific DCAI vector sharply decreased (Fig. 3, patient 1) or became undetectable (Fig. 3, patient 2) and were progressively replaced in the circulation by T cells containing the BM-specific, DCAm vector. To confirm this important finding, we evaluated two additional time points, subsequent to the data in Figs. 2 and 3, on bulk populations and on T lymphocyte clones. Thirty-eight clones from patient 1 were analyzed for their origin; 26 were derived from marrow, 6 could not be unequivocally determined, and 9 contained the DCAI vector. Similarly, of 49 clones obtained from patient 2, 6 could not be clearly determined, 6 contained the DCAI vector, and all others were derived from marrow.

These results show that short-term immune reconstitution was sustained in the two patients by a population of peripheral blood–derived, ADA-producing lymphocytes with a life-span in the circulation ranging between 6 and 12 months. We have previously shown that this population contains both mature T cells and immature, or naïve, precursors (*11*, *18*). Conversely, long-term reconstitution resulted almost exclusively from transduced, BM-derived hematopoietic stem and progenitor cells capable of generating multilineage progenies of ADA-producing cells, that is, lymphocytes, granulocytes, and (more recently) erythrocytes.

A fundamental hypothesis underlying this study was the possibility that genetically corrected cells would benefit from a selective advantage over noncorrected cells. Our experimental design has made it possible to obtain data in support of this hypothesis. The first line of evidence comes from the progressive appearance of marrow-derived PBLs, generated over time from a relatively small number of genetically modified precursors contained in the transduced marrow cell population (Figs. 2 and 3). Additional evidence comes from the analysis of the integrated retroviral vectors. In a recent comparative analysis of different vector constructs designed for gene transfer of reporter genes in human PBLs, we demonstrated that the DC construct carries an inherent instability that results in loss of the gene inserted in the viral LTR (*18*). Such instability could affect 50% of integrated proviruses, depending on the size and nature of the inserted gene. In the present study, the analysis of over 200 T cell clones obtained at different times during the follow-up of the two patients showed no rearrangement that might have eliminated the ADA gene, and consequently its expression. Conversely, loss of the ADA gene could be detected only in marrow-derived colonies and T cell clones that had been transduced and cultured in vitro, in the absence of any positive selection (*41*). These observations indicate that, in ADA$^-$ SCID patients, ADA-producing cells have a selective advantage over noncorrected ADA$^-$ cells, as previously suggested in the

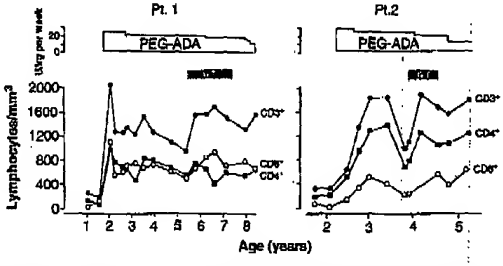

Fig. 4. Immune reconstitution during the PEG-ADA and gene therapy trial for patient 1 (left) and patient 2 (right). CD3$^+$, CD4$^+$, and CD8$^+$ lymphocyte counts are plotted against age for the duration of the trial. Doses of PEG-ADA administered to the patients are shown in the upper part of the graphs. The black boxes (GT) indicate the period of administration of genetically modified PBLs and BM cells (ticks indicate individual injections).

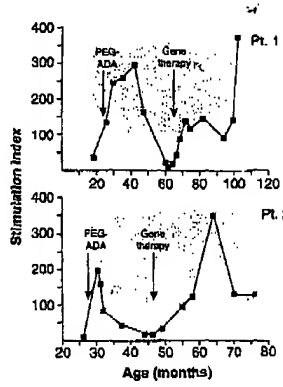

Fig. 5. Immune reconstitution during the PEG-ADA and gene therapy trial for patient 1 (top) and patient 2 (bottom). T cell proliferative response to mitogenic stimulus is presented as stimulation index (cpm of stimulated samples divided by cpm of unstimulated cells) and is plotted against age of the patients. Shaded areas indicate the range of the stimulation index of normal internal controls. Response to TT followed a comparable kinetics. Arrows indicate initiation of enzyme replacement therapy (PEG-ADA) and administration of genetically modified cells (gene therapy).

Table 1. Quantitation of isoagglutinin titer, and antigen-specific antibody production and proliferative response after vaccination with tetanus toxoid (TT). IgG, immunoglobulin G; ND, not done.

Time of test	Anti-B isoagglutinin titer		Serum titer of anti-TT IgG*		Proliferative response (10^3 cpm)†	
	Patient 1	Patient 2	Patient 1	Patient 2	Patient 1	Patient 2
Before immunization	ND	1/2	2.4	0.2	0.5	1.6
PEG-ADA response	1/8	1/16	1600	130	26.4	15.7
PEG-ADA failure	1.8	1.5	ND	34	1.8	1.5
After gene therapy I	1/16	1/32	ND	88	50.3	67.6
After gene therapy II	1/32	1/32	ND	ND	82.2	96.5

*Anti-TT IgG production was determined in a standard enzyme-linked immunosorbent assay and is reported as international units to a reference standard (Biagini Reference Standard, Biagini, Florence, Italy). †TT-specific T cell lines were tested for their capacity to proliferate in response to TT in the presence of autologous antigen-presenting cells (*45*). Proliferation in response to antigen-presenting cells alone was always <1000 cpm. Both patients received the full immunization schedule with TT (three doses) while on PEG-ADA. Patient 2 showed signs of immune deterioration during the immunization schedule. Isoagglutinin titer, TT-specific IgG titer, and TT-specific T-cell proliferation were measured at the following times: before immunization and before use of PEG-ADA (2 years and 5 months of age for patient 1 and 2 years and 10 months for patient 2), at the time of peak response to PEG-ADA (2 years since the beginning of PEG-ADA treatment for patient 1 and 1 year for patient 2), at PEG-ADA failure, and twice after gene therapy (6 and 8 years of age for patient 1 and 4.5 years and 5 years for patient 2).

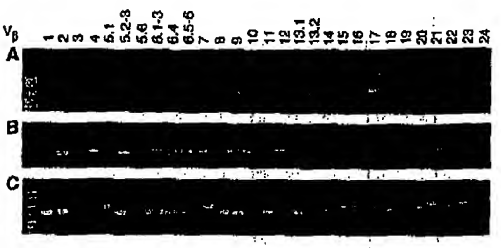

Fig. 6. Development of a normal T cell receptor repertoire in patient 1 after gene therapy treatment. Different T cell receptor V_β-chain usage at the time of failure of the PEG-ADA treatment (**A**), 1 year after the beginning of gene therapy (**B**), and 1 year after discontinuation of transduced cell administration (**C**), as analyzed by RT-PCR amplification with V_β chain-specific primers (*48*).

human PBL–SCID mouse preclinical model (*10, 11*).

Immune reconstitution induced by PEG-ADA treatment lasted for over 3 years in patient 1 and for a shorter period in patient 2, despite administration of a 50% higher PEG-ADA dose in the latter (Figs. 4 and 5). In association with a progressive decline in PBL counts, the immune response decreased markedly over a short period of time (Figs. 4 and 5 and Table 1). Administration of genetically modified cells rapidly restored immune functions in both patients, resulting in normalization of total lymphocyte counts (Fig. 4) and cellular and humoral responses, including sustained isohemagglutinin titer, antigen-specific antibody production, and mitogen- and antigen-specific proliferation (Fig. 5 and Table 1). The T cell receptor repertoire, analyzed by the V_β chain usage, normalized progressively (Fig. 6). In patient 2, the overall response to gene therapy was similar to that of patient 1, despite administration of a smaller number of genetically modified PBLs and BM cells. There have been no serious infections in the two patients throughout the PEG-ADA treatment and after the beginning of gene therapy. The patients received no other treatment, except for high-dose immunoglobulins administered intravenously and prophylactic antibiotic treatment, both of which were discontinued after indications of full immunologic reconstitution. Before the beginning of the PEG-ADA treatment, the patients showed severe growth failure, ranging below the fifth percentile for height and weight. Enzyme replacement and gene therapy had a marked clinical impact, resulting in normalization of height and weight. Patient 2, who had a very limited initial response to PEG-ADA, resumed normal growth only after gene therapy. Serum chemistry values, blood counts, and urinalysis indicated no toxicity from PEG-ADA or gene therapy treatments. Monitoring of the two patients for the presence of recombinant helper virus was consistently negative.

The results of the long-term follow-up have two main implications: the selection of an optimal treatment for ADA$^-$ SCID patients and, more generally, the potential application of similar gene therapy approaches to the treatment of genetic and acquired diseases. Our study clearly indicates the feasibility of direct BM cell gene therapy; however, in specific circumstances, genetically modified PBLs may provide a prompt supply of immune effector cells until development of BM-derived lymphocytes. If it is proven to be efficacious over time, this procedure could represent a less toxic alternative to unrelated or HLA-mismatched marrow transplants. In the prospective extension of these results to the design of other gene therapy clinical trials, gene transfer into hematopoietic progenitors can be achieved also in the absence of the stress conditions associated with cytoreduction and BM transplantation. However, in steady-state hematopoiesis a considerable time lag may be required before appearance of genetically modified cells in the blood. Under these conditions, the positive selection may represent an absolute requirement for favoring the appearance of vector-transduced cells. Such positive selection may be "naturally" present in other genetic or acquired diseases [for example, acquired immunodeficiency syndrome (AIDS)] or could be built into the vector as a drug-resistance gene.

REFERENCES AND NOTES

1. E. R. Giblett, J. E. Anderson, F. Cohen, B. Pollara, H. J. Meuwissen, *Lancet* ii, 1067 (1972).
2. R. Hirschorn, V. Roegner-Maniscalco, L. Kuritsky, F. Rosen, *J. Clin. Invest.* **68**, 1387 (1981).
3. Y. Reisner *et al.*, *Blood* **61**, 341 (1983).
4. R. J. O'Reilly, C. A. Keever, T. N. Small, J. Brochstein, *Immunodefic. Rev.* **1**, 273 (1989).
5. M. S. Hershfield *et al.*, *N. Engl. J. Med.* **316**, 589 (1987).
6. R. Parkman, *Science* **232**, 1373 (1986).
7. T. Friedmann, *Ibid.* **244**, 1275 (1988).
8. W. F. Anderson, *Ibid.* **256**, 808 (1992).
9. R. C. Mulligan, *Ibid.* **260**, 926 (1993).
10. G. Ferrari *et al.*, *Ibid.* **251**, 1363 (1993).
11. G. Ferrari *et al.*, *Blood* **80**, 1120 (1992).
12. C. Bordignon *et al.*, *Hum. Gene Ther.* **4**, 513 (1993).
13. C. von Kalle *et al.*, *Blood* **84**, 2850 (1994).
14. M. Flasshove *et al.*, *Ibid.* **85**, 566 (1995).
15. M. Bregni *et al.*, *Ibid.* **80**, 1418 (1992).
16. A. Kasid *et al.*, *Proc. Natl. Acad. Sci. U.S.A.* **87**, 473 (1990).
17. K. Culver *et al.*, *Ibid.* **88**, 3155 (1991).
18. F. Mavilio *et al.*, *Blood* **83**, 1988 (1994).
19. M. K. Brenner *et al.*, *Lancet* **341**, 85 (1993).
20. M. K. Brenner *et al.*, *Ibid.* **342**, 1134 (1993).
21. C. Dunbar *et al.*, *Blood* **85**, 3048 (1995).
22. N. M. Kredich and M. S. Hershfield, in *The Metabolic Bases of Inherited Disease* (McGraw-Hill, New York, 1983), pp. 1157–1183.
23. M. S. Hershfield *et al.*, *N. Engl. J. Med.* **316**, 589 (1987).
24. S. H. Polmar *et al.*, *Ibid.* **295**, 1337 (1976).
25. Y. Levy, M. Hershfield, C. Fernandez-Mejia, S. Polmar, *J. Pediatr.* **113**, 312 (1988).
26. A. Abuchowski, T. Van Es, N. C. Palczuk, J. R. McCoy, F. F. Davis, *Cancer Treat. Rep.* **63**, 1127 (1979).
27. R.-L. Chen, A. Abuchowski, T. Van Es, N. C. Palczuk, F. F. Davis, *Biochim. Biophys. Acta* **600**, 293 (1981).
28. B. Davis, E. Linney, H. Fan, *Nature* **314**, 550 (1985).
29. M. S. Hershfield, S. Chaffee, R. U. Sorensen, *Pediatr. Res.* **33**, S42 (1993).
30. L. D. Notarangelo *et al.*, *Eur. J. Pediatr.* **151**, 811 (1992).
31. Both patients were vaccinated with tetanus toxoid (TT; Swiss Serum Institute, Bern, Switzerland). To evaluate the number of precursor lymphocytes specific to TT, the frequency of cells capable of proliferating in the presence of irradiated autologous PBLs that had been pulsed overnight with TT was evaluated in a limiting dilution assay. At two different times after vaccination, the frequency of TT-specific lymphocyte precursors was 1:2500 and 1:5000 in patient 1. This range is comparable to that of normal individuals at the same time after immunization. Patient 2 showed signs of immune deterioration during the immunization schedule (Table 1).
32. P. A. Hantzopoulos, B. A. Sullenger, G. Ungers, E. Gilboa, *Proc. Natl. Acad. Sci. U.S.A.* **86**, 3519 (1989).
33. The double-copy DCA retroviral vector, carrying a human ADA minigene, has been described previously (*32*) and is indicated as DCA/ in this report. The DCA/*rn* vector was obtained by digestion, Klenow-filling, and religation of the DCA/ plasmid at the Mlu I restriction site in the polylinker region of the 3′ LTR, thus generating a new Bss HII site. The Am12/DCA*rn*-7 and the Am12/DCA/-16 clonal packaging cell lines were generated by the transinfection protocol, as described (*18*).
34. High molecular weight DNA was obtained from cells by standard phenol-chloroform extraction (*42*). A Neo-specific, 362-bp fragment located in the coding region of the NeoR gene or a DCA-specific 400-bp fragment spanning the 3′ end of the ADA cDNA, the polylinker, and part of the LTR U3 region, were amplified from 0.5 μg of genomic DNA by 30 cycles of PCR with 5 U of Taq polymerase (Perkin Elmer, Norwalk, CT) and 25 pmol of the primers Neo-1 (5′-GGAAGCCGGTCTTGTCGATC-3′), Neo-3 (5′-AGAGTCCCGCTCAGAAGAAC-3′), DCA-5 (5′-TCAATGCGGGCAAATCTAG-3′), and DCA-6 (5′-GCTGTTCCATCTGTTCCTGA-3′). DCA-specific PCR products were digested by Bss HII and Mlu I restriction enzymes (Boehringer Mannheim GmbH, Mannheim, Germany). Reaction mixtures (1/10th of the total volume) were separated on a 1.5% agarose gel, and DNA was visualized by ethidium bromide staining. DNA was transferred to a nylon membrane (Hybond-N, Amersham, Buckinghamshire, UK) by DNA capillary blotting (*42*) and hybridized to 10^7 dpm of ^{32}P-labeled, 1.2-kb Hind III–Sma I fragment of pSV2-neo (*43*), or 1.9 Kb Xho I fragment of the ADA cDNA. Filters were washed under high-stringency conditions and exposed to Kodak X-AR5 film for 30 min to overnight at −70°C.
35. Freshly isolated ADA$^-$ PBLs were obtained from ADA$^-$ SCID patients, Ficoll-fractionated, and grown at 10^6 cells/ml in 24-well tissue culture plates under phytohemagglutinin (PHA) (2 μg/ml; Boehringer Mannheim GmbH) and human recombinant IL-2 (hu-rIL-2, 100 U/ml; Eurocetus B.V., Amsterdam, Netherlands) stimulation in lipopolysaccharide-free RPMI 1640 medium supplemented with 2 mM L-glutamine and 5% human serum. In subsequent experiments similar levels of gene transfer could be obtained at 50 or 100 U of hu-rIL-2 per milliliter, in the absence of any additional stimulus (C. Benati *et al.*, in preparation). After 72 to 96 hours of stimulation, T lymphocytes were cocultivated with irradiated (10,000 roentgen) vector-producing cells for 72 hours in complete Dul-

becco's minimum essential medium (DMEM) in the presence of polybrene (8 μg/ml) as described (18). Cells were washed twice in phosphate-buffered saline (PBS), resuspended in fresh medium, and cultured for 3 to 4 days. Transduced cells were tested for the presence of helper virus and cryopreserved until use.

36. BM mononuclear cells were obtained as a Ficoll fraction and grown for 2 to 3 days in complete DMEM at a density of 6×10^5 to 8×10^5 cells/cm^2 (35). T cell depletion and progenitor cell enrichment were obtained as described (3, 35). Gene transfer was carried out by multiple infection cycles with cell-free, helper virus–tested viral supernatants in the presence of polybrene (8 μg/ml) (35). BM cells were maintained in a long-term culture system over adherent layers without addition of exogenous growth factors, and infected during the first 3 days of culture. Transduced cells were tested for the presence of helper virus and cryopreserved until use. At that time, the transduced cells were washed, resuspended in normal saline containing 4% human albumin, and reinfused into the patient.
37. C. Bordignon *et al.*, *Proc. Natl. Acad. Sci. U.S.A.* 86, 6748 (1989).
38. PHA blasts or antigen-specific T cells were cloned by limiting dilution. The relative frequencies of transduced cells was obtained by comparing the precursor frequency in the absence and presence of G418 (800 μg/ml). G418-resistant T cell clones were isolated and maintained as described (44, 45).
39. The relative frequencies of transduced BM progenitor cells were obtained by comparing the frequency of CFU-G, CFU-GM, BFU-E, and CFU-GEMM cells in the absence and presence of increasing doses of G418 (0.7, 1.0, 1.5 mg/ml) as described (37). In selected experiments, individual G418-resistant colonies were collected for analysis of vector transduction and expression.
40. M. J. Barnett *et al.*, *Blood* 84, 724 (1994).
41. C. Bordignon *et al.*, data not shown.
42. J. Sambrook, E. F. Fritsch, T. Maniatis, *Molecular Cloning: A Laboratory Manual* (Cold Spring Harbor Laboratory, Cold Spring Harbor, NY, ed. 2, 1989).
43. P. J. Southern and P. Berg, *J. Mol. Appl. Genet.* 1, 327 (1982).
44. A. Lanzavecchia, *Nature* 314, 537 (1985).
45. P. Panina-Bordignon *et al.*, *Eur. J. Immunol.* 19, 2237 (1989).
46. Y. Choi *et al.*, *Proc. Natl. Acad. Sci. U.S.A.* 86, 8941 (1989).
47. E. Y. Loh, J. F. Elliot, S. Cwirla, L. L. Lanier, M. M. Davis, *Science* 243, 217 (1989).
48. T cell receptor V_β-chain usage was analyzed on transduced T cell lines by reverse transcriptase–PCR. Briefly, total RNA was reverse transcribed with oligo(dT) and oligo(dG) primers and subjected to PCR with V_β- or C_β-specific oligonucleotides (46) or to anchored PCR with a C_β-specific oligonucleotide as described (47). Amplified products were analyzed by agarose gel electrophoresis.
49. We are indebted to L. Ruggieri and A. Wack for performing some of the ex vivo and in vitro analyses of gene transfer frequency; to the nurses and clinical staff of the Clinica Pediatrica, School of Medicine, University of Brescia, for skilled and dedicated care; to A. Amghini and A. Crescenzo for clinical assistance in the extended care of the two patients; to A. Plebani for dosing specific antibody production; to M. Hershfield, P. Dellabona, and A. Ballabio for helpful discussions; and to Enzon, Inc., and Orphan Europe for providing PEG-ADA before commercial distribution. Supported by grants from Telethon, the Italian National Research Council, and the Italian Ministry of Health (IV-VII AIDS Projects).

26 May 1995; accepted 27 September 1995

T Lymphocyte–Directed Gene Therapy for ADA$^-$ SCID: Initial Trial Results After 4 Years

R. Michael Blaese,* Kenneth W. Culver, A. Dusty Miller, Charles S. Carter, Thomas Fleisher, Mario Clerici,† Gene Shearer, Lauren Chang, Yawen Chiang, Paul Tolstoshev, Jay J. Greenblatt, Steven A. Rosenberg, Harvey Klein, Melvin Berger, Craig A. Mullen,‡ W. Jay Ramsey, Linda Muul, Richard A. Morgan, W. French Anderson§

In 1990, a clinical trial was started using retroviral-mediated transfer of the adenosine deaminase (ADA) gene into the T cells of two children with severe combined immunodeficiency (ADA$^-$ SCID). The number of blood T cells normalized as did many cellular and humoral immune responses. Gene treatment ended after 2 years, but integrated vector and ADA gene expression in T cells persisted. Although many components remain to be perfected, it is concluded here that gene therapy can be a safe and effective addition to treatment for some patients with this severe immunodeficiency disease.

The possibility of using gene transfer as a therapy for human disease has great appeal. The decision to enter clinical trials awaited the development of safe and efficient techniques of gene transfer and improved understanding of the basic pathology and biology underlying likely candidate diseases and target cells. The advent of useful retroviral vectors that permitted relatively high efficiency gene transfer and stable integration was a critical advance (*1*, *2*), as was the demonstration that this procedure of gene transfer could be effectively and safely used in humans (*3*).

Severe combined immunodeficiency secondary to a genetic defect in the purine catabolic enzyme adenosine deaminase [ADA$^-$ SCID] is characterized by defective T and B cell function and recurrent infections, often involving opportunistic pathogens. Large amounts of deoxyadenosine, an ADA substrate, are present in these patients; deoxyadenosine is preferentially converted to the toxic compound deoxyadenosine triphosphate in T cells, disabling the immune system (*4*).

Because this disease is curable by allogeneic bone marrow transplantation given without pretransplantation cytoreductive conditioning, it was initially assumed that gene therapy should be directed at the bone marrow stem cell. However, initial attempts to use stem cell gene transfer in primates resulted in only low-level, transient gene expression, insufficient for clinical use. The observation that the only donor cells detected in some patients "cured" by allogeneic bone marrow transplantation was their T cells—the others remaining ADA-deficient (*5*)—raised the possibility that T cell–directed gene therapy also might be a useful treatment.

The introduction of enzyme replacement with ADA-containing erythrocytes (*6*) or with bovine ADA conjugated with polyethylene glycol (PEG-ADA) (*7*) has made this approach feasible. PEG-ADA has provided noncurative, life-saving treatment for ADA$^-$ SCID patients; with this treatment, most patients have experienced weight gain and decreased opportunistic infections. Full immune reconstitution has been less regularly achieved with enzyme therapy. T cell function as measured by in vitro mitogen responses improved in most patients, but fewer patients recovered consistent immune responses to specific antigens [for instance, as measured by normal delayed-type hypersensitivity (DTH) skin test reactivity] (*8*–*10*). Nearly all PEG-ADA–treated patients showed increased peripheral T cell counts, which provided a source of T cells for gene correction not available without enzyme therapy. Furthermore, enzyme treatment could be continued during the gene therapy trial so that the ethical dilemma of withholding or stopping a life-saving therapy to test an unknown treatment could be avoided.

The adenosine deaminase complementary DNA (cDNA) (*11*) is 1.5 kb and fits within a retroviral vector. With the use of an ADA-containing retroviral vector, ADA-deficient T cell lines were transduced to express normal amounts of ADA; this rendered them normally resistant to intoxication and growth inhibition when challenged with deoxyadenosine (*12*, *13*). Next, studies in mice, rabbits, and nonhuman primates using T cells modified with retroviral vectors showed normal cell survival and function after their reintroduction into recipient animals (*14*). Finally, Bordignon and colleagues (*15*) showed that ADA gene–corrected T cells acquired a survival advantage compared with uncorrected ADA-deficient cells when transplanted into immunodeficient, but ADA-

Successful Peripheral T-Lymph cyte–Directed Gene Transfer for a Patient With Severe Combined Immune Deficiency Caused by Adenosine Deaminase Deficiency

By Masafumi Onodera, Tadashi Ariga, Nobuaki Kawamura, Ichiro Kobayashi, Makoto Ohtsu, Masafumi Yamada, Atsushi Tame, Hirofumi Furuta, Motohiko Okano, Shuzo Matsumoto, Hitoshi Kotani, Gerard J. McGarrity, R. Michael Blaese, and Yukio Sakiyama

Ten patients with adenosine deaminase deficiency (ADA$^-$) have been enrolled in gene therapy clinical trials since the first patient was treated in September 1990. We describe a Japanese ADA$^-$ severe combined immune deficiency (SCID) patient who has received periodic infusions of genetically modified autologous T lymphocytes transduced with the human ADA cDNA containing retroviral vector LASN. The percentage of peripheral blood lymphocytes carrying the transduced ADA gene has remained stable at 10% to 20% during the 12 months since the fourth infusion. ADA enzyme activity in the patient's circulating T cells, which was only marginally detected before gene transfer, increased to levels comparable to those of a heterozygous carrier individual and was associated with increased T-lymphocyte counts and improvement of the patient's immune function. The results obtained in this trial are in agreement with previously published observations and support the usefulness of T lymphocyte-directed gene transfer in the treatment of ADA$^-$SCID.

ADENOSINE DEAMINASE (EC3.5.4.4; ADA) is an enzyme in the purine salvage pathway that is critical for the deamination of adenosine and deoxyadenosine and consequent formation of inosine and deoxyinosine, respectively. The deficiency of ADA impairs the function of the human immune system resulting in severe combined immunodeficiency (SCID) characterized by severe T lymphocyte dysfunction and agammaglobulinemia.[1-3] The clinical course of inherited ADA deficiency (ADA$^-$) ranges from the rapidly fatal, early onset of classical ADA$^-$SCID to the minimally dysfunctional immune system of patients presenting "partial" ADA deficiency.[4,5] A recent review classified ADA deficiency into four types as determined by the age at clinical onset and suggested that these variants are the result of different, specific mutations resulting in various severities of enzyme dysfunction.[6]

Although the current treatment of choice for ADA$^-$SCID is an HLA-matched bone marrow transplant,[7] less than one third of patients have access to an appropriate donor. An alternative is enzyme replacement using polyethene glycol-modified bovine ADA (PEG-ADA). This represents a life saving, but costly, therapeutic option for the patients that do not have an HLA-matched donor.[8,9] Although enzyme replacement with PEG-ADA partially reconstitutes the immune function of most patients with ADA$^-$SCID, a few patients have been unresponsive to PEG-ADA.

The determination of the complete sequence of both the ADA cDNA[10-12] and the genomic ADA structural gene[13] has facilitated the molecular analysis of ADA$^-$ patients and permitted identification of various genetic mutations in unrelated ADA$^-$ patients. Early identification of the mutant gene led ADA$^-$SCID to become the first disorder to be treated by gene therapy. Two ADA$^-$SCID patients who had manifested differing levels of severity of persistent immunodeficiency despite continuous treatment with PEG-ADA thus were enrolled in 1990.[14] Since then, 10 patients with ADA$^-$SCID have undergone gene therapy as recently described.[14-17] The strategies adopted in these trials have differed and the efficacy of treatment has varied.

We report the molecular analysis of the genetic defect in an ADA$^-$SCID patient enrolled in the first gene therapy protocol in Japan and analyze the clinical results obtained during the first 18 months of this clinical trial.

MATERIALS AND METHODS

Cell culture. B-lymphoblastoid cell lines (B-LCL) were established from our ADA$^-$SCID patient, his parents and a healthy volunteer by Epstein-Bar Virus (EBV) transformation. B-LCL were maintained in RPMI-1640 medium (GIBCO-BRL, Grand Island, NY) with 10% fetal calf serum (FCS; GIBCO-BRL) and 50 mmol/L β-mercaptoethanol (Sigma Chemical Co, St Louis, MO).

Sequence analysis of patient's ADA cDNA and genomic DNA. For the analysis of the ADA cDNA sequence, total cellular RNA was isolated from B-LCL using TRIZOL Reagent (GIBCO-BRL). First-strand cDNA was synthesized from 2 μg of total cellular RNA (First strand synthesis kit; Promega, Madison, WI). Full-length ADA cDNA fragments extending from the translation start site codon to 230 base pair (bp) 3′ of the stop codon were amplified by reverse transcriptase-polymerase chain reaction (RT-PCR). Oligonucleotide primers for RT-PCR were as follows: sense primer; CCATGGCCCAGACGCCCGCCTT, antisense primer; ACCATAGCCCATGTGCAAGGGC. Reactions containing 0.5 μL (2.5 U) *Taq* polymerase (*TaKaRa Ex Taq*, TaKaRa Shuzo Co, Ltd, Tokyo, Japan) were incubated for 30 cycles of 60 seconds at 92°C, 90 seconds at 58°C, and 180 seconds at 72°C with the extension time at 72°C increased to 10 minutes in the last cycle. Amplified products were isolated from 1.0% agarose gel and then subcloned into pCR II vector (Invitrogen, San Diego, CA). Sequence analysis of double-stranded DNA was performed using Sequenase version II DNA sequencing kit (Amersham Life Science, Arlington

From the Department of Pediatrics, Hokkaido University School of Medicine, Sapporo, Japan; Clinical Gene Therapy Branch, National Human Genome Research Institute, National Institutes of Health, Bethesda, MD; Institute of Medical Science, Health Sciences University of Hokkaido, Ainosato, Sapporo, Japan; and Genetic Therapy, Inc, Gaithersburg, MD.

Submitted May 28, 1997; accepted August 20, 1997.

Supported by the grant for Scientific Research Expenses for Health and Welfare Programs (Funds of Highly Advances Medical Research), Tokyo, Japan.

Address reprint requests to Yukio Sakiyama, MD, PhD, Department of Pediatrics, Hokkaido University School of Medicine, North 15, West 7, Kita-ku, Sapporo, 060 Japan.

The publication costs of this article were defrayed in part by page charge payment. This article must therefore be hereby marked "advertisement" in accordance with 18 U.S.C. section 1734 solely to indicate this fact.

0006-4971/98/9101-0006$3.00/0

Heights, IL) with [^{35}S]dATP (Amersham Life Science) and a series of ADA-specific primers. Amplified products were sequenced through a 6% acrylamide gel (National Diagnostics, Atlanta, GA). To analyze the ADA genomic sequence, high molecular DNA was obtained from B-LCL by standard techniques.[18] Primers and PCR conditions for amplification of ADA all exons have also been described previously.[19-21] Amplified products were isolated from agarose gel and sequenced directly using the Thermal Cycler DNA sequencing kit (Circum Vent; New England Biolabs Inc, Beverly, MA). ADA cDNA sequences are numbered relative to the start site of translation and genomic DNA according to Wiginton et al.[13]

Southern blot analysis. High molecular weight DNA from B-LCL was digested with restriction endonuclease *Rsa* I, separated in 1.0% agarose gel, and transferred onto a nylon membrane (Biotrace HP; Gelman Sciences, Ann Arbor, MI). Filters were then hybridized to a ^{32}P randomly labeled 444-bp *Rsa* I-*Pst* I fragment from the ADA cDNA.

Retroviral-mediated gene transfer into patient's peripheral T cells. The clinical protocol used here has been described elsewhere.[22] Briefly, peripheral T lymphocytes from the patient were obtained by apheresis (CS3000 plus, Baxter Corp, Chicago, IL), isolated by density gradient centrifugation, and then maintained in AIM-V medium (GIBCO-BRL) supplemented with 5% FCS (GIBCO-BRL), 100 U/mL of recombinant human IL-2 (rIL-2, SHIONOGI, Osaka, Japan) and 10 ng/mL of anti-CD3 antibody (Orthoclone OKT3 Injection; Ortho, Raritan, NJ) in gas-permeable culture bags (Nipro Pretobag; Nishyo, Osaka, Japan). After 72 hours, half of the medium was removed and replaced with supernatant containing the LASN retroviral vector[23] supplemented with interleukin-2 (IL-2) and 10 μg/mL of protamine (Shimizu, Shimizu City, Japan). The LASN supernatant, prepared under Good Manufacturing Practices guidelines, was supplied by Genetic Therapy Inc (Gaithersburg, MD). The transduction procedure was repeated twice following an optimized transduction protocol combining low-temperature (32°C) incubation and centrifugation.[24] After two rounds of transduction, the virus supernatant was replaced with fresh medium supplemented with IL-2 and the cells were cultured for an additional 6 days. At the 11th day of culture, the cells were harvested and washed extensively with saline containing 0.5% human albumin and then reinfused into the patient.

Analysis of the inserted proviral genome by semi-quantitative PCR. Sense (GAGGCTGTGAAGAGCGGCAT) and anti-sense (CTCGAAGTGCATGTTTTCCT) primers were designed to match the sequence of the start site of exon 7 and the end of exon 8, respectively. Using these primers, the amplification of DNA samples from vector-containing cells generates two bands; the larger one (250 bp) derived from the endogenous ADA gene containing intron 7 (76 bp) and the smaller one (174 bp) from the LASN provirus. To evaluate the frequency of transduced cells in the patient's peripheral blood, a standard curve was prepared from a serial dilution of in vitro-transduced and G418-selected B-LCL with untransduced cells. The ratio of the amount of amplified ADA cDNA derived from the integrated vector and the amplified genomic sequence was calculated after hybridization with an ADA cDNA probe.

Thin-layer chromatography (TLC) analysis of ADA enzyme activity. Mononuclear cells were washed twice with phosphate-buffed saline to remove FCS and then suspended in 100 mmol/L Tris, pH 7.4 containing 1% bovine serum albumin. Cell lysates were obtained by 5 rapid freeze-thaw cycles. Cellular debris was removed by centrifugation and the lysates were stored at −80°C until used. ADA enzyme activity was assayed by the measurement of the conversion of [^{14}C] adenosine (Amersham Life Science) to [^{14}C] inosine and [^{14}C] hypoxanthine followed by TLC separation of the reaction products performed as previously described.[25] The results were expressed as nanomoles of inosine and hypoxanthine produced per min by 10^8 cells (nmol/min/10^8 cells).

RESULTS

Clinical course. The patient is a 5-year-old Japanese male. Symptoms including a chronic productive cough and a purulent nasal discharge began at 8 months of age. At 10 months he developed respiratory distress and was hospitalized for the treatment of severe pneumonia that was unresponsive to antibiotics. On admission at age 10 months, the patient had lymphopenia (absolute lymphocyte count 520/μL), with few mature T and B lymphocytes (CD3, 125/μL; CD4, 62/μL; CD8, 41/μL; CD19, 26/μL) and low serum Ig levels (IgG, 342 mg/dL; IgA, 18 mg/dL; and IgM, 60 mg/dL). Both humoral and cellular immunity were defective, with undetectable isohemagglutinins and absent T-cell proliferative responses to phytohemagglutinin, Concanavalin A, and pokeweed mitogen. Since ADA activity in his red blood cells (RBCs) was undetectable and the deoxyadenosine triphosphate (dATP) level was 506 nmol/mL RBCs (normal <2 nmol/mL), the diagnosis of SCID due to ADA deficiency of the "delayed onset" type[6] was established. In the absence of a suitable bone marrow donor, PEG-ADA therapy was initiated at 15 months of age and supplemented with intravenous Ig (IVIG). After treatment with PEG-ADA (37.5 U/kg/wk), the plasma ADA activity in the patient's peripheral blood increased from 0.14 to 53.15 μmol/h/mL and the peripheral blood lymphocyte (PBL) count increased to the range of 1,000 to 2,000/μL. Despite continuous PEG-ADA treatment, however, his Ig levels remained below normal and the lymphopenia recurred during the second year of enzyme replacement. The PBL count decreased to less than 1,000/μL with CD3$^+$ cell counts of 400/μL before the start of gene therapy (PBL, 702/μL; CD3, 400/μL; CD4, 205/μL; CD8, 191/μL; CD19, 57/μL on protocol day 0).

Identification of mutations responsible for ADA deficiency. To analyze mutations in our patient, we amplified full-length ADA cDNA from the patient's EBV transformed B-LCL by RT-PCR. Sequence analysis revealed that all of the clones (6/6) carried a G^{632} to A transition resulting in replacement of the arginine residue by histidine at codon 211 (Fig 1A). The mutation eliminates a recognition site for the restriction enzyme *Rsa* I. We took advantage of this feature to distinguish the mutated allele from the normal allele.[19] High molecular weight DNA extracted from the patient's B-LCL was digested with *Rsa* I, blotted and hybridized to an ADA cDNA probe spanning the region from this mutation site in exon 7 to the end of exon 11 (Fig 1B). *Rsa* I digestion showed both a normal (3.1 kb) and a larger fragment (4.4 kb) in the patient lane, indicating that the patient was heterozygous for loss of the *Rsa* I recognition site in exon 7. To determine the parental derivation, amplified genomic fragments spanning intron 6 to intron 9 of the patient and his parents were digested with *Rsa* I and electrophoresed in 2% agarose gel (Fig 1C). The patient's digestion pattern was identical to that obtained from the analysis of the father's DNA, indicating that this mutation was derived from the paternal allele.

Northern blot analyses showed that the quantity of the ADA message from both the patient and his mother was reduced to approximately half of control (data not shown). All cDNA clones carried the paternal missense mutation, suggesting that the mutation derived from the maternal allele resulted in undetectable mRNA. To characterize this mutation, we ana-

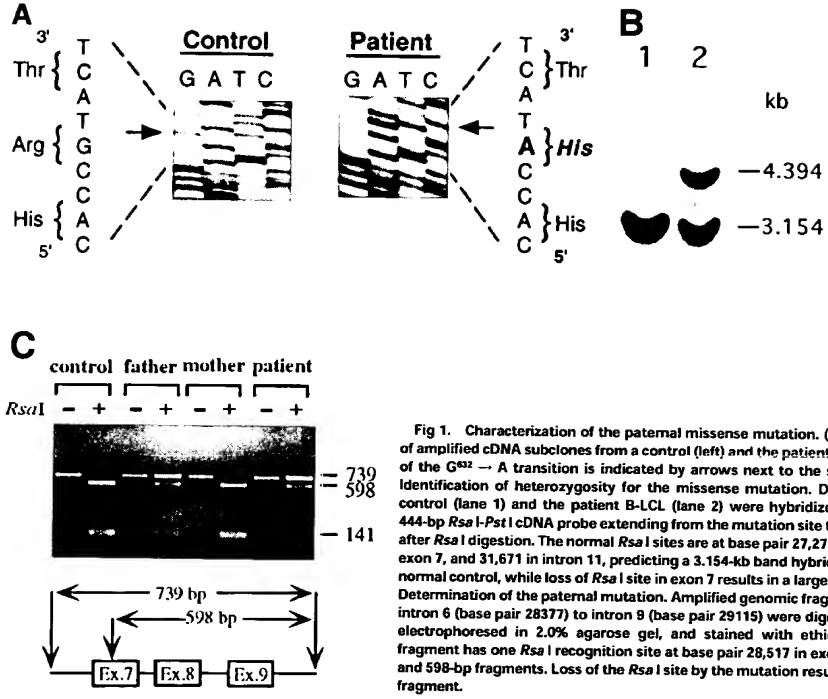

Fig 1. Characterization of the paternal missense mutation. (A) Sequence (sense) of amplified cDNA subclones from a control (left) and the patient (right). The position of the $G^{632} \rightarrow A$ transition is indicated by arrows next to the sequence ladder. (B) Identification of heterozygosity for the missense mutation. DNA samples from a control (lane 1) and the patient B-LCL (lane 2) were hybridized to a radiolabeled 444-bp *Rsa* I-*Pst* I cDNA probe extending from the mutation site to the end of exon 11 after *Rsa* I digestion. The normal *Rsa* I sites are at base pair 27,276 in exon 6, 28,516 in exon 7, and 31,671 in intron 11, predicting a 3.154-kb band hybridized to the probe in normal control, while loss of *Rsa* I site in exon 7 results in a larger band (4.394 kb). (C) Determination of the paternal mutation. Amplified genomic fragments (739 bp) from intron 6 (base pair 28377) to intron 9 (base pair 29115) were digested with *Rsa* I and electrophoresed in 2.0% agarose gel, and stained with ethidium bromide. The fragment has one *Rsa* I recognition site at base pair 28,517 in exon 7, predicting 141- and 598-bp fragments. Loss of the *Rsa* I site by the mutation results in an undigested fragment.

lyzed exons 1 to 11 by PCR amplification of genomic DNA and direct sequencing. Sequence analyses of the amplified fragments including exon 2 showed the patient to be heteroallelic for a splice site mutation at the first position of intron 2 ($G^{+1} \rightarrow A$ transversion) (Fig 2A). This mutation eliminates a recognition site for the restriction enzyme *Bsp*MI. *Bsp*MI digestion showed that the patient and his mother were heterozygous for this mutation, while the father showed a normal individual digestion pattern (Fig 2B). Reports of mutation analyses of other patients have shown that a mutation affecting a mRNA splicing mechanism may give rise to a nonfunctional or unstable mRNA.[26,27] This mechanism is also supported by the fact that *Rsa* I digestion showed that all full-length cDNA clones (48/48) from the patient's B-LCL carried the paternal G^{632} to A missense mutation.

Retroviral mediated gene transfer into peripheral T cells. At the age of 4, the patient was enrolled in a clinical gene therapy trial that repeated the protocol of the first gene therapy experiment at the National Institutes of Health (NIH) in 1990.[22] The patient's peripheral mononuclear cells, obtained by apheresis, were stimulated with IL-2 (100 U/mL) and anti-CD3 antibody (OKT3; 10 ng/mL). After 72 hours of stimulation, they were transduced twice during the next 48 hours by exposure to the ADA retroviral vector LASN, expanded 20- to 50-fold in number by culturing for 6 days after the beginning of transduction, and then reinfused into the patient (see Materials and Methods). No selection procedure to enrich for gene-transduced cells was performed. Semiquantitative PCR of the cells in the first and second infusions revealed that the frequency of the vector-carrying cells ranged from 3% to 7% (data not shown).

Clinical course after gene therapy. The patient received a total of 10 infusions over the 18-month period (Fig 3). A striking increase in lymphocyte number was observed early in the trial, followed by a gradual return to the basal level. This was followed by a sustained increase after the 8th infusion (protocol day 322) and the patient's PBL count has since remained in the normal range (PBL, 1,980/μL; CD3, 1,822/μL; CD4, 240/μL; CD8, 1,538/μL; CD19, 154/μL on protocol day 429). Progressive inversion of CD4/CD8 ratio has been observed since the 4th infusion due to an increase of the absolute $CD8^+$ cell count. This phenomenon is thought to be the result of preferential proliferation of $CD8^+$ cells during in vitro culture and transduction. ADA enzyme activity, nearly undetectable in the patient's lymphocytes before gene therapy, also increased progressively after the 7th infusion (protocol day 252) and reached 27 U on protocol day 476, which is approximately comparable to that of a heterozygous carrier individual (the patient's mother, 34.8 U).

The number of transduced cells in the patient's peripheral blood were assessed by semiquantitative PCR using PBL obtained before each infusion (Fig 4). The frequency of the genetically modified cells increased with the number of infusions of the ADA gene transduced lymphocytes and exceeded 10% of total circulating mononuclear cells just before the 5th infusion (on protocol day 126; Fig 4, lane 4). The frequency

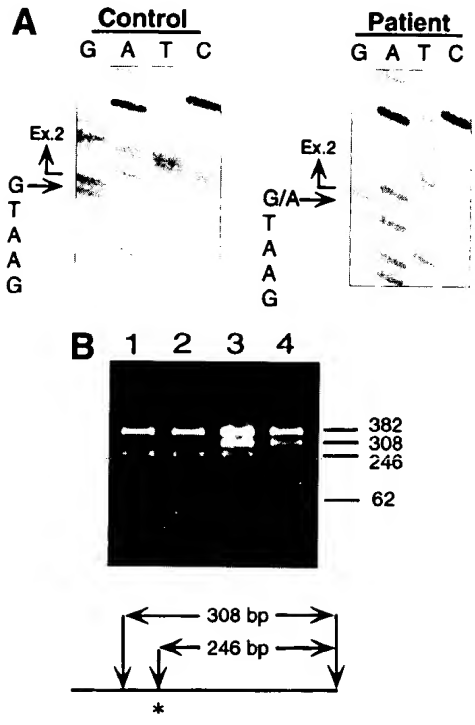

Fig 2. Identification of the maternal mutation at the splice donor site in intron 2. (A) Sequence (sense) of the exon 2/intron 2 junction in amplified genomic DNA. Genomic fragments containing exon 2 were amplified from a control (left) and the patient (right) and sequenced directly. A mutation at the splice donor site in intron 2 ($G^{+1} \rightarrow A$) is indicated by arrows. (B) Detection of the splice site mutation by the *Bsp*MI digestion. Amplified genomic fragments (690 bp) from intron 1 (bp 14,901) to intron 2 (base pair 15,590) was digested with *Bsp*MI, electrophoresed in 2.0% agarose gel, and stained with ethidium bromide. The fragment has two *Bsp*MI recognition sites at bp 15,282 and 15,344, predicting 62-, 246-, and 382-bp fragments in the control lane. Loss of the *Bsp*MI site (base pair 15,282) by the mutation results in the undigested fragment (308 bp). Lane 1, control; lane 2, father; lane 3, mother; and lane 4, patient. *Bsp*MI digestion shows the patient and his mother were heterozygous for the splice site mutation.

measured before each of the 6th through 10th infusions (on protocol days 210 to 462) has remained stable at 10% to 20%.

To evaluate the functional consequences of the ADA enzyme activity that had been induced by gene transfer, we compared the patient's immune function before and after the treatment (Table 1). Eleven months after beginning gene therapy, the patient's isohemagglutinin titer (IgG) increased from undetectable to 1:16 and delayed-type hypersensitivity (DTH) skin test responses became stronger. The interval between IVIG infusions which were given monthly before gene therapy, was widened and eventually stopped after gene therapy. Despite this, the patient's serum Ig levels gradually increased and have remained normal for more than a half year without additional IVIG treatment (Fig 3 and Table 1). These results suggest that the accumulated genetically corrected T lymphocytes in the patient's peripheral blood are associated with improvement of cellular and humoral immune responses and an increase in his circulating lymphocyte count. Although he sometimes became transiently febrile after infusions, the patient showed no serious adverse reactions to the treatments.

DISCUSSION

Advances in molecular biology during the past 3 decades have suggested that gene transfer could provide a new approach to the treatment of inherited diseases as well as acquired disorders such as cancer and acquired immune deficiency syndrome.[28] The number of active gene therapy protocols has increased greatly since the first clinical gene therapy trial.[29] ADA-SCID is one of the few early candidate disorders suitable for such interventions.[30] Accordingly, 10 ADA-SCID patients have been enrolled in gene therapy clinical protocols that employed different strategies, retroviral vector designs, and target cell populations. The results obtained from these trials have recently been reported.[14-17]

This trial of gene therapy for an ADA-SCID patient in Japan began in August 1995. Over the next 18 months he received a total of 10 infusions of cultured-expanded autologous T cells that had been transduced with the LASN retroviral vector. After an initial period of fluctuating counts, the patient's T cells stabilized in the normal range and this has been sustained for the last half year. The frequency of integrated provirus in the patient's peripheral blood increased to approximately 15% (0.1 to 0.2 proviral copies/cell) by the 4th infusion and has remained stable since that time. The patient's cell associated adenosine deaminase enzyme activity has increased from barely detectable before treatment to values approaching those found in the peripheral mononuclear cells of his heterozygous carrier mother. Delayed hypersensitivity skin tests, a measure of T-cell function, have improved. Isohemagglutinin titers have also increased and his dependence on infusions of normal gammaglobulin has eased. The patient has gained 3 kg in weight during this trial. He is still receiving periodic PEG-ADA replacement and is attending public school with no more infections than his classmates.

The period of observation has simply not been sufficient to assess the full breadth or the duration of this improved clinical status and immune responsiveness. Further, additional studies will be required to reconcile the apparent dissociation between the level of T-cell ADA observed and the proportion of cells containing integrated vector at different time points. Also, the effect of withdrawal of the exogenous PEG-ADA treatment must await more complete characterization of the quality of the patient's immune system and the repertoire of specificities represented in the transduced T-cell population.

Four gene therapy clinical trials including 10 ADA-SCID patients have been performed since the first trial in 1990. Although these trials provided much data that suggested how future gene therapy might be improved by changing retroviral vector design, transduction methods and target cell populations, we found it difficult to compare the efficacy of these various trials because of differences inherent within these basic strate-

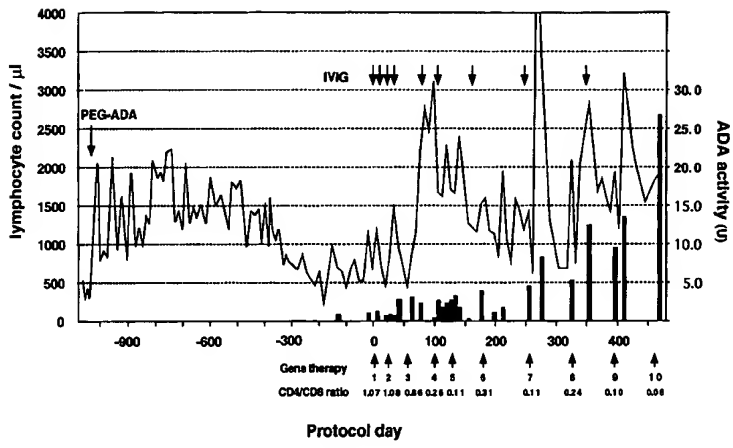

Fig 3. Clinical course before and after gene therapy. Gene therapy started on August 1, 1995 (protocol day 0) with the patient receiving a total of 10 infusions to date. PEG-ADA therapy was initiated at 15 months of age. The lymphocyte count is indicated by a solid line and CD4/CD8 ratio was measured using PBL before infusion. ADA activity shown by a solid bar is expressed as nanomoles of inosine and hypoxanthine produced per minute by 10^6 cells. Replacement of IVIG after gene therapy is shown as an arrow. The patient received a Ig replacement (2.5 g) monthly before gene therapy.

gies. Our trial has been performed following the identical protocol and vector preparations and autologous T lymphocyte isolation procedures that were used in the NIH trial. From this perspective, our trial provides an additional opportunity to evaluate the effectiveness of peripheral T lymphocyte-directed gene therapy for ADA$^-$SCID patients. Interestingly, the clinical course of our patient is quite similar to that observed in patient 1 in the NIH trial. Both trials have shown high gene transfer efficiency, remarkable increase of the ADA enzyme activity and eventual improvement of immune function. In contrast, patient 2 in the NIH trial experienced a low gene transfer efficiency and no significant increase in the ADA enzyme activity even though she exhibited some increase in immunological function. Although the factors leading to this difference have not yet been completely identified, a striking difference in the transduction efficiency of peripheral T cells between the three patients may be relevant. Transduction efficiencies before infusion were 3% to 7% for the present case, 1% to 10% for patient 1 and 0.1% to 1% for patient 2 in the NIH trial. An abbreviated proliferative capacity of patient 2 in the NIH trial was also observed. In addition, a contribution of the development of an immune response to the neomycin resistance gene must be considered since the existence of dominant selectable markers of nonhuman origin may result in unwanted immune reactivity that could eliminate or functionally impair transgene-expressing cells.[31]

The severity of the underlying ADA gene defects could also affect gene transfer. In addition to the mutation analysis reported here, specific ADA gene defects have also been reported for the two NIH patients.[20] These three cases can be classified by the severity of their clinical presentation. Both the present case and patient 1 in the NIH trial are of the "delayed onset" type, have splice site mutation defects and have achieved significant levels of "gene-corrected" circulating cells. However, the NIH patient 2 carries compound missense mutations and has manifested low transduction efficiency despite her less severe "late onset" type of presentation at age 5. Although there are insufficient numbers of treated patients to draw firm conclusions at this point, it does appear thus far that the responses of patients with "more severe" gene defects and clinical presentations are at least as responsive as cases with "milder ADA defects."

It should be noted that the ADA gene transduced T lymphocytes possess a selective advantage over the nontransduced cells due to the latter's high intracellular concentration of deoxyadenosine.[32,33] In the ADA$^-$ newborn trial using gene-corrected CD34$^+$ cells obtained from the patient's umbilical cord blood,[16] LASN vector was detected in the peripheral blood T cells of these patients at a stable frequency of approximately 0.01% during the first 18 months of observation. Then, after a 50% reduction in their weekly dose of PEG-ADA, the proportion of

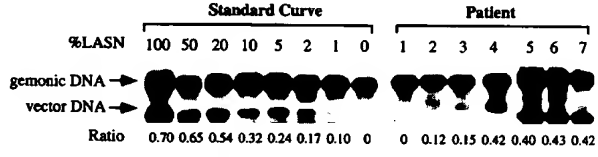

Fig 4. Semiquantitative PCR analysis to evaluate the frequency of vector-carrying cells in the patient's peripheral blood. Patient's mononuclear cells were obtained before the indicated infusion: before gene therapy (lane 1), 2nd infusion (protocol day [D] 21-lane 2), 4th infusion (D 98-lane 3), 5th infusion (D 126-lane 4), 6th infusion (D 175-lane 5), 8th infusion (D 322-lane 6, and 10th infusion (D 462-lane 7), and assayed for the frequency of vector containing cells by semiquantitative PCR. A standard was prepared by diluting cells containing the LASN vector with nontransduced cells. The ratio was determined by comparing the density of the cDNA derived band to that of the genomic DNA derived band.

Table 1. Isohemagglutinin Titer, DTH Skin Test Reactivity, and Ig Levels Before and After Gene Therapy

		Before	After
Isohemagglutinin titer	(IgG)	<2	16
DTH skin test (mm)	PPD*	8 × 7	12 × 10
	Candida	3 × 3	18 × 9
	Tetanus	N.D.	6 × 5
Igs	IgG	720	811
	IgA	20	53
	IgM	84	128

Isohemagglutinin titer and DTH skin tests were tested using standard protocols before gene therapy (before) and at 11 months after the beginning of gene therapy (after) while on PEG-ADA. The patient serum Ig levels were measured just before the Ig replacement on protocol day −60 (before) and 478 (after). The patient received the last Ig replacement at protocol day 348.

*The patient had been immunized with BCG at 5 months of age.

ADA vector-containing T cells in the blood increased to approximately 10% in each case (D.B. Kohn, personal communication, September 1995). In the present case, the dosage schedule of PEG-ADA enzyme has remained constant since the beginning of the trial (18 U/kg/wk on the protocol day 431), during which time the patient's immune function has substantially improved. It might be expected that the proportion of the transduced cells in the patient's PBL will increase as the PEG-ADA dosage is decreased.

To date, three clinical trials have been performed to assess the possibility of treating ADA-SCID patients by correcting hematopoietic progenitor cells.[15-17] The results obtained from these trials suggest that cord blood provides a stem cell population more suitable for efficient retroviral-mediated gene transfer than does bone marrow. Taken with the observations made in the NIH trial, our results strongly suggest that the effectiveness of T lymphocyte-directed gene transfer is a viable addition to the treatment programs that should be considered for ADA-SCID patients. After additional courses of treatment and continued observation to determine the breadth and durability of these positive responses, we hope to reduce or eliminate exogenous ADA enzyme supplementation in this patient. Improvements in vector design to permit higher levels of ADA expression and innovative strategies that provide greater efficiency of stem cell gene transduction may make gene therapy the treatment of choice for ADA-SCID patients.

ACKNOWLEDGMENT

We are grateful to Dr M.S. Hershfield for measuring some ADA activities and providing PEG-ADA, Dr A. Wakisaka for semiquantitative PCR, Drs L.M. Muul, C. Carter, and C. Wannebo for the transduction methods, Drs R.A. Knazek, F. Candotti, and D.M. Nelson for their critical review for the manuscript.

REFERENCES

1. Giblett ER, Anderson JE, Cohen F, Pollara B, Meuwissen HJ: Adenosine-deaminase deficiency in two patients with severely impaired cellular immunity. Lancet 2:1067, 1972

2. Kredich NM, Hershfield MS: Immunodeficiency disease associated with adenosine deaminase deficiency and purine nucleoside phosphorylase deficiency, in Scriver CM, Beaudet AL, Sly WS, Valle D (eds): The metabolic basis of inherited disease (ed 5). New York, NY, McGraw Hill, 1989, p 1045

3. Hirschhorn R: Adenosine deaminase deficiency, in Rosen FS, Seligmann M (eds): Immunodeficiency Reviews, vol 2. London, UK, Harwood Academic, 1990, p 175

4. Morgan G, Levinsky RJ, Hugh-Jones K, Fairbanks LD, Morris GS, Simmonds HA: Heterogeneity of biochemical, clinical and immunological parameters in severe combined immunodeficiency due to adenosine deaminase deficiency. Clin Exp Immunol 70:491, 1987

5. Hirschhorn R, Ellenbogen A: Genetic heterogeneity in adenosine deaminase (ADA) deficiency: Five different mutations in five new patients with partial ADA deficiency. Am J Hum Genet 38:13, 1986

6. Hirschhorn R: Overview of biochemical abnormalities and molecular genetics of adenosine deaminase deficiency. Pediatr Res 33:S35, 1993 (suppl 1)

7. Chen SH, Ochs HD, Scott CR, Giblett ER, Tingle AJ: Adenosine deaminase deficiency: Disappearance of adenine deoxynucleotides from a patient's erythrocytes after successful marrow transplantation. J Clin Invest 62:138, 1978

8. Hershfield MS, Buckley RH, Greenberg ML, Melton AL, Schiff R, Hatem C, Kurtberg J, Markert ML, Kabayashi RH, Kobayashi AL, Abuchowski A: Treatment of adenosine deaminase deficiency with polyethyleneglycol-modified adenosine deaminase. N Engl J Med 316:589, 1987

9. Hershfield MS, Chaffee S, Sorensen RU: Enzyme replacement therapy with polyethylene glycol-adenosine deaminase in adenosine deaminase deficiency: overview and case reports of three patients, including two now receiving gene therapy. Pediatr Res 33:S42, 1993 (suppl 1)

10. Daddona PE, Shewach DS, Kelley WN, Argos P, Markham AF, Orkin SH: Human adenosine deaminase. cDNA and complete primary amino acid sequence. J Biol Chem 259:12101, 1984

11. Valerio D, McIvor RS, Williams SR, Duyvesteyn MG, van Ormondt H, van der Eb AJ, Martin DW Jr: Cloning of human adenosine deaminase cDNA and expression in mouse cells. Gene 31:147, 1984

12. Wiginton DA, Adrian GS, Hutton JJ: Sequence of human adenosine deaminase cDNA including the coding region and a small intron. Nucleic Acids Res 12:2439, 1984

13. Wiginton DA, Kaplan DJ, States JC, Akeson AL, Perme CM, Bilyk IJ, Vaughn AJ, Lattier DL, Hutton JJ: Complete sequence and structure of the gene for human adenosine deaminase. Biochemistry 25:8234, 1986

14. Blaese RM, Culver KW, Miller AD, Carter CS, Fleisher T, Clerici M, Shearer G, Chang L, Chiang Y, Tolstoshev P, Greenblatt JJ, Rosenberg SA, Klein H, Berger M, Mullen CA, Ramsey WJ, Muul L, Morgan RA, Anderson WR: T lymphocyte-directed gene therapy for ADA-SCID: Initial trial results after 4 years. Science 270:475, 1995

15. Bordignon C, Notarangelo LD, Nobili N, Ferrari G, Casorati G, Panina P, Mazzolari E, Maggioni D, Rossi C, Servida P, Ugazio AG, Mavilio F: Gene therapy in peripheral blood lymphocytes and bone marrow for ADA- immunodeficient patients. Science 270:470, 1995

16. Kohn DB, Weinberg KI, Nolta JA, Heiss LN, Lenarsky C, Crooks GM, Hanley ME, Annett G, Brooks JS, el-Khoureiy A, Lawrence K, Wells D, Moen RC, Bastian J, Williams-Herman DE, Elder M, Wara D, Bowen T, Hershfield MS, Mullen CA, Blaese RM, Parkman R: Engraftment of gene-modified umbilical cord blood cells in neonates with adenosine deaminase deficiency. Nat Med 1:1017, 1995

17. Hoogerbrugge PM, van Beusechem VW, Fischer A, Debree M, le Deist F, Perignon JL, Morgan G, Gaspar B, Fairbanks LD, Skeoch CH, Moseley A, Harvey M, Levinsky RJ, Valerio D: Bone marrow gene transfer in three patients with adenosine deaminase deficiency. Gene Ther 3:179, 1996

18. Sambrook J, Fritsch EF, Maniatis T: Molecular Cloning: A Laboratory manual (ed 2). Cold Spring Harbor, NY, Cold Spring Harbor Laboratory, 1989

19. Hirschhorn R, Ellenborgen A, Tzall S: Five missense mutations at the adenosine deaminase locus (ADA) detected by altered retraction fragments and their frequency on ADA$^-$ patients with severe combined immunodeficiency. Am J Med Genet 49:201, 1992

20. Santisteban I, Arredondo-Vega FX, Kelly S, Mary A, Fischer A, Hummell DS, Lawton A, Sorensen RU, Stiehm ER, Uribe L, Weinberg K, Hershfield MS: Novel splicing, missense, and deletion mutations in seven adenosine deaminase-deficient patients with late/delayed onset of combined immunodeficiency disease. Contribution of genotype to phenotype. J Clin Invest 92:2291, 1993

21. Hirschhorn R, Yang DR, Israni A: An Asp8Asn substitution results in the adenosine deaminase (ADA) genetic polymorphism (ADA 2 allozyme): Occurrence on different chromosomal backgrounds and apparent intragenic crossover. Ann Hum Genet 58:1, 1994

22. Blaese RM, Anderson WF, Culver KW: The ADA human gene therapy clinical protocol. Hum Gene Ther 1:327, 1990

23. Hock RA, Miller AD, Osborne WR: Expression of human adenosine deaminase from various strong promoters after gene transfer into human hematopoietic cell lines. Blood 74:876, 1989

24. Bunnell BA, Muul LM, Donahue RE, Blaese RM, Morgan RA: High-efficiency retroviral-mediated gene transfer into human and nonhuman primate peripheral blood lymphocytes. Proc Natl Acad Sci USA 92:7739, 1995

25. Kohn DB, Mitsuya H, Ballow M, Selegue JE, Barankiewicz J, Cohen A, Gelfand E, Anderson WF, Blaese RM: Establishment and characterization of adenosine deaminase-deficient human T cell lines. J Immunol 142:3971, 1989

26. Aebi M, Hornig H, Padgett RA, Reiser J, Weissmann C: Sequence requirements for splicing of higher eukaryotic nuclear pre-mRNA. Cell 47:555, 1986

27. Krawczak M, Reiss J, Cooper DN: The mutational spectrum of single base-pair substitutions in mRNA splice junctions of human genes: Causes and consequences. Hum Genet 90:41, 1992

28. Miller AD: Human gene therapy comes of age. Nature 357:455, 1992

29. Marcel T, Grausz JD: The TWC worldwide gene therapy enrollment report, end 1996. Hum Gene Ther 8:775, 1997

30. Blaese RM: Development of gene therapy for immunodeficiency: Adenosine deaminase deficiency. Pediatr Res 33:S49, 1993 (suppl 1)

31. Riddell SR, Elliott M, Lewinsohn DA, Gilbert MJ, Wilson L, Manley SA, Lupton SD, Overell RW, Reynolds TC, Corey L, Greenberg PD: T-cell mediated rejection of gene-modified HIV-specific cytotoxic T lymphocytes in HIV-infected patients. Nat Med 2:216, 1996

32. Ferrari G, Rossini S, Giavazzi R, Maggioni D, Nobili N, Soldati M, Ungers G, Mavilio F, Gilboa E, Bordignon C: An in vivo model of somatic cell gene therapy for human severe combined immunodeficiency. Science 251:1363, 1991

33. Hirschhorn R, Yang DR, Puck JM, Huie ML, Jiang CK, Kurlandsky LE: Spontaneous *in vivo* reversion to normal of an inherited mutation in a patient with adenosine deaminase deficiency. Nat Genet 13:290, 1996

Successful *ex vivo* gene therapy directed to liver in a patient with familial hypercholesterolaemia

Mariann Grossman[1], Steven E. Raper[1], Karen Kozarsky[1], Evan A. Stein[2], John F. Engelhardt[1], David Muller[1], Paul J. Lupien[3] & James M. Wilson[1]

[1]Departments of Internal Medicine, Surgery, and Biological Chemistry, The University of Michigan Medical Center, Ann Arbor, Michigan 48109-0656, USA
[2]Medpace Christ Hospital Lipid Cardiovascular Research Center, Division of Lipid Metabolism and Preventive Atherosclerosis, and Clinical Research Laboratories, Cincinnati, Ohio 45219, USA
[3]Lipid Research Center, Laval University Hospital Medical Research Center, Québec, Canada G1V4G2

Present address for M.G., S.E.R., K.K., E.A.S. & J.M.W.: Institute for Human Gene Therapy, University of Pennsylvania, Wistar Institute, Room 204, 3601 Spruce Street, Philadelphia, Pennsylvania 19104-4268, USA

Correspondence should be addressed to J.M.W.

An *ex vivo* approach to gene therapy for familial hypercholesterolaemia (FH) has been developed in which the recipient is transplanted with autologous hepatocytes that are genetically corrected with recombinant retroviruses carrying the LDL receptor. We describe the treatment of a 29 year old woman with homozygous FH by *ex vivo* gene therapy directed to liver. She tolerated the procedures well and *in situ* hybridization of liver tissue four months after therapy revealed evidence for engraftment of transgene expressing cells. The patient's LDL/HDL ratio declined from 10–13 before gene therapy to 5–8 following gene therapy, improvements which have remained stable for the duration of the treatment (18 months). This represents the first report of human gene therapy in which stable correction of a therapeutic endpoint has been achieved.

Familial hypercholesterolaemia (FH) has emerged as an important model for the development of human gene therapies[1]. This disorder, caused by inherited deficiency of LDL receptors, is associated with severe hypercholesterolaemia and premature coronary artery disease[1]. The homozygous form of FH is an excellent candidate for early applications of gene therapy because it is a lethal disorder that is refractory to conventional therapies. Measurement of serum lipid profiles provides a convenient and clinically relevant endpoint to evaluate response to therapy, and orthotopic liver transplantation has been shown to correct the underlying dyslipidemia indicating that hepatic reconstitution of LDL receptor expression is sufficient for metabolic correction[2,3].

The original paradigm for liver-directed gene therapy was based on transplantation of autologous hepatocytes genetically modified *ex vivo* with recombinant retroviruses. The efficacy and safety of this approach for treatment of FH has been demonstrated in a variety of animal models. A strain of rabbits genetically deficient in LDL receptors, called the Watanabe Heritable Hyperlipidemic (WHHL) rabbit, was used to demonstrate the potential efficacy of *ex vivo* gene therapy. Analysis of recipient animals demonstrated stable engraftment of genetically modified hepatocytes and persistent reductions in serum cholesterol for the duration of the experiment — 6.5 months[4]. Experiments in larger animals including dogs and baboons documented the feasibility and safety of *ex vivo* gene therapy directed to the liver[5,6]. *In situ* hybridization analysis of liver tissue from baboons harvested 1.5 years after gene therapy demonstrated stable engraftment of transgene expressing hepatocytes, providing further support for the efficacy of this therapy (unpublished data).

Based on the encouraging results obtained in animal models, we proposed a clinical protocol to treat FH homozygous patients with *ex vivo* gene therapy. We received permission from the US Recombinant DNA Advisory Committee (RAC) and the US Food and Drug Administration to treat three patients who had developed overt coronary artery disease and therefore would have a poor prognosis. Our experience with the first patient, described here, supports the efficacy and safety of liver-directed *ex vivo* gene therapy in humans.

First recipient of liver-directed gene therapy

The first clinical application of liver-directed gene therapy in humans used the *ex vivo* approach in a patient with homozygous FH. Although we were allowed to treat FH patients of any age, the RAC suggested that we enroll an adult as the initial patient to simplify the informed consent process. Patient FH1 underwent gene therapy on June 5, 1992. This French Canadian woman, who at the time of gene therapy was 28 years old, had a myocardial infarction at the age of 16 and required coronary artery bypass at the age of 26. Her dyslipidemia — which at baseline included a total serum cholesterol concentration of 545 mg dl^{-1}, LDL of 482 mg dl^{-1} and HDL of 43 mg dl^{-1} — was refractory to treatment with a variety of drugs including HMG CoA reductase inhibitors and bile acid binding resins. Genotype analysis indicated she was homozygous for a missense mutation (Trp66Gly, exon 3) that renders the LDL receptor incapable of binding to its ligands[7]. Cardiac evaluation performed prior to gene therapy revealed failure of one of her grafts and diffuse disease in her native coronary arteries, however, she was not overtly symptomatic.

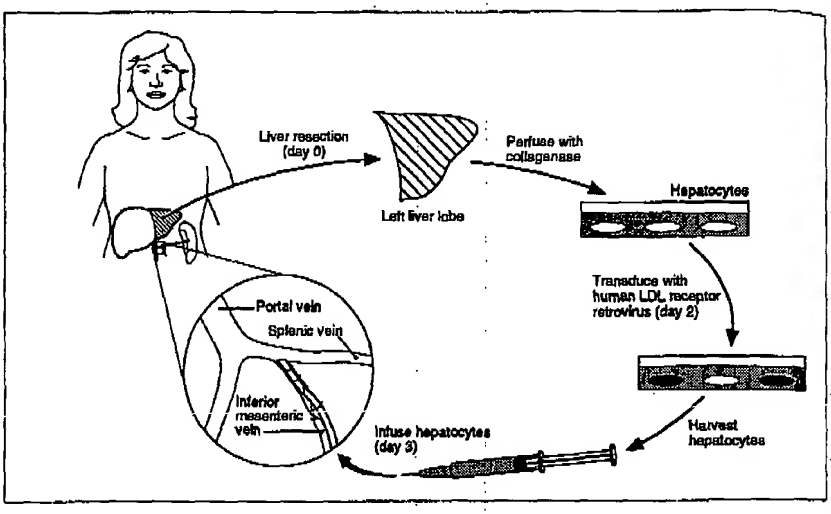

Fig. 1 Strategy of *ex vivo* gene therapy for familial hypercholesterolaemia.

Ex vivo gene therapy to liver is feasible and safe

The clinical protocol approved by the RAC has been published[9]; the general strategy is summarized in Fig. 1. The left lateral segment of the patient's liver, comprising approximately 15% of its total mass, was removed through a left subcostal incision. A 9.6 fr Hickman catheter was inserted into her inferior mesenteric vein, and the distal end of the catheter was brought through her incision thereby providing convenient access to the portal circulation for subsequent cell infusions. The resected liver, weighing 250 g, was perfused with collagenase to release hepatocytes; 3.2×10^9 cells were recovered (98% viability) and seeded into 800 10 cm^2 plates. Medium containing the LDL receptor expressing recombinant retroviruses was placed onto the cultured hepatocytes 48 hours after the initial seeding. Following a 12–18 h exposure to virus, the cells were analysed for LDL receptor expression and harvested for transplantation; 2×10^9 viable cells were recovered from the plates by treatment with trypsin. Incubation of the transduced cells with fluorescent labelled LDL revealed uptake in approximately 20% of the cells exposed to the LDL receptor expressing virus and no uptake in duplicate plates of cells not exposed to virus (Fig. 2).

Prior to infusion of the cells, a portal venogram was performed to confirm the placement of the catheter and patency of the portal circulation (Fig. 3*a*). The genetically corrected hepatocytes were harvested in three aliquots and each aliquot was manually infused at 4 h intervals directly into the catheter over a 30 minute period (a rate of ~2 cc min^{-1}). During the cell infusions the patient was carefully monitored in the intensive care unit; her vital signs measured during this time are presented in Fig. 4. She tolerated the cell infusions well except for a transient tachycardia early in the day, thought to be secondary to anxiety, and fevers that were present before cell infusion which resolved subsequently.

One concern was the potential development of portal

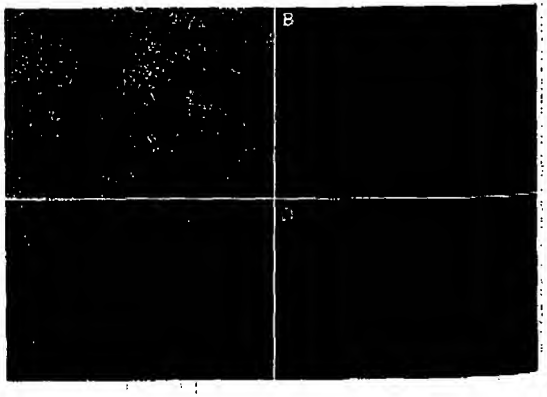

Fig. 2 Expression of recombinant LDL receptor in primary hepatocytes. Primary cultures of hepatocytes were infected with recombinant retroviruses and analysed for LDL receptor expression using an assay based on uptake of fluorescent labelled LDL. Mock infected cells visualized under the phase contrast (*a*) and fluorescent microscope (*b*), and LDL receptor transduced cells visualized under the phase contrast (*c*) and fluorescent microscope (*d*) are presented. Magnification, 100×.

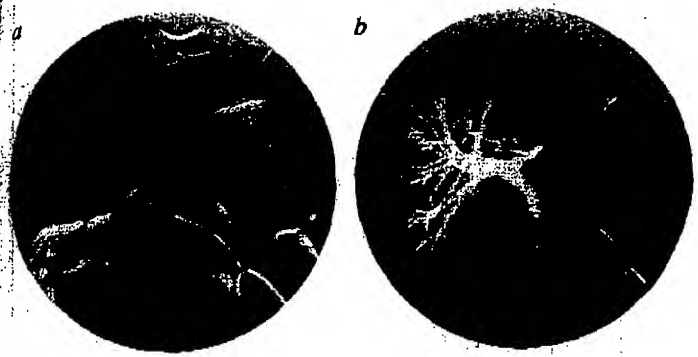

Fig. 3 Portal venograms before and after hepatocyte infusion. *a*, Portal venogram immediately prior to cell reinfusion (postoperative day 3). Note surgical absence of the left lateral segment of the liver, absence of portal vein thrombosis and good position of the catheter. *b*, Portal venogram immediately prior to catheter removal (postoperative day 10). Note patent portal vein without evidence of intraluminal thrombus.

vein thrombosis and/or portal hypertension as a result of introducing a large cell mass into this low pressure venous circulation. Portal pressures measured via the catheter three days before cell infusion (9.8 ± 1.3, mean ± s.d., n=4) were indistinguishable from those measured five days after cell infusion (10.9 ± 2.1 mean ± s.d. n=12) with transient increases (lasting <4 h) of 4 and 8 cm H_2O occurring after the second and third cell infusions, respectively. Repeat portal venography performed at the time of catheter removal seven days after cell infusion revealed a fully patent portal circulation without evidence of intraluminal clot (Fig. 3*b*).

Prolonged improvement in dyslipidemia

Liver tissue was harvested by percutaneous biopsy four months after gene therapy. No histopathology was noted in plastic embedded sections prepared for light and electron microscopy (data not shown). Frozen sections were analysed for the presence of transgene expressing cells by *in situ* hybridization using an RNA probe specific for the recombinant derived LDL receptor transcript. Figure 5 presents an example of an hepatocyte that hybridized to the antisense probe (*c* and *d*); this kind of focal hybridization was not present in serial sections incubated with the sense probe (*a* and *b*) or in sections pretreated with RNase prior to hybridization with the antisense probe (data not shown). Analysis of a limited number of sections revealed hybridization to the antisense probe in 1:1,000 to 1:10,000 cells. It is unlikely that the results obtained from a single small block of liver tissue from FH1 accurately represents the abundance and distribution of transgene expressing cells throughout the liver. Similar experiments performed in three baboons who underwent

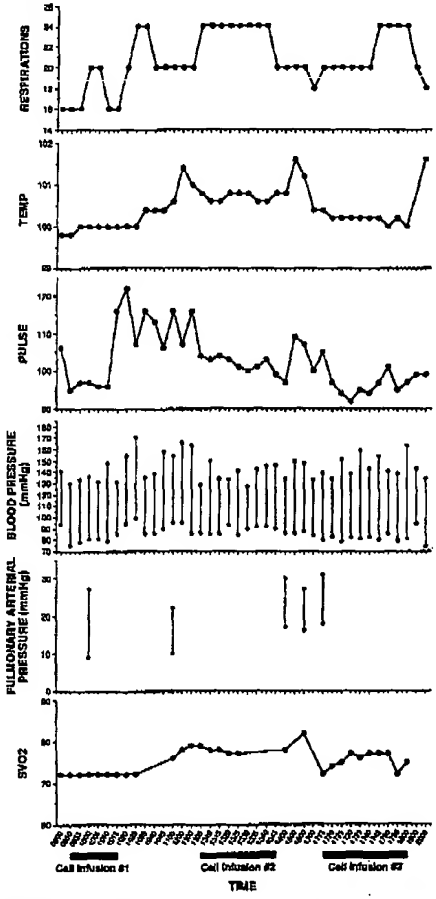

Fig. 4 Clinical response during hepatocyte infusion. During the cell infusions the patient was invasively monitored with a radial arterial line and pulmonary arterial line while in the intensive care unit. Six clinical parameters (respiration rate, oral temperature, pulse, systemic blood pressure (mm Hg), pulmonary arterial pressure (mm Hg), and oxygen saturation in mixed venous blood (SVO_2)) are presented. The actual times are indicated along the bottom with the periods during which the cells were infused indicated by the bars. Note that the time coordinates have been expanded during the periods of cell infusion.

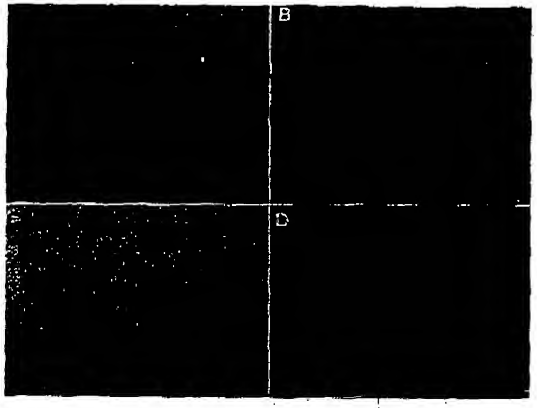

Fig. 5 *In situ* hybridization of liver tissue after gene therapy. Liver tissue (50 mg) was harvested by percutaneous biopsy four months after gene therapy. The majority of the sample was fixed, embedded, sectioned and analysed by light and electron microscopy for evidence of pathology. A small block was analysed for cells expressing recombinant LDL receptor by *in situ* hybridization. Tissue sections were hybridized with the sense probe (*a* and *b*) or antisense probe (*c* and *d*) and visualized by bright field (left panels) and dark field (right panels) microscopy. The clustering of signal seen in panels c and d indicates a cell that hybridized to the antisense probe. Magnification, 50×.

ex vivo liver-directed gene therapy demonstrated marked regional variation of recombinant LDL receptor expressing cells within large biopsies of liver, illustrating the limitations in quantitatively assessing engraftment from the small quantity of tissue sampled from a percutaneous biopsy (unpublished data).

The effect of gene therapy on the patient's lipid profiles, presented as ΔLDL, ΔHDL and LDL/HDL ratio, is presented in Fig. 6; Table 1 summarizes the lipid data with relevant statistical analyses. The patient has been followed for 18 months after gene therapy in the context of four treatment periods: pre gene therapy — on (period A) and off (period B) lovastatin; and post gene therapy — off (period C) and on (period D) lovastatin. The original protocol was designed to establish baseline lipids when the patient was off all lipid lowering medications and to reinitiate pharmacologic therapy four months after gene therapy. This initial analysis allowed comparisons between periods B, C and D.

Blood samples were coded and submitted to a referen

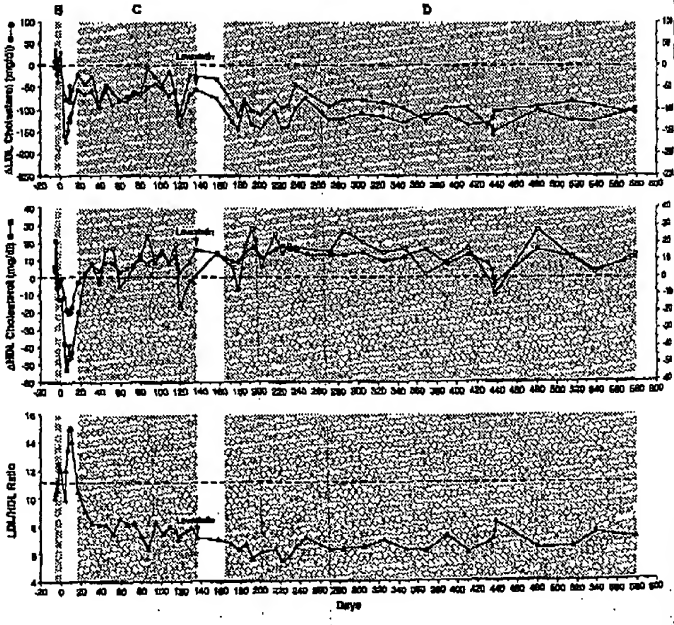

Fig. 6 Lipid profiles. The study was performed using three treatment periods. Period B spans 8 days immediately prior to gene therapy during which 7 lipid profiles were obtained. Period C represents a 131 day interval after gene therapy before she was started on lovastatin during which 19 lipid profiles were obtained. Interpretation of data obtained 8 days following gene therapy was confounded because of additional effects on lipids of the stress of the procedure and decreased nutritional intake; these data were deleted from the analysis of Period C. Period D represents a 15 month interval following Period C during which the patient was treated with lovastatin. Data obtained during a 30 day period after initiation of lovastatin was not included in analysis of Period D to allow for the effect of the drug. Data are presented as ΔLDL and Δapo B (top panel); ΔHDL and Δapo AI (middle panel); and LDL/HDL ratio (bottom panel). Three treatment periods are indicated: period B — pre-gene therapy, off medications; period C — post-gene therapy, off medications; and period D — post-gene therapy, on lovastatin.

Table 1 Summary of lipid profiles for patient FH1

	Pre-gene therapy		Post-gene therapy		Statistical comparisons (p values)		
	+Lovastatin period A	–Lovastatin period B	–Lovastatin period C	+Lovastatin period D	B–C	C–D	A–D
Cincinnati ref. lab.							
LDL	–	482 ± 19 (7)	404 ± 24 (19)	356 ± 22 (27)	0.0001	0.0001	–
HDL	–	43 ± 3.4 (7)	51.4 ± 5.9 (19)	54 ± 5 (27)	0.0014	0.10	–
LDL/HDL	–	11 ± 1.0 (7)	7.9 ± 0.9 (19)	6.6 ± 0.6 (27)	0.0001	0.0001	–
apoAI	–	115 ± 12 (7)	121 ± 11 (18)	130 ± 9 (24)	0.22	0.005	–
apoB	–	352 ± 23 (7)	299 ± 30 (18)	260 ± 23 (24)	0.0004	0.0002	–
Quebec ref. lab.							
LDL	448 ± 30 (6)	–	–	366 ± 25 (7)	–	–	0.0001
HDL	44.5 ± 4.1 (6)	–	–	47.6 ± 4.1 (7)	–	–	0.16
LDL/HDL	10.2 ± 1.0 (6)	–	–	7.6 ± 0.6 (7)	–	–	0.0001

All samples represent mean ± 1. s.d. with *n*=number of determinations. Statistical analyses performed as described in the text.

laboratory in Cincinnati for analysis. Serum LDL dropped by 180 mg dl^{-1} immediately after cell infusion and regained a new baseline that was 17% lower than pre treatment levels (482±19 before therapy versus 404 ± 24 after therapy, p=0.0001). Coincident with the diminution in LDL was an increase in HDL from 43 ± 3.4 to 51.4 ± 5.9 (p=0.0014) that translated to a decline in LDL/HDL ratio from 11 ± 0.4 to 7.9 ± 0.9 (p=0.0001). The mechanism(s) responsible for increased HDL following gene therapy remain unexplained, however, similar effects have been described in FH homozygotes who underwent orthotopic liver transplantation[2,3]. Initiation of lovastatin four months after gene therapy was associated with further improvements in this patient's dyslipidemia including a reduction in LDL (404 ± 24 to 356 ± 22, p=0.0001), increase in HDL (51.4 ± 5.9 to 54 ± 5, p=0.10), and decline in LDL/HDL ratio (7.9 ± 0.9 to 6.6 ± 0.6, p=0.0001). The changes in LDL and HDL noted in each treatment period were associated with parallel and equally significant changes in apo B and apo AI, respectively (Table 1 and Fig. 6).

An attempt was made to evaluate further the effect of gene therapy using lipid profiles that were obtained in Quebec during period A, spanning a two year interval from Feb. 1990–Dec. 1991; during this time the patient was treated with lovastatin in a single drug regimen at approximately the same dose she has been taking during period D (that is, following gene therapy). Additional samples were obtained during period D and analysed by the same reference laboratory in Quebec that was used to measure the patient's lipids in 1990–91. Direct comparison of the patient's lipids on lovastatin before and after gene therapy revealed a diminution in LDL from 448 ± 30 to 366 ± 25 (p=0.0001), a modest increase in HDL from 44.5 ± 4.1 to 47.6 ± 4.1 (p=0.16), and a decline in LDL/HDL ratio from 10.2 ± 1.0 to 7.6 ± 0.6 (p=0.0001).

Discussion

FH represents a unique model for developing and evaluating the principle of liver-directed gene therapy in humans. This fatal disease is easily evaluated for reconstitution of hepatic gene expression by serial measurements of serum lipids which are considered relevant endpoints for clinical efficacy. Critical to the early development of this clinical model was the availability of an authentic animal model, the WHHL rabbit.

Ex vivo approaches to liver-directed gene therapy emerged as the initial paradigm for treating hepatic metabolic diseases such as FH. In this strategy, stable reconstitution of hepatic gene expression can be achieved by transplanting hepatocytes transduced *ex vivo* with retroviruses. The development of safe and effective *ex vivo* gene therapies to liver presents unique experimental challenges. *Ex vivo* correction of the defect is complicated because the target cell for gene transfer, the hepatocyte, must be isolated from surgically resected tissue and it cannot be maintained and expanded in culture. The ultimate success of this approach depends on the efficient and stable engraftment of the transduced cells and their progeny. The likelihood that this will occur with transduced hepatocytes is difficult to predict because of the paucity of information available regarding stem cells and lineage in the liver, and ultimately must be answered experimentally. Clinical application of this form of gene therapy was further confounded because it does not resemble existing forms of therapy as is the case with bone marrow directed gene therapy, which conceptually is a modification of a commonly used therapy, autologous bone marrow transplantation. However, there should be no immunological barriers associated with *ex vivo* gene therapy other than the problem of an immune response to the therapeutic gene product, a potential concern that is generic to all forms of gene therapy for deficiency states. A variety of animal models, in addition to the WHHL rabbit, have been useful in developing the requisite technology and providing sufficient preclinical studies to justify a human trial[4,9,10].

The outcome of our first clinical experience supports the safety and feasibility of *ex vivo* gene therapy directed to liver. Molecular and metabolic data suggest that the genetically modified hepatocytes have engrafted stably in this patient and continue to express the recombinant gene (after at least 18 months). The level of metabolic correction achieved in this patient was similar to that detected in the WHHL rabbits who received autologous genetically corrected hepatocytes[4]. In this animal model, control experiments performed with mock transfected hepatocytes had no effect on cholesterol except for a transient elevation suggesting that the persistent diminution in lipoproteins observed in FH1 was not an artefact of the surgical

procedures but due to expression of the recombinant gene. Subsequent to gene therapy, the patient's serum lipids consistently remained at levels significantly lower than those measured by at least two reference laboratories over several years before gene therapy. It is unclear, however, whether the partial correction of hypercholesterolaemia achieved in this patient will translate to improved clinical outcome. It is encouraging that she tolerated gene therapy well without short or long term sequelae and that her coronary artery disease, as documented by serial angiography, has not progressed during the 18 months since the treatment (data not shown).

The response of this patient to lovastatin following gene therapy is interesting given that she failed to respond to this drug on multiple occasions prior to gene therapy. Lovastatin is thought to deplete intracellular cholesterol which leads to up regulation of LDL receptor expression[1], probably at the transcriptional level[11]. The recombinant LDL receptor gene does not contain the transcriptional elements necessary to confer cholesterol mediated regulation suggesting the response to lovastatin is unrelated to the recombinant gene or that its effect is in part mediated by posttranscriptional regulation of LDL receptor. This is consistent with previous studies that indicate the endogenous LDL receptor gene is regulated at both a transcriptional and posttranscriptional manner[12].

One potential concern about gene therapy for diseases caused by loss of gene function is that the protein product of the therapeutic gene will be recognized by the recipient as a neoantigen leading to an immune response against the genetically corrected cells. Several observations suggest this did not occur in FH1. Western blot analysis of the patient's sera failed to detect antibodies to the recombinant human LDL receptor protein (data not shown). Also, there was no clinical or pathological evidence for autoimmune hepatitis following gene therapy. It will be interesting to see if similar results are obtained in FH patients undergoing gene therapy who have mutations that totally ablate LDL receptor protein expression as opposed to the mutation in FH1 that leads to the expression of a dysfunctional protein[7].

Our study demonstrates the feasibility, safety and potential efficacy of *ex vivo* liver-directed gene therapy in humans and supports the initial hypothesis that selective reconstitution of LDL receptor expression in hepatocytes of FH homozygotes should be sufficient for metabolic improvement. This represents the first example of stable correction of a therapeutic endpoint by gene therapy, in contrast to clinical trials that require repeated administration of short-lived target cells such as lymphocytes for treatment of adenosine deaminase deficiency. Translation of this technology to the treatment of other lethal liver metabolic diseases (such as, ornithine transcarbamylase deficiency) should proceed rapidly if the principle of *ex vivo* liver-directed gene therapy is confirmed in a larger number of homozygous FH patients. Ultimately, a more effective and clinically practical approach to liver directed gene therapy, based on *in vivo* gene delivery, must be developed. Gene transfer technologies using recombinant adenoviruses, liposomes and molecular conjugates have shown promising results in animal models[13–19]. Problems with efficiency and stability of recombinant gene expression as well as destructive and/or blocking immune responses to the delivery vehicles or genetically modified cells must be overcome before the potential of *in vivo* approaches can be realized.

Methodology

Surgical procedures. During the procedure and for the first three postoperative days the patient was carefully monitored with a pulmonary arterial catheter and radial arterial line. Following induction of anesthaesia, the left lobe of the liver was exposed by a left subcostal incision which was extended up the midline to the xiphoid. A self-retaining retractor was used to retract the costal margin. The left triangular ligament was divided to the level of the left hepatic vein from lateral to medial. A rubber-shod, non-crushing intestinal bowel clamp was tested for fit just to the left of the falciform ligament. The clamp was applied and using a scalpel, the liver surface was rapidly transected (<90 s) and transferred to the human applications laboratory for cell isolation. Bleeding from the cut hepatic vein was easily controlled with direct pressure until surgical hemostasis was applied. The cut ends of the portal vein and hepatic vein were sutured with 5-0 running non-absorbable monofilament. The open surface of the liver was controlled with 3-0 silk interlocking vertical mattress sutures placed in the liver tissue protruding from the clamp. Once haemostasis was achieved, the clamp was removed and individual bile ducts or blood vessels were ligated with additional 3-0 silk sutures. The inferior mesenteric vein was identified at the paraduodenal fossa. The vein was sharply dissected for a distance of 3 cm and individual branches were ligated with 5-0 silk ligatures. Silk ties (2-0) were placed at either end of the dissected vessel, and the ligature placed at the end of the vein nearest to the colon was tied. A 9.6 Fr. Hickman-type catheter was brought obliquely through the abdominal wall about 3 cm below the lateral aspect of the incision and secured in place with a 3-0 nylon stitch. The catheter was trimmed to the correct length, a bevel was placed at the cut end to facilitate insertion, and the catheter was primed with heparinized saline (100 U ml^{-1}). A venotomy was made with a number 11 scalpel blade. The ideal location for catheter placement is the confluence of the inferior mesenteric vein and the splenic vein, a position that was identified by palpation. The catheter was secured by tying the ligature nearest the portal vein around the inferior mesenteric vein making sure not to occlude the catheter. A 3-0 chromic suture was tied around the inferior mesenteric vein and the outside of the catheter to further protect against premature dislodgement (see Fig. 1). A final inspection of the cut surface of the liver was made and the liver bed was drained with a closed suction drainage catheter to remove any residual bile or serum. The wound was closed in two fascial layers with a running absorbable monofilament suture. The skin was closed with interrupted subcuticular 4-0 chromic sutures and surgical tapes.

Preparation of virus and isolation of hepatocytes. The recombinant retrovirus used in this study has been described[6]. A full length human LDL receptor cDNA is expressed from a chicken β-actin promoter in combination with an enhancer from the immediate early gene of cytomegalovirus. The cell line that produced this virus, called 132-10, was characterized in accordance with recommendations of the RAC and the FDA. Supernatants containing the LDL receptor viruses were cryopreserved and aliquots were analysed for the presence of contaminants and replication competent virus. Certified lots of cryopreserved virus were used in the clinical trial.

Hepatocytes were isolated by collagenase perfusion, plated in culture and infected with retroviruses as described previously[20]. Plates of cells were infected with virus from 132-10 (LDL receptor virus) and analysed for LDL receptor expression using the previously described assay; cells were incubated in RPMI 1640 medium containing lipoprotein deficient serum (10%) and fluorescent labelled LDL (10 μg ml^{-1}) for 4 h[16]. Following completion of this incubation, the medium was removed, and the cells were washed in PBS and visualized under the fluorescent microscope. In preparation for transplantation, hepatocytes were removed from the plates by incubation with trypsin and washed extensively in RPMI 1640. Hepatocytes were harvested in three batches each of which contained cells recovered from one third of the total prep. Each batch was washed and resuspended in normal saline (50 ml) containing 10 U ml^{-1} of heparin in preparation for infusion.

Analyses of biopsied liver tissue. The tissue block for *in situ* analysis

was frozen in OCT, and cryosections (6 μM) were mounted on gelatin poly(L-lysine)-coated slides and fixed with 4% paraformaldehyde in phosphate buffered saline[17]. Sections were hybridized to a ^{35}S labelled RNA probe complementary to retroviral envelope acquences that are uniquely present in the 3' untranslated region of the recombinant derived LDL receptor RNA[4]. Sense probes and RNAse pretreatment with antisense probes were used as controls for hybridization specificity.

Analysis of metabolic parameters. Blood samples were obtained, coded and sent to reference laboratories in Cincinnati and Quebec for determination of lipid profiles. LDL cholesterol, HDL cholesterol, ApoA1 and ApoB were measured directly using previously published techniques. Differences in LDL, HDL and LDL/HDL profiles obtained during the four treatment periods were evaluated using random intervention testing and randomized testing methodologies.

Received 27 December 1993; accepted 31 January 1994.

1. Brown, M.S. & Goldstein, J.L. A receptor-mediated pathway for cholesterol homeostasis. *Science* 232, 34–37 (1986).
2. Starzl, T.E. *et al.* Heart-liver transplantation in a patient with familial hypercholesterolemia. *Lancet* 1, 1382–1383, (1984).
3. Bilheimer, D.W. *et al.* Liver transplantation to provide low density lipoprotein receptors and lower plasma cholesterol in a child with homozygous familial hypercholesterolemia. *New Engl. J. Med.* 311, 1658–1664 (1984).
4. Chowdhury, J.R. *et al.* Long term improvement of hypercholesterolemia after *ex vivo* gene therapy in LDLR deficient rabbits. *Science* 254, 1802–1805 (1991).
5. Grossman, M., Wilson, J.M. & Raper, S.E. A novel approach for introducing genetically modified hepatocytes into the portal circulation. *J. Lab. clin. Med.* 121, 472–478 (1993).
6. Grossman, M., Raper, S.E. & Wilson, J.M. Transplantation of genetically-modified autologous hepatocytes in non-human primates. *Hum. gene Ther.* 3, 501–510 (1992).
7. Leitersdorf, E., Tobin, E.J., Davignan, J., & Hobbs, H. Common low-density lipoprotein receptor mutations in the French Canadian population. *J. clin. Invest.* 85, 1014–1023 (1990).
8. Wilson, J.M. *et al.* Clinical protocol: *ex vivo* gene therapy of familial hypercholesterolemia. *Hum. gene Ther.* 3, 179–222 (1992).
9. Armentano, D., Thompson, A.R., Darlington, G. & Woo, S.L.C. Expression of human factor IX in rabbit hepatocytes by retrovirus-mediated gene transfer: potential for gene therapy of hemophilia B. *Proc. natn. Acad. Sci. U.S.A.* 87, 6141–6145 (1990).
10. Kay, M.A. *et al.* Expression of human α$_1$-antitrypsin in dogs after autologous transplantation of retroviral transduced hepatocytes. *Proc. natn. Acad. Sci. U.S.A.* 89, 89–93 (1992).
11. Sighof, T.C., Russell, D.W., Brown, M.S. & Goldstein, J.L. 42 bp element from LDL receptor gene confers end-product repression by sterols when inserted into viral TK promoter. *Cell* 48, 1061–1069 (1987).
12. Sharkey, M.F. *et al.* Post-transcriptional regulation of retroviral vector-transduced low density lipoprotein receptor activity. *J. lipid Res.* 31, 2167–2176 (1990).
13. Jaffe, H.A. *et al.* Adenovirus-mediated *in vivo* gene transfer and expression in normal rat liver. *Nature Genet.* 1, 372–378 (1992).
14. Kaneda, Y., Iwai, K. & Uchida, T. Increased expression of DNA cointroduced with nuclear protein in adult rat liver. *Science* 243, 375–378 (1988).
15. Wu, C.H., Wilson, J.M. & Wu, G.Y. Targeting genes: delivery and persistent expression of a foreign gene driven by mammalian regulatory elements *in vivo*. *J. biol. Chem.* 264, 16985–16987 (1989).
16. Grossman, M., Raper, S. & Wilson, J.M. Towards liver-directed gene therapy: retrovirus mediated gene transfer into human hepatocytes. *Som. Cell molec. Gen.* 17, 601–607 (1991).
17. Engelhardt, J.F. *et al.* Submucosal glands are the predominate site of CFTR expression in human bronchus. *Nature Genet.* 2, 240–248 (1992).

Acknowledgements

We thank physicians and staff at the University of Michigan, the Biostatistical and Computing core of the GCRC at University of Pennsylvania. K. Wu, M. Lucey and J. Cornicelli for their help and contribution to this work. This work was supported by the University of Michigan Medical Center, the Department of Internal Medicine at the University of Michigan and NIH Grants R01-DK42193 (J.M.W.), P01-DK42718 (J.M.W.), and 3M01RR00042-32S2 (General Clinical Research Center at the University of Michigan).

HUMAN GENE THERAPY 13:1201–1211 (July 1, 2002)

Enhancement of Bone Healing Based on *Ex Vivo* Gene Therapy Using Human Muscle-Derived Cells Expressing Bone Morphogenetic Protein 2

JOON YUNG LEE,[1,2,3*] HAIRONG PENG,[1,2*] ARVYDAS USAS,[1] DOUGLAS MUSGRAVE,[1] JAMES CUMMINS,[1] DALIP PELINKOVIC,[1] RON JANKOWSKI,[1] BRUCE ZIRAN,[2] PAUL ROBBINS,[3] and JOHNNY HUARD[1,3]

ABSTRACT

Molecular biological advances have allowed the use of gene therapy in a clinical setting. In addition, numerous reports have indicated the existence of inducible osteoprogenitor cells in skeletal muscle. Because of this, we hypothesized that skeletal muscle cells might be ideal vehicles for delivery of bone-inductive factors. Using *ex vivo* gene transfer methods, we genetically engineered freshly isolated human skeletal muscle cells with adenovirus and retrovirus to express human bone morphogenetic protein 2 (BMP-2). These cells were then implanted into nonhealing bone defects (skull defects) in severe combined immune deficiency (SCID) mice. The closure of the defect was monitored grossly and histologically. Mice that received BMP-2-producing human muscle-derived cells experienced a full closure of the defect by 4 to 8 weeks posttransplantation. Remodeling of the newly formed bone was evident histologically during the 4- to 8-week period. When analyzed by fluorescence *in situ* hybridization, a small fraction of the transplanted human muscle-derived cells was found within the newly formed bone, where osteocytes normally reside. These results indicate that genetically engineered human muscle-derived cells enhance bone healing primarily by delivering BMP-2, while a small fraction of the cells seems to differentiate into osteogenic cells.

OVERVIEW SUMMARY

Segmental bone defects and nonunions are relatively common in the craniofacial skeleton. Osteogenic proteins, including bone morphogenetic proteins 2 and 4 (BMP-2 and BMP-4), can promote bone healing in segmental bone defects, but the short half-lives and rapid clearance of the osteogenic proteins by the bloodstream limit the success of this technology. Gene therapy and tissue-engineering approaches that can achieve efficient and long-term expression of these proteins may help to further improve craniofacial bone healing. We observed that a population of muscle-derived stem cells isolated from mouse skeletal muscle can differentiate into the osteogenic lineage and improve bone healing. In this paper, we have attempted to determine whether human muscle-derived cells can be genetically engineered with adenovirus and retrovirus to express human BMP-2, and subsequently be used in an *ex vivo* gene transfer protocol to improve bone healing in mice. Our results suggest that human skeletal muscle–derivedcells can be used for delivery of BMP-2 and as a possible source of inducible osteoprogenitor cells to participate in bone formation, and consequently improved bone healing.

INTRODUCTION

In 1965, Marshall Urist conducted a series of experiments that suggested the existence of osteoinductive factors in demineralized bone. Subsequent research efforts have led to the isolation of what are now known as bone morphogenetic proteins (BMPs) (Urist, 1965; Urist *et al.*, 1984; Reddi, 2001).

[1]Growth and Development Laboratory, Department of Orthopaedic Surgery, Children's Hospital of Pittsburgh and University of Pittsburgh, Pittsburgh, PA 15260.
[2]Department of Orthopaedic Surgery, University of Pittsburgh Medical Center, Pittsburgh, PA 15260.
[3]Department of Molecular Genetics and Biochemistry, University of Pittsburgh, Pittsburgh, PA 15260.
*These authors contributed equally to this paper.

Characterizations and numerous uses of BMPs in animal studies have generated the idea of healing bone by molecular biological means. Currently, biological methods to treat segmental bone defects, nonunions, and delayed unions with BMP-2 are being investigated.

Investigations have focused on the use of gene therapy to deliver BMPs into the diseased bone. Vectors such as retrovirus and adenovirus have been tested in experimental settings to deliver exogenous genes such as bone-inductive factors (Verma and Somia, 1997; Robbins *et al.*, 1998; Romano *et al.*, 1998). These vectors have been efficient *in vitro* for delivering the gene of interest but have been fraught with disadvantages when used for direct *in vivo* gene delivery. For example, retroviral vectors require actively dividing cells for integration of the foreign gene and thus inefficiently transduce postmitotic cells *in vivo* (Robbins *et al.*, 1998). First-generation adenovirus seems to induce an immune response in hosts that may decrease the efficiency of gene transfer (Yang *et al.*, 1994; Vilquin *et al.*, 1995). In addition, some of these vectors are cytotoxic, and their systemic effects on the host are unknown (Verma and Somia, 1997).

To circumvent these complications, the *ex vivo* method of gene transfer was developed (Dai *et al.*, 1992; Lieberman *et al.*, 1999; Engstrand *et al.*, 2000; Musgrave *et al.*, 2000; Peng *et al.*, 2001). This method involves transducing the desired population of cells *in vitro*, and then reimplanting the genetically engineered cells into the host. The obvious advantage of this method is that the investigator can choose, screen, and manipulate the target cell easily and efficiently *in vitro*. The technique allows target cell screening before implantation for efficiency of protein production, oncogenic potential, and survivability posttransduction. Furthermore, the use of autologous cells decreases the possibility of immune rejection, ensuring longer expression of the protein of interest. The only disadvantage of the *ex vivo* method is that it requires an additional step of cultivating and growing the desired cells.

The most beneficial aspect of *ex vivo* gene therapy is that the investigator can choose the cell population to use as the vehicle for delivery. Although the target tissue may be bone, the vehicle for protein (BMP) delivery does not necessarily have to be osteoblastic cells. Any cell population that can be harvested in a noninvasive manner and can survive postimplantation to efficiently produce the protein of interest can act as the vehicle for protein delivery.

For treatment of segmental bone defects by *ex vivo* gene therapy, an obvious cell choice would be bone marrow stromal cells (Caplan, 1991; Young *et al.*, 1995; Lieberman *et al.*, 1999; Pittenger *et al.*, 1999). Bone marrow stroma has been shown to harbor mesenchymal stem cells, which have the potential to differentiate into osteoblasts (Caplan, 1991; Young *et al.*, 1995). Therefore, these cells provide the added advantage of implanting inducible osteoprogenitor cells into the bone defect while introducing exogenous bone-inductive protein. One study of syngeneic rats has shown that rat bone marrow stromal cells can heal segmental bone defects efficiently when used as a vector for BMP-2 delivery (Lieberman *et al.*, 1999). Thus far, bone marrow stromal cells and human gingival and dermal fibroblasts have been tested for *ex vivo* gene therapy to improve bone healing (Lieberman *et al.*, 1999; Krebsbach *et al.*, 2000).

Several previous studies provided evidence of the existence of inducible osteoprogenitors in skeletal muscle (Urist, 1965; Urist *et al.*, 1984; Katagiri *et al.*, 1994; Bosch *et al.*, 2000; Lee *et al.*, 2000, 2001; Musgrave *et al.*, 2000, 2002). *In vitro* (Katagiri *et al.*, 1994; Bosch *et al.*, 2000; Musgrave *et al.*, 2000, 2002) and *in vivo* (Urist, 1965; Urist *et al.*, 1984; Bosch *et al.*, 2000) studies have shown that a subpopulation of muscle-derived cells can differentiate into osteogenic cells with BMP-2 stimulation. Although the identity of these cells is being investigated by the use of stem cell markers (Lee *et al.*, 2000) and is not fully established, the existence of these inducible osteoprogenitor cells in skeletal muscle makes them a potential vehicle for delivery of bone-inductive factors. They provide the same added advantage of osteoprogenitors in bone marrow stromal cells, and can be obtained via a noninvasive small muscle biopsy. In addition, the injured muscle postbiopsy can rapidly regenerate due to the activation of satellite cells, which support muscle regeneration and promote muscle repair postinjury (Bischoff, 1986, 1994).

We used mouse muscle-derived cells in a critical-sized defect model to enhance bone healing (Lee *et al.*, 2000, 2001). A small population of cells in mouse skeletal muscle was shown to differentiate into osteocytes *in vivo* to participate in bone formation (Lee *et al.*, 2000, 2001). However, no data on the use of human muscle cells to improve bone healing are available. In this study, we examined whether human muscle-derived cells can enhance bone healing. Using a critical-sized defect model in mice, we show that human muscle-derived cells can efficiently deliver human BMP-2 and significantly enhance bone healing. In addition, by using fluorescence *in situ* hybridization (FISH) with human probes to monitor the fate of these human cells and distinguish donor cells from host cells, we observed that only a small percentage of these cells can be found within the bone, a location where osteocytes reside; this suggests that the injected cells can differentiate into osteogenic cells. These results suggest that human muscle-derived cells can improve bone healing primarily by delivering BMP-2, whereas a small percentage of cells seems to be capable of differentiating into bone lineage.

MATERIALS AND METHODS

Isolation of human muscle-derived cells

Primary human muscle cells were isolated on biopsy of the gastrocnemius of a 19-year-old male patient (IRB protocol 9902222). Approximately 1 to 3 g of muscle tissue were minced into a slurry. This slurry was then digested by serial 1-hr incubations at 37°C in 0.2% type XI collagenase (Sigma, St. Louis, MO), dispase (grade II, 240 units; Sigma), and 0.1% trypsin (GIBCO-BRL, Gaithersburg, MD). The cell suspension was passed through 18-, 20-, and 22-gauge needles, centrifuged at 3000 rpm for 5 min, resuspended in growth medium (Dulbecco's modified Eagle's medium [DMEM] supplemented with 10% fetal bovine serum, 10% horse serum, 0.5% chick embryo extract, and 2% penicillin–streptomycin; all from GIBCO-BRL), and plated in collagen-coated flasks. This technique of plating muscle-derived cells in collagen-coated flasks has been termed "the preplating technique" and has been used to purify desmin-expressing myogenic cells (Richler and Yaffe, 1970;

Rando and Blau, 1994; Qu *et al.*, 1998; Qu and Huard, 2000). We then used this technique to purify the human muscle-derived cells. During the initial 7 days, floating cells in the medium were centrifuged at 3000 rpm for 5 min and replated into the same culture flask with fresh medium. Most of the fibroblasts that rapidly adhered in the initial culture flask were eliminated (Richler and Yaffe, 1970; Rando and Blau, 1994; Qu *et al.*, 1998; Qu and Huard, 2000). After 7 days, medium changes were conducted routinely and no attempts were made afterward to separate myogenic cells from residual fibroblasts.

Human muscle cells were stained for the myogenic marker desmin, using a basic immunohistochemistry method as previously described (Lee *et al.*, 2000). These cells were also analyzed by flow cytometry for the expression of myogenic marker CD56 (specific to human myoblasts) and stem cell marker CD34, using a standard protocol (Lee *et al.*, 2000). The CD56 and CD34 antibodies were purchased from BD PharMingen (Carlsbad, CA).

Adenoviral and retroviral vectors expressing human BMP-2 and LacZ

The BMP2-125 plasmid, which contains human BMP-2 cDNA, was generously provided by the Genetics Institute (Cambridge, MA). A replication-defective, E1 and E3 gene-deleted adenoviral vector was engineered to encode BMP-2 under the control of the human cytomegalovirus (CMV) promoter. The BMP2-125 plasmid was digested with *Sal*I, resulting in a 1237-base pair fragment containing the BMP-2 cDNA. The recombinant human BMP-2 (rhBMP-2) cDNA was then inserted into the *Sal*I site of the pAd.lox plasmid, which placed the gene under the control of a human CMV promoter. Recombinant adenovirus was obtained by cotransfection of pAd.lox with ψ-5 viral DNA into CRE-8 cells. The adenovirus–BMP-2 construct (adBMP2) was stored at −80°C until further use. Retroviral vector expressing BMP-2 (retroBMP2) was constructed by cloning the cDNA into retroviral vector pCLX, which was derived from pLXSN (from A. Dusty Miller, Fred Hutchinson Cancer Research Center, Seattle, WA) by removing the simian virus 40 (SV40) promoter and the neomycin resistance gene, and replacing the U3 region in the 5′ long terminal repeat (LTR) with the human CMV promoter. Vector DNA was converted into replication-defective retrovirus by cotransfection, by calcium phosphate precipitation, into packaging cell line GP-293 (Clontech, Palo Alto, CA) with plasmid pVSVG, which expresses vascular stomatitis virus glycoprotein as the viral envelope. The conditioned medium containing the retroviral particles from the transfected cells was centrifuged at 3000 rpm for 5 min to remove cellular debris, and stored at −80°C in small aliquots until use. The retroviral vector MFG-NB (Ferry *et al.*, 1991), used for the LacZ studies, was provided by the laboratory of P.D. Robbins (University of Pittsburgh, Pittsburgh, PA). This retrovirus carries a modified *lacZ* gene, which includes a nuclear localization sequence (nls-*lacZ*) cloned from the SV40 large tumor antigen, and is transcribed from the LTR.

Transduction of human muscle cells with adBMP2 and retroBMP2

After being counted with a hemocytometer, cells were washed by serial rinses in Hanks' balanced salt solution (HBSS; GIBCO-BRL). Adenovirus particles at a multiplicity of infection (MOI) of 50 were premixed into HBSS and then layered onto the culture. After 4 hr of incubation at 37°C, an equal volume of growth medium was added, and cells were allowed to recover overnight. For transduction with retroviral vector expressing BMP-2 or LacZ, human cells were incubated with retroviral vector at MOIs of 5–10 for 8–18 hr in the presence of Polybrene (8 μg/ml). This procedure was repeated three times to ensure that the majority (>70%) of cells was transduced. BMP-2 secreted from transduced cells was measured by enzyme-linked immunosorbent assay (ELISA) (Lee *et al.*, 2001) and BMP bioassay (Peng *et al.*, 2001).

Skull defect assay

All the animal experiments were conducted according to the policies and guidelines set by the U.S. Department of Health and Human Services and approved by the Animal Research and Care Committee (ARCC) of Children's Hospital of Pittsburgh (protocol 1/98). The animals used in this experiment were purchased from Jackson Laboratories (Bar Harbor, ME) and kept in the Rangos Research Center Animal Facility of Children's Hospital of Pittsburgh. One day before surgery, transduced human muscle cells were trypsinized, counted, and seeded by incubating the cell drop onto collagen matrix (6-mm disks, Helistat: Colla-Tec, Plainsboro, NJ) at a concentration of 5×10^5 cells per disk for retroBMP2 and 1×10^6 cells per disk for adBMP2. Severely combined immunodeficient (SCID) mice (8 weeks old; Jackson Laboratories) were anesthetized with methoxyflurane and placed prone on the operating table. With a number 10 blade, the scalp was dissected to the skull, and the periosteum was stripped. A 5-mm, full-thickness circular skull defect was created with a dental burr, with minimal penetration of the dura (Lee *et al.*, 2000, 2001).

Mice were divided into four groups (Table 1). Group I did

TABLE 1. DESCRIPTION OF MOUSE GROUPS

Group	Treatment	Number at: 2 weeks	4 weeks	6 weeks	8 weeks
I	None	5	4		
II	Collagen sponge (matrix) only	5	5		
III	A. Matrix + nontransduced human cells	4	5		
	B. Matrix + retroLacZ-transduced human cells			5	5
IV	A. Matrix + adBMP2-transduced human cells	4	4		
	B. Matrix + retroBMP2-transduced human cells			5	5

not receive any implants for the skull defect; group II received a collagen sponge only; group III received a collagen sponge seeded with human muscle cells with or without transduction with retroLacZ; group IV received a collagen sponge seeded with muscle-derived cells transduced with adBMP2 or retroBMP2. The scalp was closed with a 4-0 nylon suture, and the animals were allowed food and activity *ad libitum*. At designated time points, mice were killed and skull specimens were dissected free from soft tissue for digital imaging. The percent closure of the defect was calculated by the NIH Image program. The area of the original defect was calculated with a 5-mm circular standard on the digital image, and the area of the closed defect was traced and calculated with the NIH Image program. The area of the closed defect divided by the standard area yielded the fraction of skull defect closure. Bone healing after the transplantation of retrovirally transduced human cells was also monitored by radiograph.

Skull specimens were then flash frozen in 2-methylbutane precooled in liquid nitrogen. Frozen samples were cut into 5- to 10-μm sections, using a cryostat (HM 505 E; Microm, Walldorf, Germany), and stored at −20°C pending further study.

For von Kossa staining, slides were fixed in 10% neutral buffered formalin and soaked in 0.1 *M* $AgNO_3$ solution for 15 min. After exposure to light for at least 15 min, slides were washed with phosphate-buffered saline (PBS), and stained with hematoxylin and eosin for viewing by light microscopy.

Fluorescence in situ hybridization

Cryosections were fixed for 10 min in methanol–glacial acetic acid (3:1, v/v), air dried, and then denatured in 70% formamide-2× SSC (0.3 *M* NaCl, 0.03 *M* sodium citrate), pH 7.0, at 70°C for 2 min. Slides were immediately dehydrated with a series of ethanol washes (70, 80, and 95%) for 2 min at each concentration. Human probes (human-specific α-satellite 10; Vysis, Downers Grove, IL) labeled with fluorescein isothiocyanate (FITC) were used to detect human nuclei. The human probes were denatured and applied according to the manufacturer's protocols and allowed to hybridize overnight at 37°C. After hybridization, sections were rinsed with 2× SSC solution, pH 7.0, at 72°C for 5 min. Sections were then rinsed in BMS solution (0.1 *M* $NaHCO_3$, 0.5 *M* NaCl, 0.5% Nonidet P-40 [NP-40], pH 8.0). Nuclei were counterstained with 4′,6-diamidino-2-phenylindole (DAPI, 10 ng/ml) and diluted in Vectashield mounting medium (Vector Laboratories, Burlingame, CA).

Statistical methods

Data are presented as means ± the standard deviation of the mean. Statistical differences between groups were calculated by a Student *t* test.

RESULTS

Human muscle-derived cells were analyzed for the expression of myogenic markers. These cells were only 10% desmin positive (Fig. 1A), and 22% of the cells expressed CD56 (Fig. 1B), a specific surface antigen expressed on human muscle cells (Webster *et al.*, 1988). This suggests that only 10–20% of the human cells were myogenic, and the remainder of the cells were likely fibroblastic in nature. In addition, the vast majority of human muscle-derived cells did not express CD34, a widely utilized stem cell marker that was found to be expressed by mouse muscle stem cells (Lee *et al.*, 2000). Human muscle-derived cells were capable of osteogenic differentiation upon stimulation with retroBMP2, as evidenced by expression in the transduced cells of alkaline phosphatase, an early marker of osteogenesis (Fig. 1D). In contrast, human cells transduced with retroLacZ were alkaline phosphatase negative (Fig. 1C). About 70–80% of the cells were transduced after three rounds of transduction with retroviral vectors as indicated by the expression of BMP-2 or LacZ (data not shown). Human muscle-derived cells transduced with adBMP2 or retroBMP2 produced, on average, 1.0 ng of BMP-2 per million cells, whereas the nontransduced control did not produce any detectable protein. There was no apparent morphological difference between cells transduced by adBMP2 or retroBMP2.

To assess their bone-healing ability, the BMP-2-producing human muscle cells were implanted into critical-sized skull defects in SCID mice. The use of SCID mice was necessary to eliminate immune rejection of xenogeneic human muscle-derived cells. A 5-mm skull defect was previously shown to be a nonhealing, critical-sized defect in mice (Krebsbach *et al.*, 1998). A soft, bovine collagen type I sponge (Helistat) (Boyne *et al.*, 1997; Hollinger *et al.*, 1998) was used as a matrix to allow focal implantation of the cells. It has been shown previously that this collagen sponge is degraded by the host within 4 weeks in a skull defect model (Lee *et al.*, 2000, 2001).

Four groups of mice were tested (Table 1). Groups I through III were control groups, and group IV included the treated animals. Group I consisted of animals without any implants; group II mice received a collagen sponge only; group III animals received a collagen sponge and nontransduced human muscle cells or collagen sponge containing human cells retrovirally transduced to express LacZ; and group IV mice received a collagen sponge and BMP-2-producing human muscle cells retrovirally transduced to after transduction with adenovirus or retrovirus (Table 1). The healing process was monitored at 2, 4, 6, and 8 weeks for closure of the skull defect grossly and histologically, and by radiograph.

The representative gross specimens from the control groups and the treatment group are shown in Fig. 2 for comparison. The control groups (a specimen from group III is shown in Fig. 2: d/s/c [defect + collagen sponge + cells]) did not show any evidence of defect closure at either 2 weeks (Fig. 2A) or 4 weeks (Fig. 2C). However, the treatment group (group IV, defect + collagen sponge + adBMP2-transduced cells) showed robust closure of the defect at 2 weeks (Fig. 2B) and nearly complete closure of the defect at 4 weeks (Fig. 2D). The arrows in Fig. 2 show the edge of the skull defect.

The digital quantitation of the skull defect closure is summarized in Fig. 2E. The three control groups (d only, d/s, and d/s/c) showed minimal evidence of defect closure at 2 and 4 weeks. At most, only 25 to 35% closure was seen in the control groups. On the other hand, the group treated with BMP-2-producing human muscle-derived cells showed >70% closure of the defect at 2 weeks and >90% closure at 4 weeks.

Mineralized segments of newly formed bone were identified by von Kossa staining. Figure 3A and B shows representative specimens from the control group treated with a sponge matrix

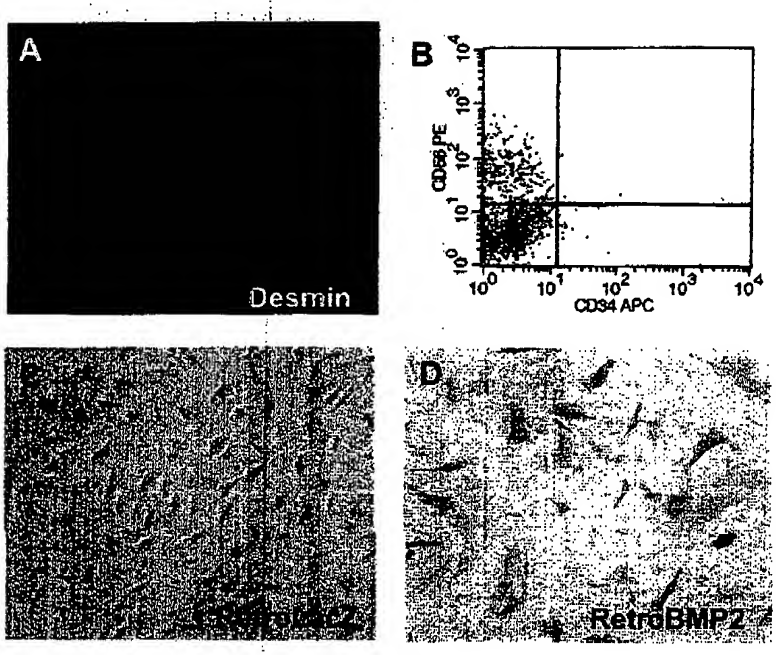

FIG. 1. Human muscle cell characterization and osteogenic differentiation induced by human BMP-2. (A) Expression of myogenic marker desmin by human muscle cells. (B) Flow cytometry analysis of CD56 and CD34 expression by human cells. (C and D) Expression of osteogenic marker alkaline phosphatase in human muscle cells transduced with retroLacZ (C) or retroBMP2 (D). Many alkaline phosphatase-expressing cells can be found among the BMP-2-expressing cells (D), in contrast to the cells retrovirally transduced to express LacZ (retroLacZ). Total magnification: (A, C, and D) ×200 objective.

and nontransduced human muscle cells (group III, d/s/c: control in Fig. 3) and from the group treated with a sponge matrix and human muscle cells transduced with adBMP2 (group IV, d/s/c/adBMP2; BMP2 in Fig. 3). The control group shows no evidence of newly formed bone at 2 weeks (Fig. 3B) or at 4 weeks (not shown). The treatment group, however, shows newly mineralized bone bridging the defect at 2 weeks (Fig. 3A) and thicker trabeculae covering the defect at 4 weeks (not shown).

Human muscle cells transduced with retroBMP2 were also capable of eliciting healing of critical-sized calvarial defects. The defects implanted with BMP-2-expressing cells were completely healed when judged by gross inspection and palpation 6 and 8 weeks after surgery. These results were confirmed by X-ray (Fig. 3E) and histologic analysis (Fig. 3C). In contrast, there was no bone healing in the control group implanted with cells transduced with retroviral vector expressing LacZ (Fig. 3D and F) tested at the same time points.

The remodeling process was also evident when the specimens were analyzed histologically (Fig. 4). At 2 weeks, all specimens in the treatment group (d/s/c/adBMP2) showed bony bridging of the skull defect with thin trabeculae (Fig. 4A). However, at 4 weeks, the new bone was remodeled to a thicker mineralized bone (Fig. 4B). Most of the newly formed bone was woven (Fig. 4A and B). A mature periosteum covered the newly formed bone at both 2 and 4 weeks (Fig. 4A and B, marked *P*). Similar results were observed in the bone-healing sites implanted with retroBMP2 at 6 and 8 weeks posttransplantation (Fig. 4C and D).

Because human muscle cells were used in a mouse model, we were able to monitor the fate of the transplanted cells and to differentiate transplanted cells from host cells using a human-specific fluorescence *in situ* hybridization (FISH) technique. By using human-specific α-satellite 10 probe, we could distinguish transplanted cells from host cells. Locations of human chromosome-positive cells were analyzed in the treatment group at 6 weeks (Fig. 5). A majority of the visualized cells (>99% by manual counting) was found localized to the periphery of the newly formed bone (Fig. 5B, arrows). A small percentage of the visualized cells (<1%) was identified within the lacunae of the new bone, where osteocytes are normally found (Fig. 5C, E, and F). A faint outline of the newly formed bone was visible because of autofluorescence of the mineralized bone (Fig. 5B–5E, arrowheads). Similar results were found in the sample implanted with human cells transduced by adBMP2 (data not shown).

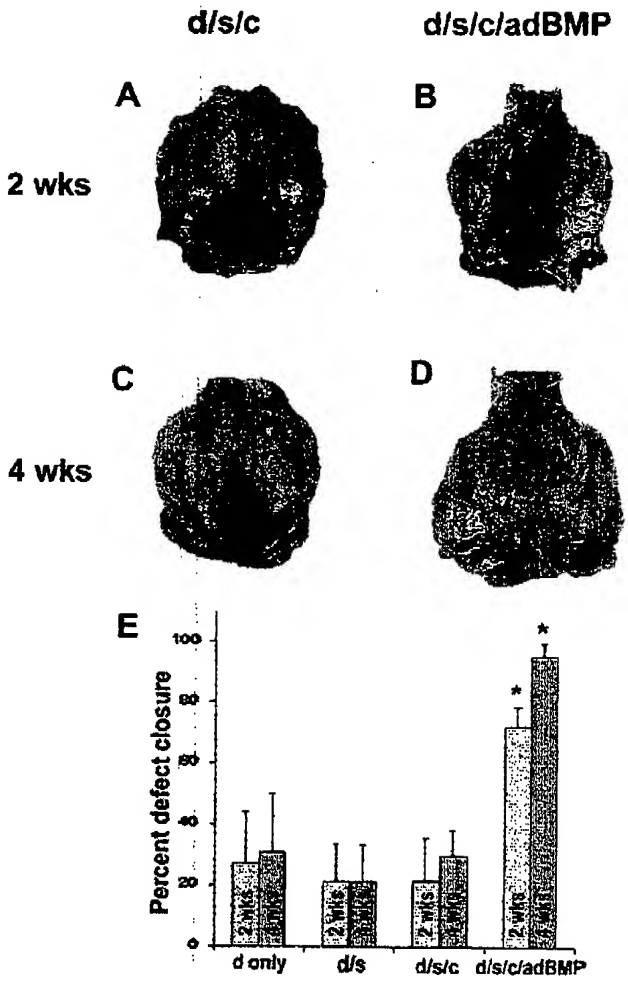

FIG. 2. Closure of skull defects by human muscle-derived cells transduced with adBMP2. (**A** and **B**) At 2 weeks, the control groups, represented here by a specimen from group III (**A**, d/s/c), showed minimal closure of the defect (arrows outline the edge of the defect). The treatment group (**B**, d/s/c/adBMP2), however, showed a significant defect closure (arrows outline the edge of the defect). (**C** and **D**) At 4 weeks, the control specimens (**C**, d/s/c) failed to show any healing progression (arrows outline the edge of the defect), whereas the treatment group (**D**, d/s/c/adBMP2) showed nearly complete closure of the defect. (**E**) Digital quantitations of skull defect closure. Mice treated with human muscle cells expressing BMP-2 showed >70% healing by 2 weeks and 90 to 100% healing by 4 weeks. All three control groups failed to show any significant healing at either 2 or 4 weeks. d, Defect only (group I); d/s, defect plus collagen sponge (group II); d/s/c, defect plus collagen sponge plus nontransduced cells (group III); d/s/c/adBMP, defect plus collagen sponge plus BMP-2-producing cells (group IV). *Significant difference from the control group ($p < 0.05$).

DISCUSSION

We have demonstrated that human muscle-derived cells can be genetically engineered by both adenoviral vector and retroviral vector to produce human BMP-2 and significantly enhance healing of a critical-sized bone defect. These cells can be induced by BMP-2, under *in vitro* conditions, to differentiate into cells expressing an early marker of osteoblasts, alkaline phosphatase. FISH analysis suggests that a small percentage of the implanted human muscle-derived cells is incorporated into the

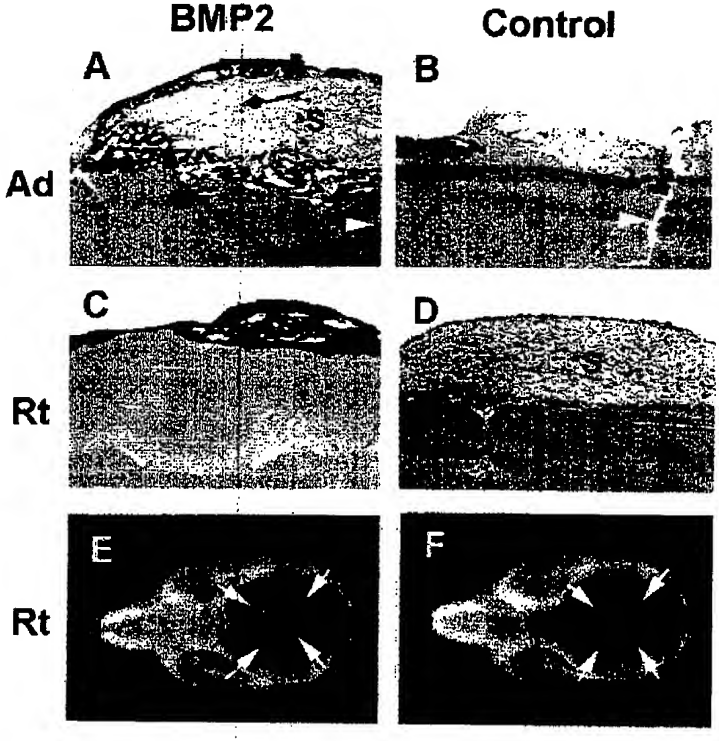

FIG. 3. Characterization of bone healing by von Kossa staining and radiography of the control and BMP-2-expressing human cell-treated mice. (A) Mice that received BMP-2-producing human muscle cells after transduction with adenovirus already show robust mineralized bone formation by 2 weeks (s, nondegraded collagen sponge). (B) The control group shows minimal new bone formation at 2 weeks. Healing of skull defects by human muscle cells transduced with retroBMP2 was also investigated. (C) von Kossa staining shows complete bone bridging of the defect at 8 weeks after the surgery, with mineralized bone covering most of the defect. (D) No bone healing was observed in the control group implanted with human muscle cells transduced with retroLacZ (s, nondegraded collagen sponge). (E and F) X-ray shows bone healing of the critical-sized calvarial defect implanted with transduced human muscle cells expressing BMP-2 (E, arrows show the edge of the defect), whereas no bone healing occurred in the defects implanted with the same cells transduced with control vector, retroLacZ (F, arrows show the edge of the defect) at 8 weeks after surgery. Total magnification: (A and B) ×100 objective; (C and D) ×40 objective.

newly formed bone, possibly differentiating *in vivo* into osteogenic cells.

Until now, the osteoprogenitor cells in skeletal muscle have been underutilized. Katagiri *et al.* (1994) initially suggested the osteogenic potential of skeletal muscle cells when they reported that clonal skeletal muscle cells from mice can express osteocalcin, alkaline phosphatase, and parathyroid-dependent 3′,5′-cAMP in response to BMP-2. Many studies have focused on potential uses of stem cell-like muscle cells for the treatment of muscle-related diseases, such as Duchenne muscular dystrophy (Barofflo *et al.*, 1996; Fan *et al.*, 1996; Qu *et al.*, 1998; Beauchamp *et al.*, 1999; Gussoni *et al.*, 1999; Qu and Huard, 2000), but only a few have explored their potential value in treating skeletal defects. We reported that mouse muscle cells could enhance bone healing and differentiate into osteogenic cells *in vivo* (Lee *et al.*, 2000, 2001). Also, we reported the potential existence of inducible osteoprogenitor cells in human muscle cells and their ability to form bone when genetically engineered to produce BMP-2 and ectopically implanted in SCID mice (Musgrave *et al.*, 2002).

The osteogenic potential of human muscle cells has not been tested in a bone defect model until now. Our data suggest that there is a small population of inducible osteoprogenitor cells in human skeletal muscle and that they can participate in bone formation *in vivo* with stimulation by BMP-2. These data suggest numerous clinical applications. If these cells could be isolated or enriched *in vitro*, they may be useful for common orthopedic procedures that require augmentation of bone healing, such as osteotomies, fusions, and procedures for segmental bone defects and failed unions. Our results show that the number of os-

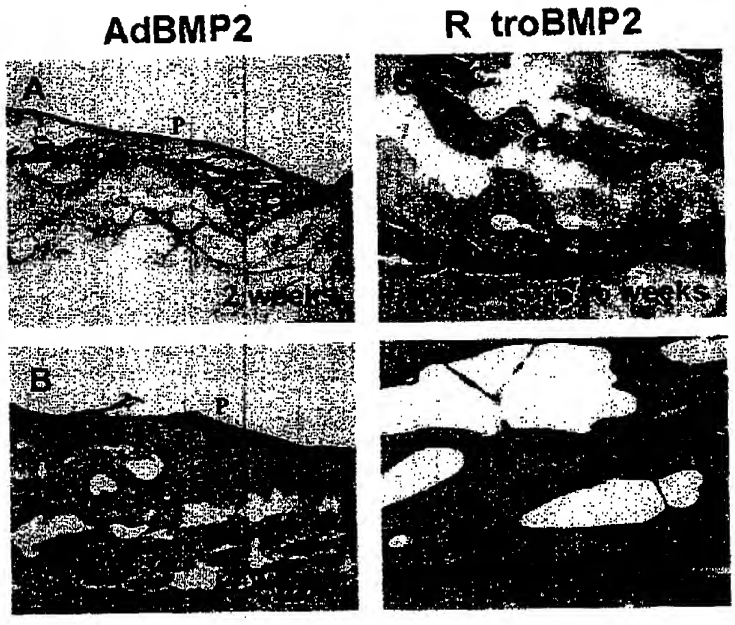

FIG. 4. Remodeling of newly regenerated bone. (**A** and **B**) H&E stain shows the newly formed woven bone induced by muscle cells transduced with adBMP2. At 2 weeks, trabeculae were coarse and thin (**A**). The newly formed bone was remodeled with thicker trabeculae by 4 weeks (**B**). Both 2- and 4-week specimens contained mature periosteal covers (P). (**C** and **D**) A similar trend is seen in new bone induced by human muscle cells transduced by retroBMP2 at 6 weeks (**C**) and 8 weeks (**D**) postimplantation. Total magnification: (**A** and **B**) ×200 objective; (**C** and **D**) ×400 objective.

teoprogenitors in human muscle cells is relatively small (<1%). This underscores the need to develop methods to rapidly isolate or enrich these muscle-derived inducible osteoprogenitor cells for future clinical use. However, our results cannot rule out the possibility that muscle-derived fibroblasts may be capable of improving bone healing by delivering BMP-2 and differentiate into the osteogenic lineage in a manner similar to that observed with gingival and dermal fibroblasts (Krebsbach *et al.*, 2000).

Our data also suggest that exogenous production of BMP-2 is required for human muscle cells to augment bone healing. This is not surprising, as previous *in vitro* data indicate that muscle-derived inducible osteoprogenitors do not express osteogenic markers until exposed to BMP-2 (Katagiri *et al.*, 1994; Bosch *et al.*, 2000; Lee *et al.*, 2000, 2001; Musgrave *et al.*, 2000, 2002). This would suggest either that these cells are noncommitted and quiescent until stimulated or that they are already committed to the muscle lineage but are redirected to the osteogenic lineage by stimulation with BMP-2. Clinically, this would mean that these cells should be used in combination with osteoinductive factors to augment bone healing. They would have to be genetically manipulated by *ex vivo* methods to achieve full osteogenic potential. However, this is not a disadvantage, as these cells can also deliver a sufficient amount of BMP-2 to stimulate host osteoprogenitors to form bone.

Skeletal muscle represents an easily accessible and abundant source of cells, given that 30–40% of our total body weight is skeletal muscle. A simple surgical muscle biopsy can provide a sufficient number of cells for use in *ex vivo* gene therapy. Because we have not compared muscle-derived cells with various other cell types such as bone marrow stromal cells or fibroblasts, it is still unclear which cell type is the most suitable candidate for bone healing. The relative advantage of these various cell types has not yet been established. If there is no major difference among these cells in terms of harvesting, efficiency of transduction, and efficacy to deliver therapeutic gene to elicit bone healing, the selection of a particular cell source depends largely on their availability. In addition, collagen matrix is a commercially available material that has already been tested in humans for maxillary sinus floor reconstruction (Boyne *et al.*, 1997). Because it allows muscle cells to adhere to its matrix, a collagen sponge proved efficient for our purposes. It is highly malleable, allowing flexible fitting into the bone defect. However, it cannot be used in a weight-bearing bone; a more solid construct is required for such a purpose. In this regard, hydroxyapatite/tricalcium phosphate-based materials can be used. In animals, a BMP-2-impregnated collagen sponge was used for repair of radius defects in rabbits (Hollinger *et al.*, 1998).

In our experiments, the newly formed bone underwent extensive remodeling during the testing period. The thin trabeculae initially seen were rapidly replaced with thicker bone by 4

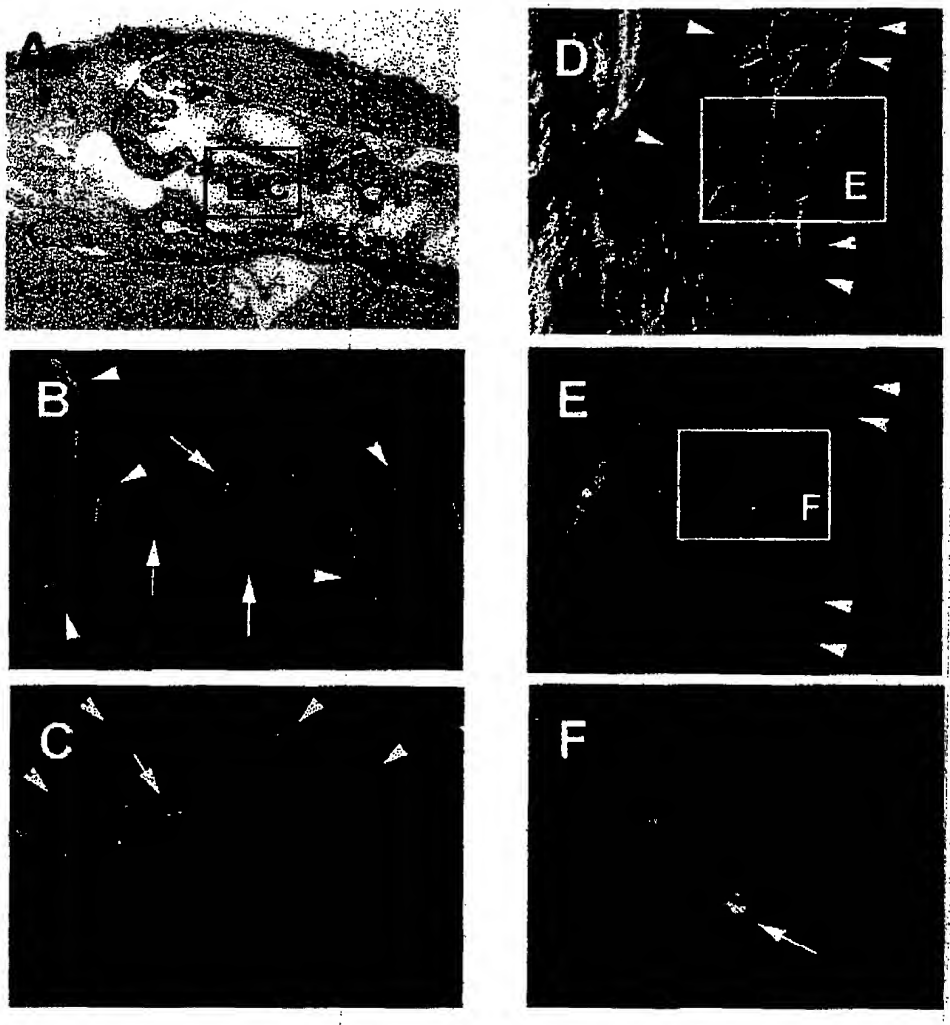

FIG. 5. FISH analysis of transplanted cells in newly formed bones. (A) H&E stain of new bone, showing the area of interest at the site implanted with human muscle cells transduced with retroBMP2. (B) Most of the implanted human cells were scattered at the periphery of the new bone (outlined by arrowheads), which was visualized by red autofluorescence. These cells were identified by bright punctate green fluorescence (arrows); nuclei are identified by purple DAPI staining. (C) A minority of the implanted human cells was identified within the lacunae of the new bone (arrows). (D) Another area of interest in the newly formed bone visualized by phase microscopy. (E and F) Human cells embedded in the newly formed bone were derived from the implanted human cell (arrow). The high magnification in (F) shows the presence of the positive signal of the human probe in the nucleus of the cells embedded in the newly regenerated bone. Total magnification: (A) ×200 objective; (B and C) ×600 objective; (D) ×400 objective; (E) ×1,000 objective.

to 8 weeks posttransplantation. The new bone, however, was not tested biomechanically, because the skull is not a weight-bearing bone. Weight-bearing models in rats and rabbits are currently under investigation to test the osteogenic capacity of muscle cells to produce biomechanically sound bone. Although both adBMP2- and retroBMP2-transduced cells were capable of eliciting complete bone healing of the defects, we observed that the healing process mediated via the retrovirally transduced

human muscle cells expressing BMP-2 was delayed when compared with the BMP-2-expressing human muscle cells transduced by adenovirus. The difference in the number of implanted cells (1×10^6 cells in adBMP2 vs. 5×10^5 in retroBMP2) is a potential explanation for these results because the levels of BMP-2 expressed from these two groups of cells were found to be similar.

In summary, human skeletal muscle cells are an important source of inducible osteoprogenitors, and their orthopedic utility in both gene therapy and tissue-engineering applications should not be ignored. Future developments to enrich, isolate, and expand these human muscle cells *in vitro* will facilitate and further expedite their use in clinical applications.

ACKNOWLEDGMENTS

The authors thank Dr. Christopher Evans, Dr. Steve Ghivizzani (adBMP2), Dr. Brian Klatt, Marcelle Pellerin, and Ryan Pruchnic for technical assistance, and Dana Och, Ryan Sauder, and Kathy Wypychowski for assistance with the manuscript. The authors also thank the Genetics Institute (Cambridge, MA) for rh-BMP-2 and rh-BMP-2 antibodies, and Stephen Hardy for graciously providing us with the Cre–*lox* adenoviral system. This work was supported by grants awarded to Dr. Johnny Huard from the National Institutes of Health (1 P60 AR44811-01 and 1 RO1 DE13420-01A2), the Pittsburgh Tissue Engineering Initiative (PTEI, Drs. Peng and Huard), and the William F. and Jean W. Donaldson Chair at the Children's Hospital of Pittsburgh.

REFERENCES

BAROFFIO, A., HAMANN, M., BERNHEIM, L., BOCHATON-PIALLAT, M.L., GABBIANI, G., and BADER, C.R. (1996). Identification of self-renewing myoblasts in the progeny of single human muscle satellite cells. Differentiation **60**, 47–57.

BEAUCHAMP, J.R., MORGAN, J.E., PAGEL, C.N., and PARTRIDGE, T.A. (1999). Dynamics of myoblast transplantation reveal a discrete minority of precursors with stem cell-like properties as the myogenic source. J. Cell Biol. **144**, 1113–1122.

BISCHOFF, R. (1986). Proliferation of muscle satellite cells on intact myofibers in culture. Dev. Biol. **115**, 129–139.

BISCHOFF, R. (1994). The satellite cells and muscle regeneration. In *Myology: Basic and Clinical*, 2nd Ed. A.G. Engel and C. Franzini-Armstrong, eds. (New York: McGraw-Hill) pp. 97–118.

BOSCH, P., MUSGRAVE, D.S., LEE, J.Y., CUMMINS, J., SHULER, F., GHIVIZZANI, S.C., EVANS, C., ROBBINS, P.D., and HUARD, J. (2000). Osteoprogenitor cells within skeletal muscle. J. Orthop. Res. **18**, 933–944.

BOYNE, P.J., MARX, R.E., NEVINS, M., TRIPLETT, G., LAZARO, E., LILLY, L.C., ALDER, M., and NUMMIKOSKI, P. (1997). A feasibility study evaluating rhBMP-2/absorbable collagen sponge for maxillary sinus floor augmentation. Int. J. Periodontics Restorative Dent. **17**, 11–25.

CAPLAN, A.I. (1991). Mesenchymal stem cells. J. Orthop. Res. **9**, 641–650.

DAI, Y., ROMAN, M., NAVIAUX, R.K., and VERMA, I.M. (1992). Gene therapy via primary myoblasts: Long-term expression of factor IX protein following transplantation in vivo. Proc. Natl. Acad. Sci. U.S.A. **89**, 10892–10895.

ENGSTRAND, T., DALUISKI, A., BAHAMONDE, M.E., MELHUS, H., and LYONS, K.M. (2000). Transient production of bone morphogenetic protein 2 by allogeneic transplanted transduced cells induces bone formation. Hum. Gene Ther. **11**, 205–211.

FAN, Y., MALEY, M., BEILHARZ, M., and GROUNDS, M. (1996). Rapid death of injected myoblasts in myoblast transfer therapy. Muscle Nerve **19**, 853–860.

FERRY, N., DUPLESSIS, O., HOUSSIN, D., DANOS, O., and HEARD, J.M. (1991). Retroviral-mediated gene transfer into hepatocytes in vivo. Proc. Natl. Acad. Sci. U.S.A. **88**, 8377–8381.

GUSSONI, E., SONEOKA, Y., STRICKLAND, C.D., BUZNEY, E.A., KHAN, M.K., FLINT, A.F., KUNKEL, L.M., and MULLIGAN, R.C. (1999). Dystrophin expression in the *mdx* mouse restored by stem cell transplantation. Nature **401**, 390–394.

HOLLINGER, J.O., SCHMITT, J.M., BUCK, D.C., SHANNON, R., JOH, S.P., ZEGZULA, H.D., and WOZNEY, J. (1998). Recombinant human bone morphogenetic protein-2 and collagen for bone regeneration. J. Biomed. Mater. Res. **43**, 356–364.

KATAGIRI, T., YAMAGUCHI, A., KOMAKI, M., ABE, E., TAKAHASHI, N., IKEDA, T., ROSEN, V., WOZNEY, J.M., FUJISAWA-SEHARA, A., and SUDA, T. (1994). Bone morphogenetic protein-2 converts the differentiation pathway of C2C12 myoblasts into the osteoblast lineage [published erratum appears in J. Cell Biol. 1995;128:following 713] J. Cell Biol. **127**, 1755–1766.

KREBSBACH, P.H., MANKANI, M.H., SATOMURA, K., KUZNETSOV, S.A., and ROBEY, P.G. (1998). Repair of craniotomy defects using bone marrow stromal cells. Transplantation **66**, 1272–1278.

KREBSBACH, P.H., GU, K., FRANCESCHI, R.T., and RUTHERFORD, R.B. (2000). Gene therapy-directed osteogenesis: BMP-7-transduced human fibroblasts form bone in vivo. Hum. Gene Ther. **11**, 1201–1210.

LEE, J.Y., QU-PETERSEN, Z., CAO, B., KIMURA, S., JANKOWSKI, R., CUMMINS, J., USAS, A., GATES, C., ROBBINS, P.D., WERNIG, A., and HUARD, J. (2000). Clonal isolation of muscle derived stem cells capable of enhancing muscle regeneration and bone healing. J. Cell Biol. **150**, 1085–1099.

LEE, J.Y., MUSGRAVE, D., PELINKOVIC, D., FUKUSHIMA, K., CUMMINS, J., USAS, A., ROBBINS, P., FU, F.H., and HUARD, J. (2001). Effect of bone morphogenetic protein-2-expressing muscle-derived cells on healing of critical-sized bone defects in mice. J. Bone Joint Surg. **83**, 1032–1039.

LIEBERMAN, J.R., DALUISKI, A., STEVENSON, S., WU, L., McALLISTER, P., LEE, Y.P., KABO, J.M., FINERMAN, G.A., BERK, A.J., and WITTE, O.N. (1999). The effect of regional gene therapy with bone morphogenetic protein-2-producing bone-marrow cells on the repair of segmental femoral defects in rats. J. Bone Joint Surg. Am. **81**, 905–917.

MUSGRAVE, D.S., BOSCH, P., LEE, J.Y., PELINKOVIC, D., GHIVIZZANI, S.C., WHALEN, J., NIYIBIZI, C., and HUARD, J. (2000). Ex vivo gene therapy to produce bone using different cell types. Clin. Orthop. **378**, 290–305.

MUSGRAVE, D.S., PRUCHNIC, R., WHALEN, J., BOSCH, P., ZIRAN, B.H., and HUARD, J. (2002). Human skeletal muscle cells in *ex vivo* gene therapy to deliver bone morphogenetic protein-2. J. Bone Joint Surg. Br. **84-B**, 120–127.

PENG, H., CHEN, S.T., WERGEDAL, J.E., POLO, J.M., YEE, J.K., LAU, K.H., and BAYLINK, D.J. (2001). Development of an MFG-based retroviral vector system for secretion of high levels of functionally active human BMP4. Mol. Ther. **4**, 95–104.

PITTENGER, M.F., MACKAY, A.M., BECK, S.C., JAISWAL, R.K., DOUGLAS, R., MOSCA, J.D., MOORMAN, M.A., SIMONETTI, D.W., CRAIG, S., and MARSHAK, D.R. (1999). Multilineage potential of adult human mesenchymal stem cells. Science **284**, 143–147.

QU, Z., and HUARD, J. (2000). Matching host muscle and donor myoblasts for myosin heavy chain improves myoblast transfer therapy. Gene Ther. **7**, 428–437.

QU, Z., BALKIR, L., VAN DEUTEKOM, J.C., ROBBINS, P.D., PRUCHNIC, R., and HUARD, J. (1998). Development of approaches to improve cell survival in myoblast transfer therapy. J. Cell Biol. **142**, 1257–1267.

RANDO, T.A., and BLAU, H.M. (1994). Primary mouse myoblast purification, characterization, and transplantation for cell-mediated gene therapy. J. Cell Biol. **125**, 1275–1287.

REDDI, A.H. (2001). Bone morphogenetic proteins: From basic science to clinical applications. J. Bone Joint Surg. **83**, S1–S6.

RICHLER, C., and YAFFE, D. (1970). The in vitro cultivation and differentiation capacities of myogenic cell lines. Dev. Biol. **23**, 1–22.

ROBBINS, P.D., TAHARA, H., and GHIVIZZANI, S.C. (1998). Viral vectors for gene therapy. Trends Biotechnol. **16**, 35–40.

ROMANO, G., CLAUDIO, P.P., KAISER, H.E., and GIORDANO, A. (1998). Recent advances, prospects and problems in designing new strategies for oligonucleotide and gene delivery in therapy. In Vivo **12**, 59–67.

URIST, M.R. (1965). Bone: Formation by autoinduction. Science **150**, 893–899.

URIST, M.R., HUO, Y.K., BROWNELL, A.G., HOHL, W.M., BUYSKE, J., LIETZE, A., TEMPST, P., HUNKAPILLER, M., and DELANGE, R.J. (1984). Purification of bovine bone morphogeneric protein by hydroxyapatite chromatography. Proc. Natl. Acad. Sci. U.S.A. **81**, 371–375.

VERMA, I.M., and SOMIA, N. (1997). Gene therapy: Promises, problems and prospects. Nature **389**, 239–242.

VILQUIN, J.T., GUERETTE, B., KINOSHITA, I., ROY, B., GOULET, M., GRAVEL, C., ROY, R., and TREMBLAY, J.P. (1995). FK506 immunosuppression to control the immune reactions triggered by first-generation adenovirus-mediated gene transfer. Hum. Gene Ther. **6**, 1391–1401.

WEBSTER, C., PAVLATH, G.K., PARKS, D.R., WALSH, F.S., and BLAU, H.M. (1988). Isolation of human myoblasts with the fluorescence-activated cell sorter. Exp. Cell Res. **174**, 252–265.

YANG, Y., NUNES, F.A., BERENCSI, K., FURTH, E.E., GONCZOL, E., and WILSON, J.M. (1994). Cellular immunity to viral antigens limits E1-defeted adenoviruses for gene therapy. Proc. Natl. Acad. Sci. U.S.A. **91**, 4407–4411.

YOUNG, H.E., MANCINI, M.L., WRIGHT, R.P., SMITH, J.C., BLACK, A.C., JR., REAGAN, C.R., and LUCAS, P.A. (1995). Mesenchymal stem cells reside within connective tissues of many organs. Dev. Dyn. **202**, 137–144.

Address reprint requests to:
Dr. Johnny Huard
Growth and Development Laboratory
4151 Rangos Research Center
Children's Hospital of Pittsburgh
3705 Fifth Avenue
Pittsburgh, PA 15213

E-mail: jhuard+@pitt.edu

Received for publication February 16, 2001; accepted after revision June 3, 2002.

Published online: June 19, 2002.